UNIVERSIDAD CARLOS III DE MADRID

TESIS DOCTORAL

BIT AND POWER LOADING FOR MIMO SYSTEMS WITH STATISTICAL CHANNEL KNOWLEDGE AT THE TRANSMITTER

Author: Li Hong

Advisor: Dra. Ana García Armada

DEPARTAMENTO DE TEORÍA DE LA SEÑAL Y COMUNICACIONES

Madrid, May, 2011

TESIS DOCTORAL
BIT AND POWER LOADING FOR MIMO SYSTEMS WITH STATISTICAL CHANNEL KNOWLEDGE AT THE TRANSMITTER

Author: Li Hong
Advisor: Dra. Ana García Armada

Firma del Tribunal Calificador:

		Firma
Presidente:	(Nombre y apellidos)	
Vocal:	(Nombre y apellidos)	
Vocal:	(Nombre y apellidos)	
Vocal:	(Nombre y apellidos)	
Secretario:	(Nombre y apellidos)	

Calificación:

Madrid, de de

Abstract

In MIMO (multiple input-multiple output) communication, the adaptation of the modulation and coding at the transmitter side according to the channel characteristics allows reducing the transmission power and/or enhancing the data rates. However, it is not always feasible to have instantaneous knowledge of the channel at the transmitter. This Thesis focuses on the case that the receiver has (perfect) instantaneous Channel State Information (CSIR) but the transmitter has only access to its distribution (CDIT). This is a practical case that applies, particularly, to situations where the channel varies rapidly. Under CDIT, the input cannot be adapted to the instantaneous state of the channel and thus SVD (singular value decomposition) cannot be used to diagonalize the channel. Achieving capacity requires a complex Gaussian input vector with a covariance that depends on the channel distribution. In practice, however, discrete constellations are used instead of Gaussian signals. Determining the optimum signalling strategy with discrete constellations is difficult in general, and thus a pragmatic approach is using the spatial signalling directions indicated by the capacity-achieving covariance. Several classical practical bit and power loading algorithms are available for parallel-channel settings. To guarantee the quality of service, a certain average bit error probability (BER) is required at the receiver side. Different types of receiver correspond to differente relationships between the BER and the SINR. With the feedback of the parameters of the SINR (Signal-to-Interference-plus-Noise Ratio) distribution, two optimization problems for single user MIMO systems with correlation at the transmitter side can be solved, namely rate maximization with a total power constraint and power minimization with a target bit rate.

The goal of this Thesis is to devise practical bit and power loading schemes for MIMO that can operate on the basis of CDIT only. For practical reasons,

three typical receivers are considered, namely zero-forcing (ZF), minimum mean squared error (MMSE) and zero-forcing with successive interference cancellation (ZF-SIC). The following problems are addressed:

- Maximization of the bit rates with discrete constellations, using the transmit directions given by the capacity achieving input covariance, at a certain average bit error probability (BER) and a constraint of total transmit power.
- Minimization of the transmit power with discrete constellations, using the transmit directions given by the capacity achieving input covariance, at a certain average bit error probability (BER) and a target transmit bit rate.
- Evaluation and comparison of the power gain when optimizing the transmission with the three mentioned types of receivers relative to a non-optimized transmission.

In order to address these items, in this work it is essential to establish a relationship between the average BER corresponding to each of the three receivers and the powers allocated at the transmitter under the premise of CDIT. By utilizing these BER approximations, two dual optimization problems, bit maximization and power minimization, are solved for the practical case of statistical channel knowledge at the transmitter side and discrete constellations. Using a Gamma or a generalized Gamma distribution of the SINR, BER approximations can be obtained through integration.

For a single user MIMO system with correlated channel, to accomplish the optimization process the mathematical methods used are a Levin-Campello algorithm for ZF, exhaustive search with additional constraints for MMSE and tree search with bit rate boundary for ZF-SIC. The accuracy of the developed expressions is verified with Monte Carlo simulations. The transmission environment is specified to be a Rayleigh flat-fading channel with correlation at the transmitter side.

The Thesis is structured as follows. An introduction is presented at the first chapter, explaining the contents of this Thesis. Following a description of the basic process which takes place at the transmitter side, the second chapter presents the characteristics of the MIMO channel. Moreover, the system models of three typical receivers are described, namely ZF, MMSE and ZF-SIC. The third chapter starts with a review of capacity, and leads to the so-called waterfilling distribution. The dual optimization problems, bit rate maximization and power minimization, are defined with the objective of enhancing the performance via processing at the transmitter side. In some practical systems, Levin-Campello develops a solution for the dual optimization problems for discrete constellations that is described. Also, in order to further understand the power minimization problem for discrete constellations considering the loss of mutual information due to a given modulation, Mercury/Waterfilling is reviewed.

In chapter IV, the BER of a ZF receiver is computed by using its SINR distribution, which is a Gamma distribution. For convenience, it is further accurately approximated at the high SNR regime. From the relationship between BER and power for different constellations, the two dual problems can be solved by a Levin-Campello algorithm, as the streams are independent with each other. To facilitate using the Levin-Campello algorithm, BER approximations are simplified to be established in convenient closed-form equations.

In chapter V, the BER of an MMSE receiver is also computed by using its SINR distribution, which can be modeled as a Gamma distribution or a generalized Gamma distribution. Some accurate closed-formed approximations are proposed and compared. In chapter VI, from these relationships between BER and power for different constellations, the two dual problems are solved by exhaustive search, as the streams are coupled with each other in the case of the MMSE receiver. In order to reduce the computational complexity, some additional constrains are added. For the two dual optimization problems, the total number of transmitted bits with an MMSE receiver cannot be less than those with a ZF receiver. Therefore, the starting point for the search is always the solution derived for ZF receivers, and the search progresses from that point towards higher loads until the constraints set in. The BER of MMSE can be approximated by the moment generating function (MGF), which includes the first three moments of SINR. Comparing two randomly selected antennas, when an increment of the number of bits is added to one of them, placing the increment in the antenna with better channel condition requires less total power to accomplish the transmission. Thus, it can be concluded that the better channel should be loaded with more bits. With this additional constraint, the computational complexity of the exhaustive search can be reduced even more reasonably.

In chapter VII, taking into account the error propagation, a closed-form BER approximation can be derived for the ZF-SIC receiver by using the total probability theorem. Moreover, since the ordering of the decoding process can dramatically impact the system performance when using this receiver, a precoder is proposed to determine the decoder ordering to minimize the total power. Moreover, a boundary of possible bit rates for ZF-SIC is presented, considering the bit rate of ZF and ZF-PSIC (perfect SIC), for the two dual optimization problems. To make the search converge more efficiently, a tree search is implemented making use of this boundary.

In the final chapter, the results obtained for the different receivers are compared to conclude the core of this Thesis. Then, some future work is outlined.

Resumen

En los sistemas de comunicaciones multiantena (MIMO: multiple input-multiple output), la adaptación de los esquemas de modulación y codificación en el extremo transmisor según las características del canal permite reducir la potencia de transmisión y/o aumentar la velocidad de transmisión. Sin embargo, no siempre es posible tener conocimiento instantáneo del canal en el transmisor. Esta Tesis se centra en el caso en que el receptor tiene (perfecta) información instantánea del canal (CSIR: Channel State Information at the Receiver), pero el transmisor únicamente tiene acceso a su distribución (CDIT: Channel Distribution Information at the Transmitter). Este es un caso práctico que sucede, en particular, en situaciones en las que el canal varía rápidamente. Con CDIT, la señal no se puede adaptar al estado instantáneo del canal y, por tanto, no es posible usar una descomposición en valores singulares para diagonalizar el canal. Alcanzar la capacidad requiere el uso de señales Gaussianas cuya correlación depende de la distribución del canal. En la práctica, sin embargo, se utilizan constelaciones discretas y no señales Gaussianas. Determinar la estrategia óptima de transmisión con constelaciones discretas es difícil en general y, por ello, tomaremos una aproximación pragmática consistente en utilizar las direcciones espaciales correspondientes a la matriz de covarianza que permite obtener la capacidad (con señales Gaussianas). Para constelaciones discretas y canales paralelos independientes existen varios algoritmos de carga adaptativa de bits y potencia (bit and power loading) clásicos, que no son directamente aplicables al sistema bajo estudio. Si deseamos garantizar la calidad de servicio, se requiere una cierta probabilidad de error promedio (BER: bit error rate) en el extremo receptor. A diferentes tipos de receptor corresponden relaciones distintas entre la BER y la relación señal a interferencia (SINR: signal to interference plus noise ratio). Con la realimentación

de los parámetros de la distribución de SINR al transmisor es posible resolver dos problemas duales de optimización en sistemas MIMO de usuario único con canal con correlación en el extremo transmisor: maximización de la tasa binaria con una restricción de potencia y minimización de la potencia transmitida con una restricción de la tasa binaria objetivo.

El objetivo de esta Tesis es diseñar esquemas prácticos de carga adaptativa de bits y potencia para sistemas MIMO, que puedan operar sobre la base de conocimiento estadístico del canal en el transmisor (CDIT) únicamente. Por motivos prácticos, consideramos tres tipos de receptores típicos: receptor de forzado a cero (ZF), receptor de mínimo error cuadrático medio (MMSE), y receptor ZF con cancelación sucesiva de interferencias (ZF-SIC). Para estos tres receptores se abordan los siguientes problemas:

- Maximizar la tasa binaria con constelaciones discretas, usando las direcciones espaciales de transmisión dictadas por la matriz de covarianza que alcanza la capacidad, garantizando una cierta probabilidad de error promedio y con la restricción de la potencia total a transmitir.
- Minimizar la potencia de transmisión con constelaciones discretas, usando las direcciones espaciales de transmisión dictadas por la matriz de covarianza que alcanza la capacidad, garantizando una cierta probabilidad de error promedio y satisfaciendo un requisito de tasa binaria.
- Obtener y comparar la ganancia de potencia de los tres tipos de receptores mencionados en relación con una transmisión sin optimizar.

Para abordar estos problemas, es esencial establecer una relación entre la probabilidad de error promedio de cada uno de los receptores y la potencia asignada en el transmisor a cada flujo de datos MIMO, bajo la premisa de conocimiento CDIT. A partir de la distribución Gamma o Gamma generalizada de la SINR, se obtienen aproximaciones para la probabilidad de error promedio mediante integración.

Para un sistema MIMO de usuario único con canal correlado, los métodos matemáticos empleados para resolver los problemas de optimización son: algoritmo “Levin-Campello” para ZF, búsqueda exhaustiva con restricciones adicionales para MMSE, y búsqueda en árbol con tasa binaria acotada para ZF-SIC. La precisión de las aproximaciones y las prestaciones de los algoritmos desarrollados se evalúan mediante simulación de Monte Carlo. El entorno de transmisión viene dado por un canal MIMO con desvanecimiento tipo Rayleigh, plano en frecuencia y con correlación en el extremo transmisor.

La estructura de la Tesis es la siguiente. En el primer capítulo se presenta una introducción y se describe el contenido de la Tesis. A continuación, tras una descripción del procesado básico que tiene lugar en el transmisor, el capítulo II presenta las características del canal MIMO. Además, se describen el modelo del sistema y los tres receptores que se van a tratar: ZF, MMSE y ZF-SIC.

El capítulo III comienza con una revisión de la capacidad, lo que conduce a la denominada distribución de "waterfilling" en sistemas MIMO. Los dos problemas de optimización duales, maximización de la tasa binaria y minimización de la potencia, se definen para mejorar las prestaciones mediante procesado en el extremo transmisor. En algunos sistemas prácticos, el algoritmo de Levin-Campello constituye una solución para estos problemas de optimización duales con constelaciones discretas, por lo que se presenta una revisión del mismo. Con el fin de comprender mejor el problema de minimización de potencia para constelaciones discretas, considerando la pérdida de información mutua debida a una modulación concreta, se revisa a continuación la distribución conocida como "mercury/waterfilling".

En el capítulo IV, se estima la probabilidad de error promedio para un receptor ZF utilizando la distribución de la SINR, que corresponde a una función de densidad de probabilidad Gama, y se encuentra una aproximación para relación señal a ruido alta que resulta muy precisa. A partir de la relación entre la BER y la potencia requerida para diferentes constelaciones, los dos problemas duales se pueden resolver mediante un algoritmo tipo "Levin-Campello", dado que los flujos de datos son independientes. Para facilitar el uso de este algoritmo, se mejoran las aproximaciones de la BER, obteniendo cómodas ecuaciones en forma compacta.

En el capítulo V, se estima la probabilidad de error promedio para un receptor MMSE, también utilizando la distribución de la SINR, que ahora corresponde a una Gama o Gama generalizada. Se proponen y comparan varias expresiones en forma cerrada.

En el capítulo VI, a partir de la relación entre la BER y la potencia requerida para diversas constelaciones, se resuelven los dos problemas duales mediante búsqueda exhaustiva, dado que en este caso los flujos de datos están acoplados debido a que el receptor MMSE no cancela la interferencia. Para reducir la carga computacional se añaden algunas restricciones. Para los dos problemas duales, el número total de bits que se pueden transmitir cuando el receptor es MMSE no puede ser menor que el correspondiente a un receptor ZF. Así pues, el punto de partida de la búsqueda es la solución para el receptor ZF y la búsqueda progresa desde ese punto hacia mayores tasas mientras lo permiten las restricciones. La probabilidad de error tras el receptor MMSE se puede aproximar a través de la MGF (moment generating function) que incluye los tres primeros momentos de la SINR. Comparando dos antenas cualesquiera se demuestra que si hay que añadir un cierto incremento de bits en una de ellas, la antena con mejor canal es la que requiere menor incremento de potencia total para transmitirlo. Así, se puede concluir que los mejores canales deben llevar mayor número de bits y esto permite añadir una restricción adicional a la búsqueda, que conlleva, de este modo, una carga computacional razonable.

En el capítulo VII, se obtiene una aproximación cerrada para la BER de un receptor ZF-SIC considerando la propagación de errores, a partir del teorema de la probabilidad total. Dado que el orden del proceso de decodificación tiene un impacto importante en las prestaciones del sistema con este receptor, se propone un precodificador que determina el orden que minimiza la potencia total. Por otra parte, se presentan unas cotas de las tasas binarias posibles con ZF-SIC, considerando las de ZF y ZF-PSIC (perfect SIC) para los dos problemas duales de optimización. Haciendo uso de estas cotas, se emplea una búsqueda en árbol para agilizar la convergencia.

En el último capítulo, los resultados obtenidos para los diferentes receptores se comparan, concluyendo la Tesis con una descripción de las líneas de trabajo futuras.

Acknowledgements

My deepest gratitude goes first and foremost to Professor Ana García Armada, my supervisor, for her constant encouragement and guidance. She has walked me through all the stages of the writing of this thesis. Without her consistent and illuminating instruction, this thesis could not have reached its present form. Second, I would like to express my heartfelt gratitude to Professor Angel Lozano, who revises the articles related with this thesis patiently and also gives me a lot of sparkling advices. I am also greatly indebted to the professors and teachers at the Department (Departamento de teoría de la señal y comunicaciones) and CEAES, who have instructed and helped me a lot in the past years. Last my thanks would go to my beloved family for their loving considerations and great confidence in me all through these years. I also owe my sincere gratitude to my friends and my fellow classmates who gave me their help and time in listening to me and helping me work out my problems during the difficult course of the thesis.

Contents

List of Figures

List of Tables

Glossary

AWGN	Additive white Gaussian noise
BER	Bit error rate
CDIT	Channel distribution information at the transmitter
CSIR	Channel state information at the receiver
DMT	Discrete multitone
HSPA	High speed packet access
MAI	Multiple access interference
MIMO	Multiple-input multiple-output
MMSE	Minimum mean squared error
MSI	Multistream interference
MW	Mercury/Waterfilling
QAM	Quadrature amplitude modulation
QPSK	Quadrature phase shift keying
SINR	Signal-to-interference-plus-noise ratio
SISO	Single-input single-output
SM	Spatial multiplexing
SNR	Signal-to-noise ratio
SVD	Singular value decomposition
WiFi	Wireless fidelity
WiMax	Worldwide interoperability for microwave access
ZF	Zero-forcing
ZF-PSIC	Zero-forcing with Perfect successive interference cancellation
ZF-SIC	Zero-forcing with successive interference cancellation
ZMCSCG	Zero mean circularly symmetric complex Gaussian
3GPP	3rd generation partnership project

1

Introduction

With the rapid development of wireless telecommunication systems, there are more requirements for higher quality of service and data transmission rate. The applications with mobility, flexible usage, convenient maintenance and flexibility are demanded more and more. Facing the increasing demand of data services, especially multimedia services, the limited bandwidth, the interference and multi-path propagation seriously restrict further development.

In wireless telecommunication systems, multiple-input multiple-output (MIMO) denotes the use of multiple antennas at both the transmitter and receiver to improve the communication performance. As a smart antenna technology, MIMO is quickly becoming a central ingredient in the design of wireless systems. MIMO techniques can provide a significant improvement in the system capacity and spectral efficiency (more bits per second per hertz of bandwidth). They offer significant increases in data throughput and link range (through the use of diversity) without additional bandwidth or transmit power. Because of these properties, MIMO is an important part of modern wireless communication standards such as IEEE 802.11n (WiFi), WiMAX, HSPA+, and 3GPP Long Term Evolution towards the 4th generation of mobile communications.

The use of bit and power optimization was first introduced in wire-line telecommunication systems and afterwards extended to wireless communications. Subsequently it was extended to MIMO systems, and it is widely used in several current communication standards. In MIMO communication, the adaptation of the modulation and coding at the transmitter side according to the channel characteristics allows reducing the transmission power and/or enhancing the data rates [Lozano et al. 2006a]. However, it is not always feasible to have instantaneous knowledge of the channel at the transmitter. This Thesis focuses on the case that the receiver has (perfect) instantaneous channel state information (CSIR) but the transmitter has only access to its distribution (CDIT). This is a practical case that applies, particularly, to situations where the channel varies rapidly. Under CDIT, the input cannot be adapted to the instantaneous state of the channel and thus SVD (singular value decomposition) cannot be used to diagonalize the channel.

On the other hand, achieving capacity requires a complex Gaussian input vector with a covariance that depends on the channel distribution [Tulino et al. 2006]. In practice, however, discrete constellations are used instead of Gaussian signals. Determining the optimum signalling strategy with discrete constellations is difficult in general, and thus a pragmatic approach is taken here, namely using the spatial signalling directions indicated by the capacity-achieving covariance.

Several classical practical bit and power loading algorithms [Chow et al. 1995; Campello et al. 1999; Cioffi; Lozano et al. 2006b; Hong et al. 2009] are available for parallel-channel settings. However, in MIMO with CDIT it is not always feasible to have parallel-channel settings as we will see. To guarantee the quality of service, a certain average bit error probability (BER) is required at the receiver side. Different types of receiver correspond to different relationships between the BER and the signal-to-interference-plus-noise ratio (SINR) [P. Li et al. 2006; Armada et al. 2009; Hong et al. 2010]. With the feedback of the parameters of the SINR distribution, two optimization problems for single user MIMO systems can be solved at the transmitter side [Cioffi; Armada et al. 2009], namely rate maximization with a total power constraint and power minimization with a target bit rate.

1.1 Objectives

The goal of this Thesis is to devise practical bit and power loading schemes for MIMO that can operate on the basis of CDIT only. For practical reasons, three typical receivers are considered, namely zero-forcing (ZF), minimum mean squared error (MMSE) and zero-forcing with successive interference cancellation (ZF-SIC) [Paulraj et al. 2003]. The following problems are addressed:

- Maximization of the bit rates with discrete constellations, using the transmit directions given by the capacity achieving input covariance, at a certain average bit error probability (BER) and a constraint of total transmit power.
- Minimization of the transmit power with discrete constellations, using the transmit directions given by the capacity achieving input covariance, at a certain average bit error probability (BER) and a target transmit bit rate.
- Evaluation and comparison of the power gain when optimizing the transmission with the three mentioned types of receivers relative to a non-optimized transmission.

In order to address these problems, in this work it is essential to establish a relationship between the average BER corresponding to each of the three receivers and the powers allocated at the transmitter under the premise of CDIT [P. Li et al. 2006; Armada et al. 2009; Hong et al. 2010].

1.2 Thesis Organization and Contributions

1.2.1 Methodology

Using a Gamma or a generalized Gamma distribution of the SINR, BER approximations can be obtained through integration [P. Li et al. 2006; Armada et al. 2009; Hong et al. 2010].

For a single user MIMO system with correlated channel, to accomplish the optimization process, the mathematical methods used are a Levin-Campello algorithm for ZF, exhaustive search with additional constraints for MMSE and tree search with bit rate boundary for ZF-SIC [P. Li et al. 2006; Armada et al. 2009; Hong et al. 2010].

The accuracy of the developed expressions and the gain obtained through transmit optimization with the proposed algorithms are evaluated using Monte Carlo simulations.

1.2.2 Organization

The Thesis is focused on the design and optimization of the transmitter in MIMO communications. The transmission environment is specified to be a Rayleigh flat-fading channel with correlation at the transmitter side. An introduction is presented at the first chapter, addressing the structure of this Thesis.

Following a description of the basic process which takes place at the transmitter side, the second chapter presents the characteristics of the MIMO channel. Moreover, the system models of three typical receivers are described, including ZF, MMSE and ZF-SIC.

The third chapter starts with a review of capacity, and leads to the so-called waterfilling distribution in MIMO systems. The dual optimization problems, bit rate maximization and power minimization, are defined to enhance the performance with processing at the transmitter side [Cioffi]. In some practical systems, Levin-Campello algorithm develops a solution for the dual optimization problems for discrete constellations [Campello et al. 99], so it is briefly reviewed. In order to further understand the power minimization problem for discrete constellations, considering the loss of mutual information due to a given modulation, Mercury/Waterfilling is also reviewed [Lozano et al. 2006b].

In chapter IV, the BER of a ZF receiver is computed by using its SINR distribution, which is a Gamma distribution, and it is also accurately approximated at the high SNR regime [Armada et al. 2009]. From the relationship between BER and power for different constellations and ZF receiver, the two dual problems can be solved by a Levin-Campello algorithm, as the streams are independent with each other [Armada et al. 2009]. To facilitate using the Levin-Campello algorithm, BER approximations are improved to be established in convenient closed-form equations [Armada et al. 2009].

In chapter V, the BER of an MMSE receiver is also computed by using its SINR distribution, which can be modelled as a Gamma distribution or a generalized Gamma distribution [P. Li et al. 2006], and some accurate closed-formed approximations are proposed and compared [Hong et al. 2010].

In chapter VI, from the relationship between BER and power for different constellations, the two dual problems can be solved by exhaustive search, as the streams are coupled with each other in the case of the MMSE receiver. In order to reduce the computational complexity, some additional constrains are necessary to be added. For the two dual optimization problems, the total number of transmitted bits with an MMSE receiver cannot be less than with a ZF receiver. Therefore, the starting point for the search is always the solution derived for ZF receivers, and the search progresses from that point towards higher loads until the constraints set.

The BER of the MMSE receiver can be approximated by the moment generating function (MGF), which includes the first three moments of SINR. Comparing two randomly selected antennas, when an increment of the number of bits is added to one of them, the antenna with better channel condition spend less total power to accomplish the transmission. Thus, it can be concluded that the better channel can be loaded with more bits. With this additional constraint, the computational complexity of the exhaustive search can be reduced even more reasonably.

In chapter VII, taking into account the error propagation, a closed-form BER approximation is derived for the ZF-SIC receiver by using the total probability theorem. Moreover, since the ordering of the decoding process can dramatically impact the system performance when using this receiver, a method is proposed to determine the decoder ordering to minimize the total power. Moreover, a boundary of possible bit rates for ZF-SIC is presented, considering the bit rate of ZF and ZF-PSIC (perfect SIC), for the two dual optimization problems.To make the search converge more efficiently, a tree search is implemented making use of this boundary.

In the final chapter, the results obtained for the different receivers are compared to conclude the core of this Thesis. Then, some future work is outlined.

1.2.3 Contributions

For a single user MIMO system, the BER of three typical receivers, ZF, MMSE and ZF-SIC, is estimated and convenient closed-form approximations are provided, by using the statistical information of the channel matrix with correlation at the transmitter side.

By utilizing these BER approximations, two dual optimization problems, bit maximization and power minimization, are solved for the practical case of statistical channel knowledge at the transmitter side and discrete constellations.

2

MIMO system and Receivers

This chapter focuses on MIMO systems and provides an overview of MIMO receivers for spatial multiplexing (SM) schemes.

2.1 System model of a MIMO system

In a MIMO system several antennas are used at the transmitter and receiver sides. Due to the propagation channel, the information sent from each of the transmit antennas will be present at the input of each receive antenna, causing the so called multistream interference (MSI). The presence of MSI is a key problem that should be solved at the MIMO receiver side, as the multiple transmit streams interfere with each other.

Fig. 2.1 illustrates the configuration of a general MIMO system and the use of a linear receiver for separating the transmitted data streams.

Let n_T and n_R denote the number of transmit and receive antennas, respectively, with $n_T \leq n_R$. The $n_T \times 1$ transmit vector is denoted by $\mathbf{x} = \mathbf{V}\mathbf{P}^{\mathbf{1/2}}\mathbf{s}$, where $\mathbf{s} = [\mathrm{s}_1, \cdots, \mathrm{s}_{n_T}]$ is a vector of unit-variance M-QAM symbols. The unitary matrix $\mathbf{V}$ represents a linear precoder whose columns define the signalling directions. In turn, $\mathbf{P} = \mathrm{diag}\left[p_1,\ \cdots,\ p_i,\ \cdots,\ p_{n_T}\right]$ with $p_i \geq 0$ the power allocated to the ith signaling vector, normalized such that $\mathrm{E}\left\{\mathrm{Tr}\left[\mathbf{x}^H\mathbf{x}\right]\right\} = n_T \geq \mathrm{Tr}\left[\mathbf{P}\right]$. Then, the $n_R \times 1$ received vector is

$$\mathbf{y} = \sqrt{\frac{\gamma}{n_T}}\mathbf{H}_c\mathbf{V}\mathbf{P}^{1/2}\mathbf{s} + \mathbf{n}, \tag{2.1}$$

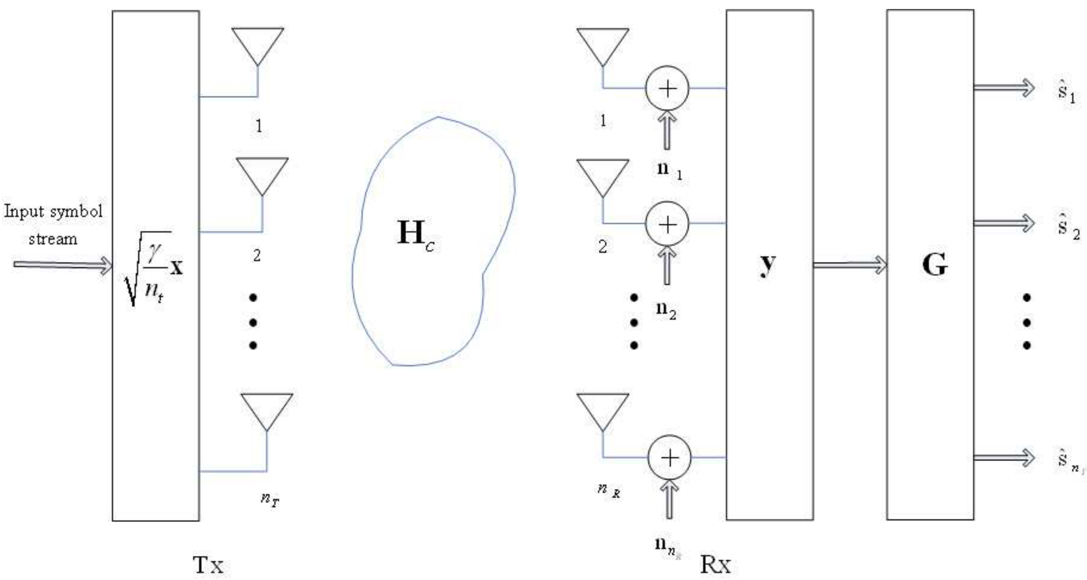

Figure 2.1: Illustration - use of a linear receiver for separating the transmitted data streams over a MIMO channel.

where $\mathbf{n}$ is a vector with independent zero-mean unit-variance complex Gaussian noise samples, $\gamma = \frac{E_s}{N_o}$ is the average signal-to-noise ratio (SNR) per receive antenna [Paulraj et al. 2003] , and $\mathbf{H}_c$ is the matrix representing the MIMO wireless channel. Allowing for arbitrary correlations among the transmit antennas, $\mathbf{H}_c = \mathbf{H}_w\mathbf{R}^{1/2}$ where the $(i,\ j)$th entry of $\mathbf{R}$ equals the correlation between the ith and jth transmit antennas, normalized such that $\mathrm{Tr}\,[\mathbf{R}] = n_T$, while $\mathbf{H}_w$ contains independent zero-mean unit-variance complex Gaussian entries. The correlations among the receiver antennas are not considered in this work.

Defining an effective channel matrix

$$\begin{aligned} \mathbf{H} &= \sqrt{\tfrac{\gamma}{n_T}}\mathbf{H}_c\mathbf{V}\mathbf{P}^{1/2} \\ &= \sqrt{\tfrac{\gamma}{n_T}}\mathbf{H}_w\mathbf{R}^{1/2}\mathbf{V}\mathbf{P}^{1/2} \end{aligned} . \tag{2.2}$$

The received signal can be simply written

$$\mathbf{y} = \mathbf{H}\mathbf{s} + \mathbf{n}. \tag{2.3}$$

For a rather general class of channel models, the precoder $\mathbf{V}$ is capacity-achieving when its columns coincide with the eigenvectors of $\mathbf{R}$ [Tulino et al. 2006]. This same precoder is also shown in [Scaglione et al. 1999] to be optimal, from an SINR standpoint. Thus the precoder $\mathbf{V}$ is found from

$$\mathbf{R} = \mathbf{V}^H \Lambda \mathbf{V}, \tag{2.4}$$

where Λ is the diagonal matrix of eigenvalues of $\mathbf{R}$.

2.2 MIMO receivers

For the purpose of reducing the decoding complexity of the ML (maximum likelihood) receiver, several receivers can separate the transmitted data streams, and then independently decode each stream. ZF, MMSE and ZF-SIC receivers are discussed below, to cancel or compensate MSI.

2.2.1 ZF receiver

The ZF matrix filter that separates the received signal into its component transmitted streams is given by

$$\mathbf{G}_{\mathrm{ZF}} = \mathbf{H}^{\dagger}, \tag{2.5}$$

where $\mathbf{H}^{\dagger}$ is the pseudo inverse of matrix $\mathbf{H}$ [Armada et al. 2009] [S. Verdú 98].

The output of a linear ZF receiver is

$$\mathbf{z}_{\mathrm{ZF}} = \mathbf{G}_{\mathrm{ZF}}\mathbf{y} = \mathbf{H}^{\dagger}\mathbf{y} = \mathbf{s} + \widehat{\mathbf{n}}. \tag{2.6}$$

The ZF receiver decouples the composite channel matrix into n_T parallel scalar channels with additive noise enhanced by $\mathbf{G}_{\mathrm{ZF}}$. Because each scalar channel is decoded independently ignoring noise correlation, ZF is sub-optimal which results in significant performance degradation, but with a very reduced complexity.

From (2.6), $\mathrm{z}_i = \mathrm{s}_i + \widehat{\mathrm{n}}_i$ is the ith element of $\mathbf{z}_{\mathrm{ZF}}$, so the detected signal $\hat{\mathrm{s}}_i$ can be obtained from a decision made on z_i.

The SINR corresponding to the reception of the signal of the ith transmit antenna can be expressed as

$$\mathrm{SINR}_{\mathrm{ZF}_i} = \frac{1}{\left[\left(\mathbf{H}^H\mathbf{H}\right)^{\dagger}\right]_{i,i}}. \tag{2.7}$$

where $[\cdot]_{i,i}$ means the ith diagonal element and $\mathbf{H}^H$ is the Hermitian transpose matrix of $\mathbf{H}$ [P. Li et al. 2006] [Armada et al. 2009].

Assuming a channel without correlation, it has been shown in [Winters et al. 1994][Gore et al. 2002] that the SINR on each of the received streams is distributed as

$$f(t) = \frac{n_T}{\gamma (n_R - n_T)!} e^{-\frac{n_T}{\gamma} t} \left(\frac{n_t}{\gamma} t \right)^{n_R - n_T} u(t). \tag{2.8}$$

So $\mathrm{SINR}_{\mathrm{ZF}_i}$ is a Chi-square random variable with $2(n_R - n_T + 1)$ degrees of freedom. Moreover, $\mathrm{SINR}_{\mathrm{ZF}_i}$ can also be characterized as a Gamma distribution [P. Li et al. 2006], with a higher accuracy as is shown in [P. Li et al. 2006].

2.2.2 MMSE receiver

At the expense of noise enhancement, the ZF receiver completely eliminates MSI. To minimize the total error, MMSE receiver can balance MSI mitigation with noise enhancement [Paulraj et al. 2003]. The MMSE receive filter is [Hong et al. 2010]

$$\mathrm{G}_{\mathrm{MMSE}} = \operatorname*{argmin}_{G} \mathrm{E} \left\{ \|\mathbf{G}\mathbf{y} - \mathbf{s}\|_F^2 \right\}. \tag{2.9}$$

Utilizing the orthogonality principle,

$$\mathrm{E}\left\{ (\mathbf{G}\mathbf{y} - \mathbf{s}) \mathbf{y}^H \right\} = 0, \tag{2.10}$$

$$\mathrm{G}_{\mathrm{MMSE}} = \left(\mathbf{I} + \mathbf{H}^H \mathbf{H} \right)^{\dagger} \mathbf{H}^H. \tag{2.11}$$

And the output of a linear MMSE receiver is

$$\mathbf{z}_{\mathrm{MMSE}} = \mathbf{G}_{\mathrm{MMSE}} \mathbf{y} = \left(\mathbf{I} + \mathbf{H}^H \mathbf{H} \right)^{\dagger} \mathbf{H}^H \mathbf{y}. \tag{2.12}$$

The SINR on the ith decoded stream can be shown to be

$$\mathrm{SINR}_{\mathrm{MMSE}_i} = \frac{1}{\left[(\mathbf{H}^H \mathbf{H} + \mathbf{I})^{\dagger} \right]_{i,i}} - 1. \tag{2.13}$$

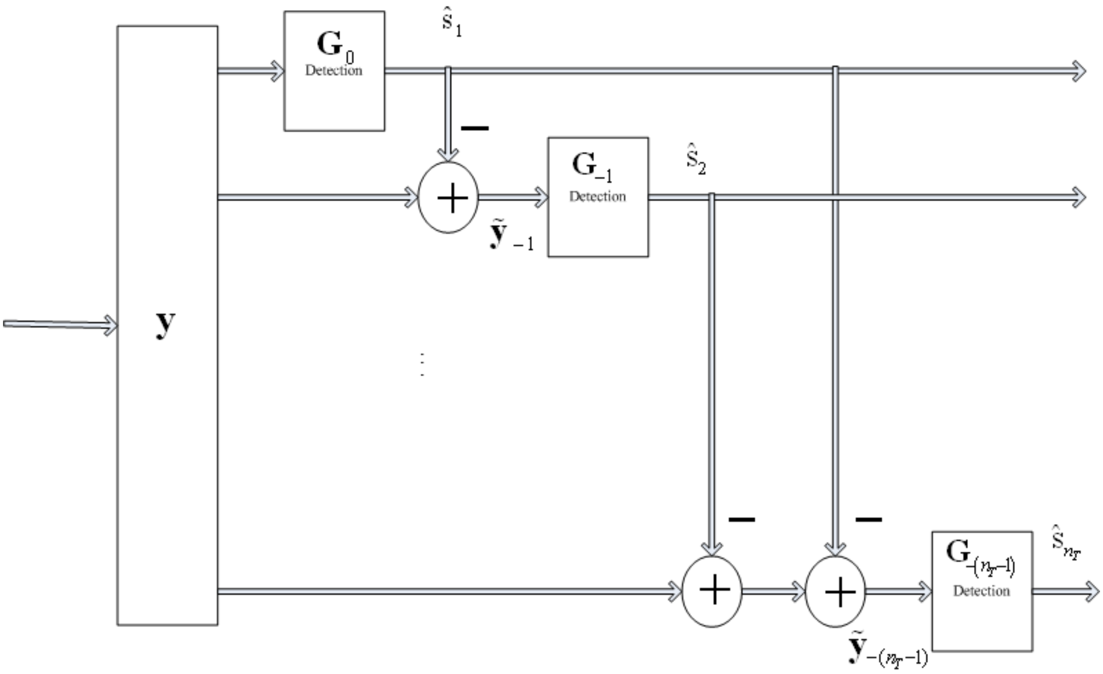

Figure 2.2: Structure - ZF-SIC receiver.

2.2.3 ZF-SIC receiver

Fig. 2.2 shows the structure of a ZF-SIC receiver.

For a ZF-SIC receiver [Paulraj 2003], there are two cases that should be analyzed respectively. First we consider the process of detection for the first stage $i = 1$, and afterwards we consider the case for any stage $i > 1$.

From Fig. 2.2 and (2.6), as $\mathbf{G}_0 = \mathbf{G}_{\mathrm{ZF}}$, $\tilde{\mathrm{z}}_1 = \mathrm{s}_1 + \widehat{\mathrm{n}}_1$ is the first element of $\mathbf{z}_{\mathrm{ZF}}$. So the detected signal $\hat{\mathrm{s}}_1$ of the first stage ($i = 1$) can be obtained from a decision made on $\tilde{\mathrm{z}}_1$.

Observing Fig. 2.2, the ith detected signal $\hat{\mathrm{s}}_i,\ i = 2, \cdots n_T$ of the ith stage can be obtained by the following steps.

Denote $\mathbf{h}_{i-1}$ as the $(i-1)$th column of $\mathbf{H}$ and $\mathbf{H}_{-(i-1)}$ is matrix $\mathbf{H}$ with the columns from first to $(i-1)$th removed.

After cancelling the interference, the ith received signal becomes

$$\tilde{\mathbf{y}}_{-(i-1)} = \mathbf{y} - \mathbf{h}_1\hat{\mathrm{s}}_1 - \cdots - \mathbf{h}_{i-1}\hat{\mathrm{s}}_{i-1}. \tag{2.14}$$

The output of the ith received signal is

$$\begin{aligned}
\mathbf{z}_i &= \mathbf{G}_{-(i-1)}\tilde{\mathbf{y}}_{-(i-1)} \\
&= \mathbf{H}^{\dagger}_{-(i-1)}\tilde{\mathbf{y}}_{-(i-1)} \\
&= \mathbf{H}^{\dagger}_{-(i-1)}\left(\left(\mathrm{s}_1 - \hat{\mathrm{s}}_1\right)\mathbf{h}_1 + \cdots + \left(\mathrm{s}_{i-1} - \hat{\mathrm{s}}_{i-1}\right)\mathbf{h}_{i-1} + \mathrm{n}_i\right) + \mathrm{s}_i
\end{aligned} \quad . \tag{2.15}$$

Denote $\tilde{\mathrm{z}}_i$ as the ith element of the vector $\mathbf{z}_i$. After the detection, the final output signal $\hat{\mathrm{s}}_i$ will be obtained from a decision made on $\tilde{\mathrm{z}}_i$.

3

Capacity and Bit loading

3.1 Capacity of the frequency-flat MIMO channel

The channel capacity is the maximum error-free data rate that a channel can support. At the beginning of this chapter, the fundamental limit on the spectral efficiency that can be supported reliably in MIMO wireless channels is shown. Claude Shannon firstly derived the channel capacity for additive white Gaussian noise (AWGN) channels [Shannon 1948]. As MIMO channels exhibit fading and encompass a spatial dimension, their capacity has been focused on the recent years.

Assuming perfect channel knowledge at the receiver side, there are two different cases for frequency-flat fading channels that will be discussed, namely channel information unknown or channel information known to the transmitter.

Assuming that the channel has a bandwidth of 1 Hz and is frequency-flat over the whole bandwidth, the input-output relation for the MIMO channel was derived in Chapter II. The capacity of the MIMO channel is defined as [Froschini 1996] [Telatar 1999]

$$C = \max_{f(\mathbf{s})} I\left\{\mathbf{s};\mathbf{y}\right\}, \tag{3.1}$$

where $f(s)$ is the probability distribution of the input vector $\mathbf{s}$ and $I\left\{\mathbf{s};\mathbf{y}\right\}$ is the mutual information between $\mathbf{s}$ and $\mathbf{y}$.

Note that

$$I\left\{\mathbf{s};\mathbf{y}\right\} = H(\mathbf{y}) - H(\mathbf{y}\,|\mathbf{s}), \tag{3.2}$$

where $H(\mathbf{y})$ is the differential entropy of the vector $\mathbf{y}$, and $H(\mathbf{y}\,|\mathbf{s})$ is the conditional differential entropy of the vector $\mathbf{y}$, when given knowledge of the vector $\mathbf{s}$. As the vectors $\mathbf{s}$ and $\mathbf{n}$ are independent, $H(\mathbf{y}\,|\mathbf{s}) = H(\mathbf{n})$, (3.2) can be simplified to

$$I\{\mathbf{s};\mathbf{y}\} = H(\mathbf{y}) - H(\mathbf{n})\,. \tag{3.3}$$

If $H(\mathbf{y})$ is maximized, the maximization of mutual information $I\{\mathbf{s};\mathbf{y}\}$ can also be achieved. The covariance matrix of $\mathbf{y}$, denoted as $\mathbf{R_{yy}} = \mathrm{E}\left\{\mathbf{y}\mathbf{y}^H\right\}$ when $\mathbf{H} = \sqrt{\frac{\gamma}{n_T}}\mathbf{H_w}\mathbf{R}^{1/2}\mathbf{P}^{1/2}$, satisfies

$$\mathbf{R_{yy}} = \mathbf{H}\mathbf{R_{ss}}\mathbf{H}^H + \mathbf{I}, \tag{3.4}$$

where $\mathbf{R_{ss}} = \mathrm{E}\left\{\mathbf{s}\mathbf{s}^H\right\}$ is the covariance matrix of $\mathbf{s}$.

The differential entropy $H(\mathbf{y})$ can be maximized, when $\mathbf{y}$ is a zero mean circularly symmetric complex Gaussian (ZMCSCG) vector [Neeser and Massey 1993]. So $\mathbf{s}$ should be a ZMCSCG vector with the distribution characterized by $\mathbf{R_{ss}}$.

Therefore, $I\{\mathbf{s};\mathbf{y}\}$ can be reduced to [Telatar 1999]

$$I\{\mathbf{s};\mathbf{y}\} = \log_2 \det\left(\mathbf{I} + \mathbf{H}\mathbf{R_{ss}}\mathbf{H}^H\right) \quad \text{bits/s/Hz}. \tag{3.5}$$

Following (3.1), the capacity of the MIMO channel is given by

$$C = \max_{\mathrm{Tr}(\mathbf{R_{ss}})=n_T} \left\{\log_2 \det\left(\mathbf{I} + \mathbf{H}\mathbf{R_{ss}}\mathbf{H}^H\right)\right\} \quad \text{bits/s/Hz}. \tag{3.6}$$

Equation (3.6) is referred to the error-free spectral efficiency, or the data rate per unit bandwidth that can be sustained reliably over the MIMO link. From here, the units bits/s/Hz will be dropped to simplify the expressions of capacity.

3.2 Capacity with channel unknown to the transmitter

If the channel is unknown to the transmitter, the vector $\mathbf{s}$ can be chosen to be statistically non-preferential $\mathbf{R_{ss}} = \mathbf{I}$ and $\mathbf{P} = \mathbf{I}$. Thus, the signals are independent and equally-powered at the transmit antennas. In the absence of channel knowledge at the transmitter side, the capacity is given by

$$C = \log_2 \det\left(\mathbf{I} + \mathbf{H}\mathbf{H}^H\right). \tag{3.7}$$

Using the eigenvalue decomposition of $\mathbf{H}\mathbf{H}^H = \mathbf{Q}\Lambda\mathbf{Q}^H$, the capacity of the MIMO channel can be expressed as

$$C = \log_2 \det\left(\mathbf{I} + \frac{\gamma}{n_T}\mathbf{Q}\Lambda\mathbf{Q}^H\right). \tag{3.8}$$

Using $\det(\mathbf{I}_m + \mathbf{AB}) = \det(\mathbf{I}_n + \mathbf{BA})$ with $\mathbf{A}$ $(m \times n)$ and $\mathbf{B}$ $(n \times m)$, (3.8) can be simplified to be

$$C = \log_2 \det\left(\mathbf{I} + \frac{\gamma}{n_T}\mathbf{P}\Lambda\right). \tag{3.9}$$

Denote r as the rank of the channel and $\lambda_i,\ i = 1, 2, \cdots, r$ are the positive eigenvalues of $\mathbf{H}\mathbf{H}^H$. Then (3.9) can be expressed equivalently

$$C = \sum_{i=1}^{r} \log_2\left(1 + \frac{\gamma}{n_T}\lambda_i\right). \tag{3.10}$$

This means that the capacity of the MIMO channel is the sum of the capacities of r single-input single-output (SISO) channels, each having power gain λ_i with the SNR γ.

Hence, in the absence of channel knowledge, multiple scalar spatial data modes between transmitter and receiver exist and equal energy is allocated to each spatial data stream.

3.3 Capacity with channel known to the transmitter

The capacity with channel known at the transmitter side can be realized via the feedback from the receiver or through the reciprocity principle in a time-duplex system.

The individual channel modes can be accessed through precoder and decoder processing at the transmitter side and the receiver side respectively [Froschini 1996; Telatar 1999; Lozano and Papadias 2002].

Equation (2.1) can be explicitly decomposed into r parallel SISO channels satisfying

$$y_i = \sqrt{\frac{\gamma p_i \lambda_i}{n_T}}s_i + n_i. \tag{3.11}$$

The capacity of the MIMO channel is the summation of these individual parallel SISO channel capacities and can be given by

$$C = \sum_{r=1}^{r} \log_2 \left(1 + \frac{\gamma}{n_T} p_i \lambda_i\right). \tag{3.12}$$

Since the special streams can be accessed at the transmitter side, the mutual information can be maximized by allocating variable energy across these streams. So the maximization of the mutual information becomes

$$C = \max_{\sum_{i=1}^{r} p_i = n_T} \sum_{r=1}^{r} \log_2 \left(1 + \frac{\gamma}{n_T} p_i \lambda_i\right). \tag{3.13}$$

3.4 Bit and power loading

3.4.1 Multi-channel modulation and SNR gap

Bit and power loading were first described to optimize a set of non-overlapping narrow input signals (multi-tone), transmitting via different types of fading channels. In this work, the input signals are specified to be Quadrature Amplitude Modulation (QAM). Multi-tone transmission uses two or more coordinated passband (QAM or QAM-like) signals to carry a single bit stream over a communication channel. The passband signals are independently demodulated in the receiver and then re-multiplexed into the original bit stream. Multi-channel modulation methods are generally considered to be the best for data transmission channels with moderate or severe intersymbol interference.

Moreover, for spatial multiplexing, multi-channel indicates that a set of input signals are independently transmitted by a set of antennas, and received by another set of antennas individually. Shannon's 1948 [Shannon 1948] constructed capacity bounds for transmission on an AWGN channel with linear ISI, effectively using multi-tone modulation. The 1958 Collins Kineplex MODEM appeared with the first uses of multi-channel modulation [Mosier and Clabaugh 1958]. Over a 30-year period, a bunch of increasingly successful attempts at the use of multi-channel modulation occurred, especially the technique with digitally implementable solutions under the name "Discrete Multitone" (DMT) emanated from Stanford University [Chow 1995].

The heuristic motivation for multitone modulation is that if the bandwidth f each of the "tones" is sufficiently narrow, then no ISI occurs on any subchannel. The individual passband signals may carry data equally or unequally. Generally, multichannel systems can be constructed as having N subchannels (parallel channels), where several pairs of these subchannels have identical gains and can be considered as two-dimensional subchannels (carrying complex symbols).

Examples of parallel channels abound in both wire-line and wireless communication [Lozano et al. 2006b]:

- *Multicarrier transmission.* Signalling takes place over a number of distinct frequency bands, each of which constitutes a parallel channel.

- *Multiantenna communication.* If multiple transmit and receive antennas are employed and the transfer coefficients between them are known, the left singular vectors of the resulting matrix can be used for signaling and the right singular vectors for reception. The outcome is a set of parallel noninteracting channels [Telatar 1999].

- *Power control for fading channels.* When the gain of an individual frequency-flat channel varies over time, it can be seen as a collection of parallel channels where each such channel encompasses a group of symbols over which the fading coefficients are identical [Goldsmith and Varaiya 1997].

- *Dispersive channels.* In linear dispersive channels, a power-preserving orthonormal linear transformation at transmitter and receiver turns the channel into one with parallel branches having uncorrelated noises.

The concept of the so-called "SNR gap", denoted as Γ, is related with parallel channels and loading algorithms.

Denoting the capacity of each of the parallel subchannels as $\bar{c}_i$, on an AWGN channel the maximum data rate or capacity corresponds to unit gap ($\Gamma = 1$)

$$\bar{c}_i = \log_2 \left(1 + \frac{\gamma}{n_T \Gamma} p_i \lambda_i \right) . \tag{3.14}$$

SNR gap is fixed to a value of 0 dB, meaning that a modulation and coding scheme are used that can achieve maximum mutual information.

The bit distribution vector for a set of parallel subchannels that in aggregate carry $\boldsymbol{b}$ total bits of information is given by

$$\boldsymbol{b} = [b_1, \cdots, b_i, \cdots b_{n_T}]\,. \tag{3.15}$$

The sum of the elements in $\boldsymbol{b}$ is clearly equal to the total number of transmitted bits,

$$b_{tot} = \sum_{i=1}^{n_T} b_i. \tag{3.16}$$

More generally, the passband signal(s) with largest channel output signal-to-noise ratio carry a proportionately larger fraction of the digital information,

$$b_i = \log_2 \left(1 + \frac{\gamma}{n_T \Gamma} p_i \lambda_i \right). \tag{3.17}$$

In (3.14) and (3.17), SNR gap Γ is defined as

$$\Gamma = \frac{2^{2\bar{c}_i} - 1}{2^{2b_i} - 1}. \tag{3.18}$$

For a given bit error rate, Γ is the SNR loss due to the actual modulation and coding schemes as compared to the ideal channel capacity. In multitone systems, SNR gap is a key parameter, that depends on several factors, as the coding gain, the shaping gain of modulation and constellation, etc [Cioffi et al. 1995; Armada 2006; Fung and Lim 2007]. A practical way to estimate its value is given in [Forney and Ungerboeck 1998]. If the SNR gap is a value of 12.8 dB, it corresponds to a BER $= 10^{-7}$ for M-QAM modulation [Forney and Ungerboeck 1998].

3.4.2 Waterfilling

The optimal power allocation named as "Waterfilling" was proposed by Cover and Thomas, [Telatar 1999; Cover and Thomas 1991; Chuah et al. 1998; Chuah et al. 2002]. Two dual problems of optimization, including rate maximization and power minimization, can be solved with a Waterfilling distribution.

3.4.2.1 Rate maximization

When the symbol rate $1/T_s$ is fixed, the data rate

$$R = \frac{1}{T_s}\sum_{i=1}^{n_T} b_i \tag{3.19}$$

for a set of parallel subchannels should be maximized with an energy constraint

$$\mathrm{Tr}\left[\mathbf{P}\right] = \sum_{i=1}^{n_T} p_i = n_T. \tag{3.20}$$

When the total power (3.20) is fixed, the sum of the number of bits (3.19) should be maximized, transmitting over a set of parallel subchannels.

When $T_s = 1s$, plugging (3.17) into (3.19) ,

$$R = \sum_{i=1}^{n_T} \log_2\left(1 + \frac{\gamma}{n_T\Gamma} p_i \lambda_i\right). \tag{3.21}$$

(3.21) can be maximized by Lagrangian methods, subject to (3.14), when

$$p_i^{opt} + \frac{n_T\Gamma}{\gamma\lambda_i} = \bar{\mu}, \quad i = 1, \cdots, r, \tag{3.22}$$

with

$$\sum_{i=1}^{r} p_i^{opt} = n_T, \tag{3.23}$$

and $\bar{\mu}$ is a constant and $(x)_+$ means

$$(x)_+ = \begin{cases} x, & if\ x \geq 0 \\ 0, & if\ x < 0 \end{cases}, \tag{3.24}$$

$\bar{\mu}$ in (3.23) can be calculated by

$$\bar{\mu} = \frac{n_T}{r}\left[1 + \frac{\Gamma}{\gamma}\sum_{i=1}^{r}\frac{1}{\lambda_i}\right]. \tag{3.25}$$

Using the value of $\bar{\mu}$, the power allocated to the ith stream can be calculated as

$$p_i = \left(\bar{\mu} - \frac{n_T\Gamma}{\gamma\lambda_i}\right)_+. \tag{3.26}$$

The optimal Waterfilling power allocation policy is accomplished when power allocated to each stream is non-negative, otherwise this channel is discarded by setting $p_i = 0$. Hence, the capacity of the MIMO channel when the channel is known, utilizing Waterfilling, is greater or equal than the capacity when the channel is unknown to the transmitter.

3.4.2.2 Power minimization

For many transmission systems, variable data rate is not desirable. In this case, the best design will maximize the performance margin at a given fixed data rate. To maximize fixed-rate margin, the designer equivalently minimizes the total energy

$$\mathrm{Tr}\left[\mathbf{P}\right] = \sum_{i=1}^{n_T} p_i \leq n_T, \tag{3.27}$$

subject to

$$R = \sum_{i=1}^{n_T} b_i = \sum_{i=1}^{n_T} \frac{1}{2}\log_2\left(1 + \frac{\gamma}{n_T\Gamma} p_i \lambda_i\right). \tag{3.28}$$

This energy-minimizing form of the loading problem is known in mathematics as "the dual form" of the rate-maximizing formulation.

Thus, the optimal power allocation should satisfy

$$p_i^{opt} = \left(\bar{\mu} - \frac{n_T\Gamma}{\gamma\lambda_i}\right)_+, \quad i = 1, \cdots, r, \tag{3.29}$$

with

$$\sum_{i=1}^{r} p_i^{opt} \leq n_T. \tag{3.30}$$

Using the value of $\bar{\mu}$, the power allocated to the th stream can be calculated by

$$p_i = \left(\bar{\mu} - \frac{n_T\Gamma}{\gamma\lambda_i}\right)_+. \tag{3.31}$$

3.4.2.3 Levin-Campello algorithm

Waterfilling algorithms produce bit distributions that can be made of any real numbers. It can be difficult to realize bit distributions with non-integer values. In practical systems, some alternative loading algorithms [Chow et al. 1995] [Campello et al. 1999] are proposed to realize bit distributions with a finite granularity.

Chow's algorithm [Chow et al. 1995] verifies that an "on/off" energy distribution can exhibit negligible loss with respect to the exact waterfilling shape, where "on" means flat energy distribution in the same used bands as waterfilling and "off" means zero energy distribution where waterfilling would be zero. The reason for the use of "on/off" energy distributions is that practical systems usually have a constraint on the maximum power spectral density along with a total energy/power constraint.

Optimum discrete loading algorithms [Campello et al. 1999] for the computation of bit distributions can be implemented amenably. The information granularity ζ of a multichannel transmission system is the smallest incremental unit of information that can be transmitted. The number of bits on any subchannel is then given by

$$b_i = g_i \zeta, \tag{3.32}$$

where $g_i \geq 0$ is an integer.

Typically, ζ takes values such as 0.25, 0.5, 0.75, 1, or 2 bit(s) with fractional bit constellations. It depends on the available modulation and coding schemes.

Any monotonically increasing relation between transmit symbol energy and the number of bits transmitted on any subchannel that is not a function of other subchannel's energies can be used by discrete loading algorithms [Campello et al. 1999]. This function can be different for each subchannel, and there need not be a constant gap used. In general, the concept of incremental energy is important to discrete loading.

The symbol energy for an integer number of information units (3.32) on each subchannel can be notationally generalized to the energy function

$$p_i\left(b_i\right), \tag{3.33}$$

where the symbol energy's dependence on the number of information units transmitted, b_i, is explicitly shown. The incremental energy to transmit b_i information units on a subchannel is the amount of additional energy required to send the g_ith information unit with respect to the g_{i-1}th information unit (that is, one more unit of ζ). The incremental energy is then

$$\Delta p_i(b_i) = p_i(b_i) - p_i(b_i - \zeta). \tag{3.34}$$

For M-QAM, an energy function with $\zeta = 1$ can be defined via the gap approximation as

$$p_i(b_i) = \frac{2n_T\Gamma}{\gamma\lambda_i}\left(2^{b_i} - 1\right). \tag{3.35}$$

Considering this incremental energy, Levin-Campello algorithm starts with any bit distribution, then it makes it "efficient" and "tight" afterwards, and the result is the optimum discrete bit distribution that solves either the rate maximization or the power minimization problems.

With this algorithm, the subchannel with the minimal incremental energy is selected each time for adding one more bit into subchannels, what is called a "greedy" algorithm.

3.4.2.4 Mercury/Waterfilling

The power distribution that maximizes mutual information for given arbitrary (i.e. not necessarily Gaussian) inputs has been recently unveiled [Lozano et al. 2006b] and it is known as Mercury/Waterfilling (MW). The work in [Lozano et al. 2006b] has been extended to the Multiuser scenario in [Lozano et al. 2008]. Mercury/Waterfilling provides a method for power loading according to a known bit distribution. Some efforts have been initiated to obtain a bit loading algorithm based on Mercury/Waterfilling. For example, [Taouk and Peacock 2006] proposes a statistical power loading and tree-search bit loading algorithm, that works under a given constellation but is not optimal for varying M-QAM modulation. [Matas and Lamarca 2007] introduces the mutual information loss of suboptimum receivers for Waterfilling and Mercury/Waterfilling, according to joint power allocation and bit loading in more general scenarios.

Mercury/Waterfilling is derived from the relation between the mutual information and the nonlinear MMSE of the input signals [Guo et al. 2005] [Lozano et al. 2006b]

$$\frac{d}{d\dot{\rho}_i} I_i(\dot{\rho}_i) = MMSE_i(\dot{\rho}_i). \tag{3.36}$$

where

$$\dot{\rho}_i = \frac{\gamma}{n_T \Gamma} \lambda_i p_i. \tag{3.37}$$

Define

$$\dot{g}_i = \frac{\gamma}{n_T \Gamma} \lambda_i, \tag{3.38}$$

the power allocation p_i^{opt} satisfies [Lozano et al. 2006b]

$$\begin{array}{l} p_i^{opt} = 0, \quad \dot{g}_i \leq \bar{\eta} \\ \dot{g}_i MMSE_i \left(p_i^{opt} \dot{g}_i \right) = \bar{\eta}, \quad \dot{g}_i > \bar{\eta} \end{array}, \tag{3.39}$$

with

$$\frac{1}{n_T} \sum_{i=1}^{n_T} p_i^{opt} = 1. \tag{3.40}$$

Denote the inverse of $MMSE_i(\cdot)$ as $MMSE_i^{-1}(\cdot)$, with domain equal to [0, 1] and $MMSE_i^{-1}(1) = 0$, the policy of the power allocation p_i^{opt} can be implemented explicitly as the following steps.

(a) Find the unique solution of $\bar{\eta}$ from the nonlinear equation

$$\frac{1}{n_T} \sum_{\substack{i=1 \\ \dot{g}_i > \bar{\eta}}}^{n_T} \frac{1}{\dot{g}_i} MMSE_i^{-1} \left(\frac{\bar{\eta}}{\dot{g}_i} \right) = 1. \tag{3.41}$$

(b) The power allocation is

$$p_i^{opt} = \frac{1}{\dot{g}_i} MMSE_i^{-1} \left(\min \left\{ 1, \frac{\bar{\eta}}{\dot{g}_i} \right\} \right). \tag{3.42}$$

An M-ary modulation defined by M discrete points, denoted by $\{s_l\}_{l=1}^M$ with probabilities $\{q_l\}_{l=1}^M$, and $\sum\limits_{l=1}^M q_l = 1$. The optimum mass probablities are generally a function of the input power. Even though it is sub-optimal in terms of mutual information, in most practical circumstances the signalling is equiprobable [Arimoto 1972; Blahut 1972; Varnica et al. 2002]. Then

$$MMSE\left(\dot{\rho}\right) = 1 - \frac{1}{\pi}\int \frac{\left|\sum\limits_{l=1}^{m} q_l s_l e^{-\left(y-\sqrt{\dot{\rho}}s_l\right)^2}\right|^2}{\sum\limits_{l=1}^{m} q_l e^{-\left(y-\sqrt{\dot{\rho}}s_l\right)^2}} dy. \tag{3.43}$$

Thus, (3.43) can be expressed distinctly in terms of different types of modulation.

For example, 4-QAM (QPSK) amounts into two BPSK constellations in quadrature, each with half the QPSK power,

$$\begin{aligned} MMSE_i^{\text{QPSK}}\left(\dot{\rho}_i\right) &= MMSE_i^{\text{BPSK}}\left(\tfrac{\dot{\rho}_i}{2}\right) \\ &= 1 - \textstyle\int_{-\infty}^{\infty} \tanh\left(2\sqrt{\dot{\rho}_i/2}x\right) \frac{e^{-\left(x-\sqrt{\dot{\rho}_i/2}\right)^2}}{\sqrt{\pi}} dx \end{aligned}. \tag{3.44}$$

In [Hong et al. 2009] Levin-Campello algorithm is compared to the Mercury Waterfilling distribution, giving the results of using other methods such as Waterfilling and Chow's algorithm as a reference. Bit rate maximization and energy minimization problems are explored using different granularities (1 or 2) for the input constellations. The influence of the SNR gap in the optimality of the power distribution obtained by Levin-Campello is analyzed [Hong et al. 2009].

4

Optimization of a MIMO system with ZF receiver

This chapter starts with the analysis of the statistical distribution of the SINR for the ZF receiver in MIMO wireless communications. The channel model is assumed to be (transmit) correlated Rayleigh flat-fading and the transmitted signals from each antenna are allowed to have unequal powers. A Gamma distribution has been proposed in the literature as approximation to the finite sample distribution of the SINR. The BER of each transmitted stream can be expressed in closed-form and will be derived using this distribution. It will be further simplified for the high SNR regime. Simulations confirm that these approximate distributions can be used to accurately estimate the probability of error even for very small dimensions (e.g., 2 transmit antennas).

For single-user MIMO communication with either uncoded or coded QAM signals, bit and power loading schemes are proposed that rely only on the channel distribution information at the transmitter. The relationship between the average bit error probability at the output of a ZF linear receiver and the bit rates and powers allocated at the transmitter is developed. This relationship, and the fact that a ZF receiver decouples the MIMO parallel channels, allows us leveraging bit loading algorithms already existing in the literature. To that end, the dual bit rate maximization and power minimization problems are solved and the performance results that illustrate the gains of the proposed scheme with respect to a non-optimized transmission are discussed.

4.1 BER of ZF receiver based on Gamma distribution

A series of works have focused on the SINR distribution at the receiver side in MIMO systems. Starting with the works related with the asymptotic properties of multiuser receivers (e.g., [Sergio V. 1998; Poor and Sergio V. 1997; Tse and Zeitouni 2000; Sergio V. and Shamai 1999; Guo et al. 2002; Tulino and Sergio V. 2004; L. Li et al. 2001; Tse and Hanly 1999]), Tse and Hanly [Tse and Hanly 1999] and Verdu and Shamai [Sergio V. and Shamai 1999] independently derived the asymptotic first moment of SINR for uncorrelated channels. For the equal power case, Tse and Zeitouni [Tse and Zeitouni 2000] proved the asymptotic Normality of SINR, and commented on the possibility of extending the result to the unequal powers scenario. The asymptotic Normality of the multiple access interference (MAI), closely related to SINR, has been proved by Zhang et. al. [Zhang et al. 2001]. For a variety of linear multiuser receivers, Guo et. al. [Guo et al. 2002] proved the asymptotic Normality of the decision statistics, considering a general power distribution and corresponding unconditional asymptotic behavior.

Poor and Verdu [Poor and Sergio V. 1997] (also in [Sergio V. 1998], [Guo et al. 2002]) proposed using the limiting BER (denoted by BER1) based on the asymptotic normality results, which is obtained as a single Q-function,

$$\mathrm{BER}_\infty = Q\left(\sqrt{\mathrm{E}\left(\mathrm{SINR}\right)_\infty}\right) = \int_{\sqrt{\mathrm{E}(\mathrm{SINR})_\infty}}^{\infty} e^{-t^2/2}dt, \tag{4.1}$$

where $\mathrm{E}\left(\mathrm{SINR}\right)_\infty$ denotes the asymptotic first moment of SINR.

Equation (4.1) is convenient and accurate for large dimensions. However, for small dimensions, more asymptotic moments should be contained in the expression to improve its accuracy [P. Li et al. 2006]. In current practice, general MIMO channels with n_T, n_R between 32 and 64 are typical and in multi-antenna systems arrays of 4 antennas are typical but arrays with 8 to 16 antennas would be considered feasible in the near future [Tulino and Sergio V. 2004]. Therefore, there is a requirement to formulate and compute error probabilities both efficiently and accurately for small and high antenna dimensions. Also for system optimization designs, a simple and accurate BER approximation is needed [Gesbert 2003], [Rungnes and Gesbert 2004].

The presence of channel correlation makes the analysis very difficult [Ralf R. M. 2002]; considering the effect of correlation tends to invalidate the independence assumption [Biglieri 2004]. Taking it into account, the asymptotic moments of SINR and several useful formulae are given for small dimensions [P. Li et al. 2006].

4.1.1 Average bit error rate based on SINR of ZF

The system model for a MIMO system with ZF receiver has been described in chapter II.

The SINR statistics can be considered as a function of the input and the channel characteristics. The ultimate goal is to relate the average BER at the receiver (through the corresponding SINR) with the power matrix $\mathbf{P}$. The output SINR for a ZF receiver on a transmit-correlated Rayleigh-faded channel with unequal powers, $n_T \leq n_R$, is characterized in [P. Li et al. 2006]. For the ith received stream it follows the Gamma distribution

$$f_g(t) = \frac{t^{\alpha-1} e^{-t/\theta_i}}{\Gamma(\alpha)\, \theta_i^{\alpha}}, \tag{4.2}$$

with parameters

$$\alpha = \alpha_{ZF} = n_R - n_T + 1, \tag{4.3}$$

$$\theta_i = \frac{1}{\left[\mathbf{R}_c^{-1}\right]_{i,i}} = p_i \lambda_i, \tag{4.4}$$

where

$$\mathbf{R}_c = \frac{\gamma}{n_T} \mathbf{P}^{\frac{1}{2}} \mathbf{V}^H \mathbf{R} \mathbf{V} \mathbf{P}^{\frac{1}{2}}. \tag{4.5}$$

Then, the average BER for the ith signal (the subindex i is dropped for notational simplicity) can be obtained from the Gamma parameters as

$$P(\alpha_{ZF},\, \theta) = \int_0^\infty P_e(t)\, f_g(t)\, dt = \int_0^\infty P_e(t)\, \frac{t^{\alpha_{ZF}-1} e^{-t/\theta}}{\Gamma(\alpha_{ZF})\, \theta^{\alpha_{ZF}}} dt. \tag{4.6}$$

where $\Gamma(\cdot)$ is the complete Gamma function and $P_e(\cdot)$ is the instantaneous BER function for the corresponding scalar signal, which depends on the modulation and coding scheme used at the transmitter. Expressions for $P_e(\cdot)$ are developed in the following subsections for uncoded and coded M-QAM modulations.

4.1.2 Approximations of Q-function

As $P_e(t)$ is derived from Q function

$$Q(t) = \frac{1}{\sqrt{2\pi}} \int_t^{\infty} \exp\left(-\frac{u^2}{2}\right) du, \tag{4.7}$$

its approximations should be analyzed at first for the further derivation.

The Q-function $Q(t)$ can be expressed in terms of the complementary error function as

$$Q(t) = \frac{1}{2} erfc\left(\frac{t}{\sqrt{2}}\right). \tag{4.8}$$

$erfc(t)$ is defined by

$$erfc(t) = \frac{2}{\sqrt{\pi}} \int_t^{\infty} e^{-u^2} du. \tag{4.9}$$

The complementary error function (11) can be approximated by the equation (14) of [Chiani et al. 2003], whose behaviour is shown in Fig.2 of [Chiani et al. 2003]. It can be seen that the curve of this approximation gives a good fit with the exact one for all SNR regimes.

Hence, from (14) of [Chiani et al. 2003], a tight and simple approximation is

$$erfc(t) \simeq \frac{1}{6} e^{-t^2} + \frac{1}{2} e^{-4t^2/3}. \tag{4.10}$$

Plugging (4.10) into (4.8),

$$\begin{aligned} Q(t) &\simeq \tfrac{1}{2}\left(\tfrac{1}{6} e^{-t^2/2} + \tfrac{1}{2} e^{-2t^2/3}\right) \\ &= 1/12 e^{-t^2/2} + 1/4 e^{-2t^2/3} \\ &= \tilde{Q}(t) \end{aligned}. \tag{4.11}$$

For high SNR, the expression (4.11) can be approximated and simplified as

$$erfc(t) \approx \frac{1}{\sqrt{\pi}} e^{-t^2}. \tag{4.12}$$

Plugging (4.12) into (4.8),

$$Q(t) \approx \frac{1}{2\sqrt{\pi}} e^{-\frac{t^2}{2}} = Q'(t). \tag{4.13}$$

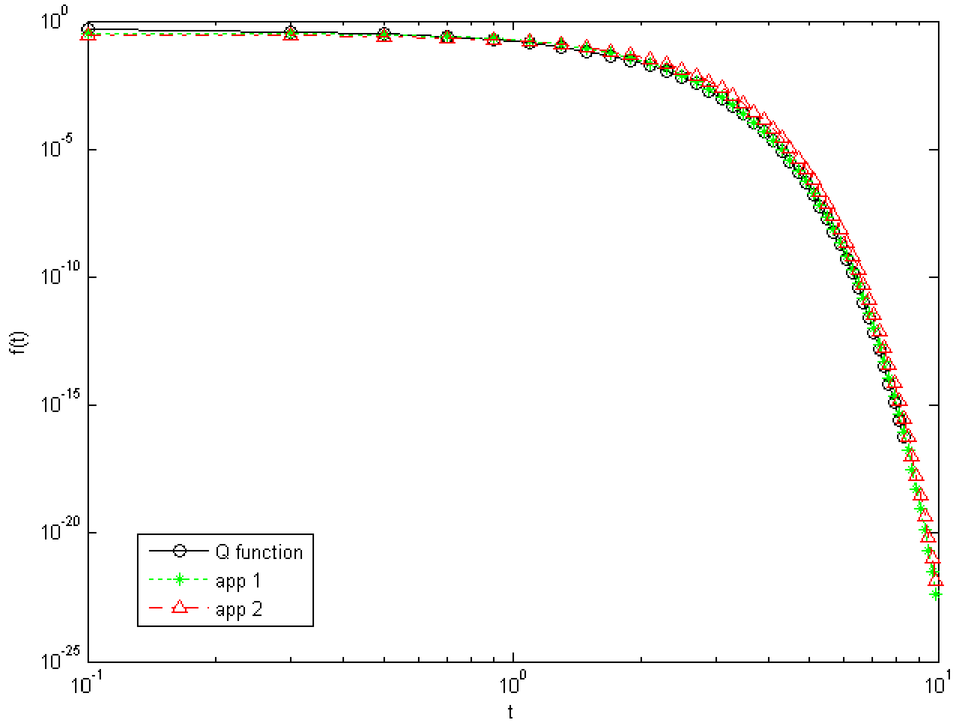

Figure 4.1: Comparison - exponential approximations for the Q function.

The behaviors of $Q(t)$, $\tilde{Q}(t)$ (app 1) and $Q'(t)$ (app 2) are compared in Fig. 4-1. Observing Fig. 4.1, it can be seen that all these three curves are close to each other, so they are good choices to accomplish the calculation for the purpose of simplification of the resulting expressions, even for low SNR.

4.1.3 Closed-form of average bit error rate for uncoded M-QAM

$P_e(t)$ is derived from the Q-function $Q(t)$, and its high SNR approximation $P'_e(t)$ is obtained from the approximated Q-function $Q'(t)$. $P_e(t)$ for uncoded M-QAM, conditioned on the fading realization, is given by the expressions [Armada et al. 2009] in Table 4.1.

	$P_e(t)$	$\tilde{P}_e(t)$	$P'_e(t)$
2-QAM	$P_e(t) = Q\left(\sqrt{2t}\right)$	$\tilde{P}_e(t) = \frac{1}{12}e^{-t} + \frac{1}{4}e^{-4t/3}$	$P'_e(t) = \frac{1}{2\sqrt{\pi}}e^{-t}$
4-QAM	$P_e(t) = Q\left(\sqrt{t}\right)$	$\tilde{P}_e(t) = \frac{1}{12}e^{-t/2} + \frac{1}{4}e^{-2t/3}$	$P'_e(t) = \frac{1}{2\sqrt{\pi}}e^{-t/2}$
M-QAM	$P_e(t) = \frac{4Q\left(\sqrt{\frac{3t}{M-1}}\right)}{\log_2 M}$	$\tilde{P}_e(t) = \frac{1}{3\log_2 M}e^{-\frac{3t}{2(M-1)}} + \frac{1}{\log_2 M}e^{-\frac{2t}{(M-1)}}$	$P'_e(t) = \frac{1}{\log_2 M}\frac{2}{\sqrt{\pi}}e^{\frac{-3t}{2(M-1)}}$

Table 4.1: Exact and approximate BER in AWGN.

Plugging these approximate P'_e expressions into (4.6) and integrating, approximate average BER expressions as function of the Gamma parameters $Gamma(\alpha_{\mathrm{ZF}},\ \theta)$ for the uncoded case are found [Armada et al. 2009].

$$P_{2qam} \approx \frac{1}{2\sqrt{\pi}}(1+\theta)^{-\alpha_{ZF}}\,. \tag{4.14}$$

$$P_{4qam} \approx \frac{1}{2\sqrt{\pi}}\left(1+\frac{\theta}{2}\right)^{-\alpha_{ZF}}, \tag{4.15}$$

$$P_{Mqam} \approx \frac{1}{\log_2 M}\frac{2}{\sqrt{\pi}}\left(1+\frac{3\theta}{2(M-1)}\right)^{-\alpha_{ZF}}. \tag{4.16}$$

Their counterparts, obtained by integrating (4.14) with the formulas in the first column of Table 4.1, can be expressed by means of the hypergeometric function

$${}_2F_1(a,b;c;d) = \frac{\Gamma(c)}{\Gamma(b)\Gamma(c-b)}\int_0^1 \frac{t^{b-1}(1-t)^{c-b-1}}{(1-td)^a}dt. \tag{4.17}$$

as follows. For 2-QAM,

$$P_{2qam} = \tfrac{1}{2\Gamma(\alpha_{ZF})} \left[\Gamma\left(\alpha_{ZF}\right) - 2\sqrt{\tfrac{\theta}{\pi}}\Gamma\left(\tfrac{1}{2} + \alpha_{ZF}\right) {}_2F_1\left(\tfrac{1}{2}, \tfrac{1}{2} + \alpha_{ZF}; \tfrac{3}{2}; -\theta\right) \right], \tag{4.18}$$

while, for 4-QAM,

$$P_{4qam} = \frac{1}{2\Gamma\left(\alpha_{ZF}\right)} \left[\Gamma\left(\alpha_{ZF}\right) - 2\sqrt{\tfrac{2\theta}{\pi}}\Gamma\left(\frac{1}{2} + \alpha_{ZF}\right) {}_2F_1\left(\frac{1}{2}, \frac{1}{2} + \alpha_{ZF}; \frac{3}{2}; \frac{-\theta}{2}\right) \right], \tag{4.19}$$

and, for M-QAM ($M > 4$),

$$\begin{aligned} P_{Mqam} = \tfrac{1}{2\log_2(M)\Gamma(\alpha_{ZF})} &\left[\Gamma\left(\alpha_{ZF}\right) - 2\sqrt{\tfrac{6\theta}{\pi(M-1)}}\Gamma\left(\tfrac{1}{2} + \alpha_{ZF}\right) \right. \\ &\left. {}_2F_1\left(\tfrac{1}{2}, \tfrac{1}{2} + \alpha_{ZF}; \tfrac{3}{2}; \tfrac{-3\theta}{2(M-1)}\right) \right] \end{aligned}. \tag{4.20}$$

On account of the excellent agreement of both sets of expressions (that will be shown in section 4.3), the much simpler expressions (4.14) - (4.16) will be used for the purpose of bit loading.

4.1.4 Closed-form expression of the average bit error rate for coded M-QAM

Consider now M-QAM modulation in conjunction with a convolutional code of rate $r_c = k_c/n_c$ and minimum distance d_f. With hard-decision decoding, maximum likelihood reduces to a minimum distance criterion and the BER at the output of the decoder is upper bounded by [Proakis 2000].

$$P_c \leq \frac{1}{k} \sum_{d=d_f}^{\infty} A_d \left(2\sqrt{P_e\left(1 - P_e\right)}\right)^d. \tag{4.21}$$

with P_e the bit error probability of the corresponding uncoded M-QAM. In turn, A_d is the number of paths in the trellis with distance d from the all-zero path that merge with this all-zero path for the first time.

At high SINR, the summation in (4.21) is dominated by the first term and, if P_e is small, it can be further approximated

$$P_c \approx \frac{1}{k} A_{d_f} 2^{d_f} P_e^{d_f/2}. \tag{4.22}$$

Using the parameter

$$D = \frac{A_{d_f}}{k} 2^{d_f/2} \pi^{-d_f/4}. \tag{4.23}$$

and with the approximate P_e expressions in Table 4.1, second column, we obtain by integrating (4.6) the following average BER expressions.

$$P_{c\_2qam} \approx D \left(1 + \frac{d_f}{2}\theta\right)^{-\alpha_{ZF}}, \tag{4.24}$$

$$P_{c\_4qam} \approx D \left(1 + \frac{d_f \theta}{4}\right)^{-\alpha_{ZF}}, \tag{4.25}$$

$$P_{c\_Mqam} \approx \frac{4}{\log_2 M} D \left(1 + \frac{3 d_f \theta}{4\,(M-1)}\right)^{-\alpha_{ZF}}. \tag{4.26}$$

4.2 Optimization problems

Denote by M_i the cardinality of the modulation applied to the ith eigenvector of $\mathbf{V}$, by P_{e_i} its average BER after the ZF receiver, and by $\overline{BER}$ the target average BER. Once the relationship between average BER and the parameters (α_{ZF}, θ) has been established and the SINR can be expressed as function of the channel correlations and the power allocation, we have the tools to solve the following dual optimization problems.

2-QAM	$\theta = (2\sqrt{\pi} P_{2qam})^{-1/\alpha_{ZF}} - 1$
4-QAM	$\theta = 2\left[(2\sqrt{\pi} P_{4qam})^{-1/\alpha_{ZF}} - 1\right]$
M-QAM	$\theta = \frac{2}{3}(M-1)\left[(1/2 \log_2(M)\sqrt{\pi} P_{Mqam})^{-1/\alpha_{ZF}} - 1\right]$

Table 4.2: Requiered θ to satisfy P_{e_i} - uncoded modulations.

2-QAM	$\theta = \frac{2}{d_{free}}\left[\left(\frac{P_{c\_2qam}}{D}\right)^{-1/\alpha_{ZF}} - 1\right]$
4-QAM	$\theta = \frac{4}{d_{free}}\left[\left(\frac{P_{c\_2qam}}{D}\right)^{-1/\alpha_{ZF}} - 1\right]$
M-QAM	$\theta = \frac{4(M-1)}{3 d_{free}}\left[\left(\frac{P_{c\_Mqam}}{4D}\log_2(M)\right)^{-1/\alpha_{ZF}} - 1\right]$

Table 4.3: Requiered θ to satisfy P_{e_i} - coded modulations.

4.2.1 Maximize Bit Rate

$$\begin{aligned} &\max \quad R = \sum_{i=1}^{n_T} \log_2 M_i \\ &s.t.\ P_{e\_i} \le \overline{\mathrm{BER}},\ 1 \le i \le n_T \\ &\quad \mathrm{Tr}\left[\mathbf{P}\right] = n_T,\ p_i \ge 0 \end{aligned} \quad . \tag{4.27}$$

Problem (4.27) can be solved by searching over all matrices $\mathbf{P}$ that satisfy Tr[$\mathbf{P}$] $=n_T$, calculating every P_{e_i} from the equations (4.14)-(4.16) and selecting the solution that satisfies $P_{e\_i} \le \overline{\mathrm{BER}}$, and achieves the maximum sum bit rate. Efficient bit and power loading algorithms available in the literature can be leveraged (cf. Chapter 4.3 of [Cioffi]).

4.2.2 Minimize Power

$$\begin{aligned} &\min \quad \mathrm{Tr}\left[\mathbf{P}\right] \\ &s.t.\ P_{e\_i} \le \overline{\mathrm{BER}},\ 1 \le i \le n_T \\ &\sum_{i=1}^{n_T} \log_2 M_i = R_{tot},\ p_i \ge 0 \end{aligned} \quad . \tag{4.28}$$

Problem (4.28) can be solved using the inverse functions that give the matrix $\mathbf{P}$ required to satisfy a given average BER per signal for each constellation cardinality. These inverse functions are shown in Tables 4.2 and 4.3 for uncoded and coded modulations, respectively [Armada et al. 2009].

4.2.3 Levin-Campello Bit Loading

As introduced in chapter III, the Levin-Campello algorithm [Campello et al. 1999] is known to optimally solve the problem of bit loading with discrete constellations at a target error probability. Its key tenet is that each additional information unit to be transmitted should be allocated to the signalling channel (spatial stream in our case) that requires the least incremental energy for its transport. Incremental energies for the modulation schemes can be obtained from Tables 4.2 and 4.3 and the application of the algorithm to the solution of Problems (4.27) and (4.28) is then quite straightforward.

4.3 Numerical examples

4.3.1 Average BER of ZF

Assuming that the transmit correlation matrix has elements $\mathbf{R}_{i,j} = \rho^{(i-j)^2}$ corresponding to suburban/rural environments with small angular spreads at the transmitter [Chu et al. 1997]

$$\mathbf{R} = \begin{bmatrix} 1 & \rho & \rho^4 & \cdots & \rho^{(n_T-1)^2} \\ \rho & 1 & \rho & \cdots & \rho^{(n_T-2)^2} \\ \rho^4 & \rho & 1 & \cdots & \rho^{(n_T-3)^2} \\ \vdots & \vdots & \vdots & \ddots & \vdots \\ \rho^{(n_T-1)^2} & \cdots & \rho^4 & \rho & 1 \end{bmatrix}. \tag{4.29}$$

Fig. 4.2 is obtained with the power matrix $\mathbf{P} = \mathbf{I}$ and precoding matrix $\mathbf{V}$ contains the eigenvectors of (2.4). It shows the excellent agreement between the exact values of BER (exa) in (4.18)-(4.20) and those approximations (app) in (4.14)-(4.16), for the operational range of interest ($P_e \leq 10^{-1}$).

4.3.2 Bit loading and power allocation for ZF

The following three scenarios, in terms of modulation and coding schemes available at the transmitter, are considered.

- 8 uncoded bit rates: M_i takes values in the set {0, 2, 4, 8, 16, 32, 64, 128, 256}. Although cardinalities beyond 64 might be unpractical, this scenario illustrates what would happen if the modulation cardinality were unbounded.

- 6 uncoded bit rates: M_i takes values in the set {0, 2, 4, 8, 16, 32, 64}. This is a more realistic uncoded scenario.

- 12 bit rates with convolutional coding: M_i takes values in the set {0, 2, 4, 8, 16, 32, 64}. Each of the signals will either be uncoded or coded with a rate - 1/2 convolutional code of generator polynomials (133, 171) and $d_f = 10$.

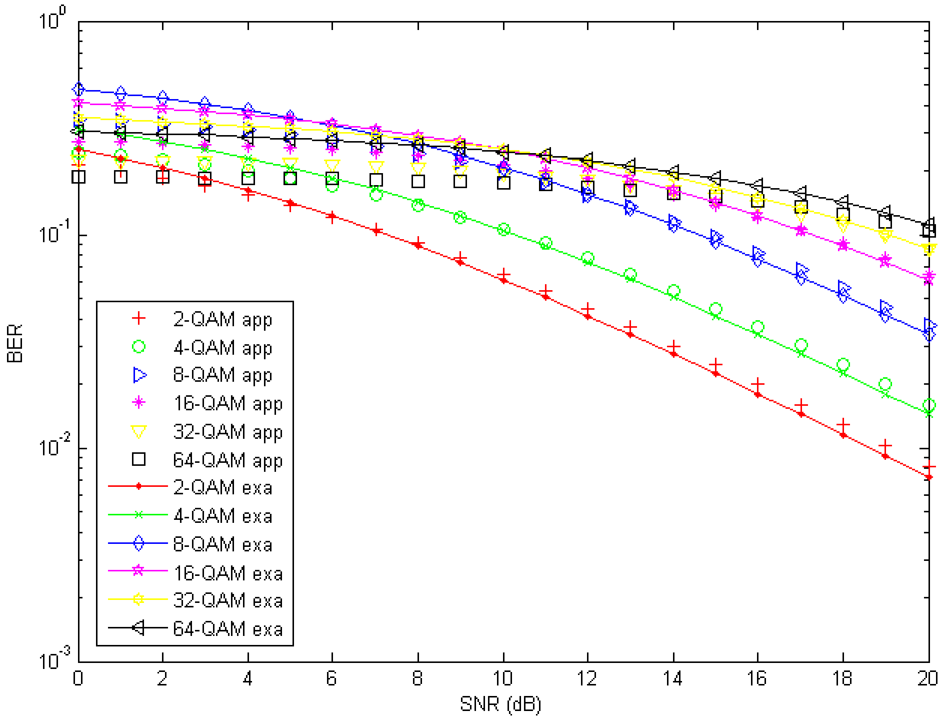

Figure 4.2: Exact and approximate average BER for uncoded QPSK - i.i.d Rayleigh flat-fading channel.

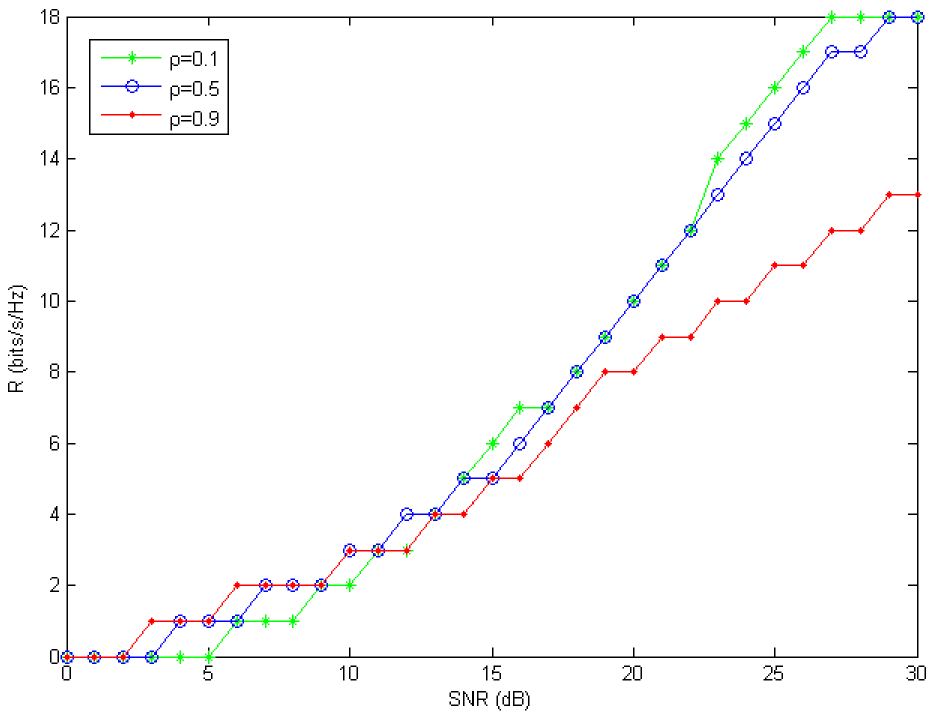

Figure 4.3: Bit rate vs. SNR - 6 uncoded bit rates with $n_T = 3$, $n_R = 4$ and $\overline{\mathrm{BER}} = 10^{-2}$.

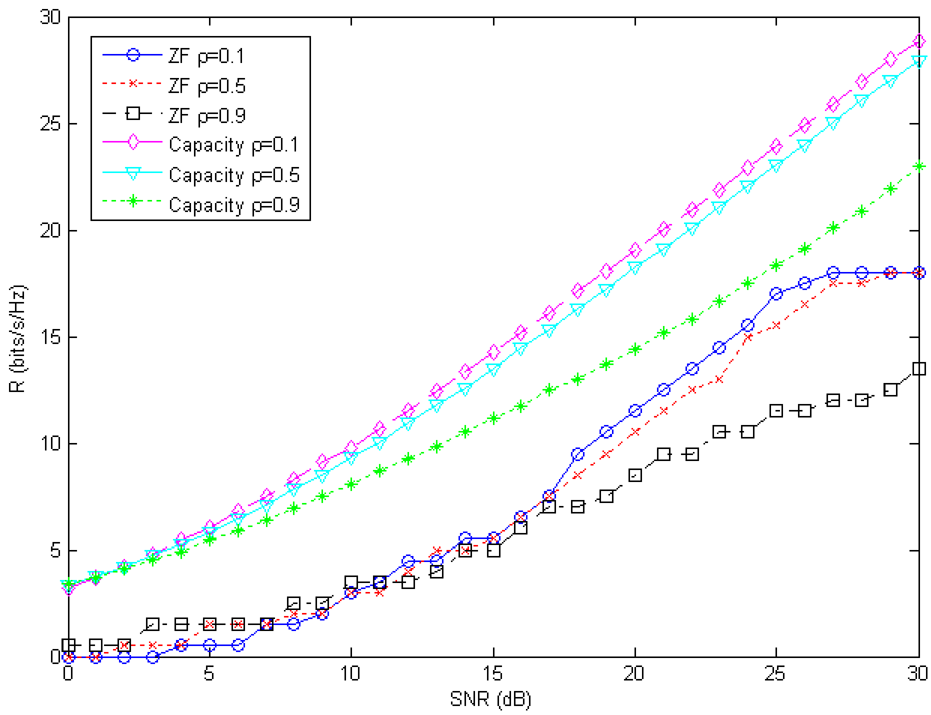

Figure 4.4: Bit rate vs. SNR - 12 uncoded bit rates with $n_T = 3$, $n_R = 4$ and $\overline{\text{BER}} = 10^{-2}$.

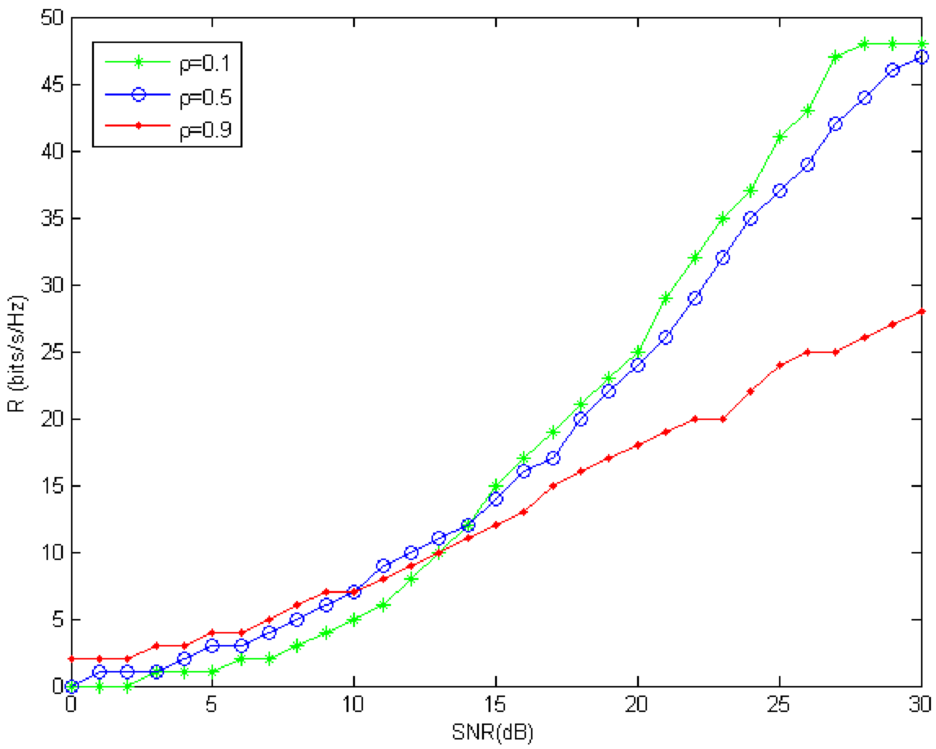

Figure 4.5: Bit rate vs. SNR - 6 uncoded bit rates with $n_T = 8$, $n_R = 10$ and $\overline{\mathrm{BER}} = 10^{-2}$.

4.3.2.1 Bit Rate Maximization

Figs. 4.3-4.5 show the achievable bit rate R as a function of the SNR - γ of (2.1) - when the power allocation $\mathbf{P}$ is optimized in comparison with the case $\mathbf{P} = \mathbf{I}$. Different values for the channel correlation parameter ρ (cf. eq. 4.29) are used while $n_T = 3$, $n_R = 4$ and $\overline{\mathrm{BER}} = 10^{-2}$. By optimizing $\mathbf{P}$, higher bit rates are always achieved. The gains in bit rate are larger when ρ is high since, in that case, optimizing $\mathbf{P}$ allows adapting to the fact that the output $\mathrm{SINR}_{\mathrm{ZF}}$ of each stream become very different. Also, optimizing $\mathbf{P}$ allows extending the range of operational SNR since nonzero bit rates are possible at low SNRs even when transmission is not possible using simply $\mathbf{P} = \mathbf{I}$. With a richer set of bit rates via coding, this range extension is more pronounced as can be seen by comparing both figures.

It is known that correlation has the following effect on the CDIT capacity (with the optimum transmit covariance): correlation is beneficial at low SNR and it is detrimental above a critical SNR [Tulino et al. 2005]. Figure 4.4 shows the CDIT capacity according to [Tulino et al. 2006] for the channel model. Interestingly, correlation has the same effect on the bit rate achieved by the proposed bit loading with ZF receiver, with the particularity that the critical SNR is higher in this case. With simple convolutional codes and a ZF receiver, the proposed scheme is seen to perform with 9 dB of capacity at $\overline{\mathrm{BER}} = 10^{-2}$ and SNR = 20dB.

To illustrate the applicability of the optimization procedure to settings with large numbers of antennas, Fig. 4.4-4.5 presents some achievable bit rates as function of the SNR with 8 transmit and 10 receive antennas and SNR = 20dB.

4.3.2.2 Power Minimization

Let us now examine the power gain defined as the dB difference that results from optimizing $\mathrm{Tr}\left[\mathbf{P}\right]$ versus using $\mathbf{P} = \mathbf{I}$. Fig. 4.6 shows this gain for $n_T = 3$, $n_R = 4$ and $\overline{\mathrm{BER}} = 10^{-2}$ with 6 uncoded bit rates. Gains in excess of 10 dB can be obtained for high ρ. In order to show the dependence on BER, Fig. 4.7 plots the same scenario of Fig. 4.6 except with $\overline{\mathrm{BER}} = 10^{-4}$. The impact of BER in the power gain is seen to be negligible.

In Figs 4.8-4.9, the extreme cases are explored when the required bit rate is either $R = n_T$ or $R = 6n_T$. This provides insight on the low- and high-SNR behaviors,

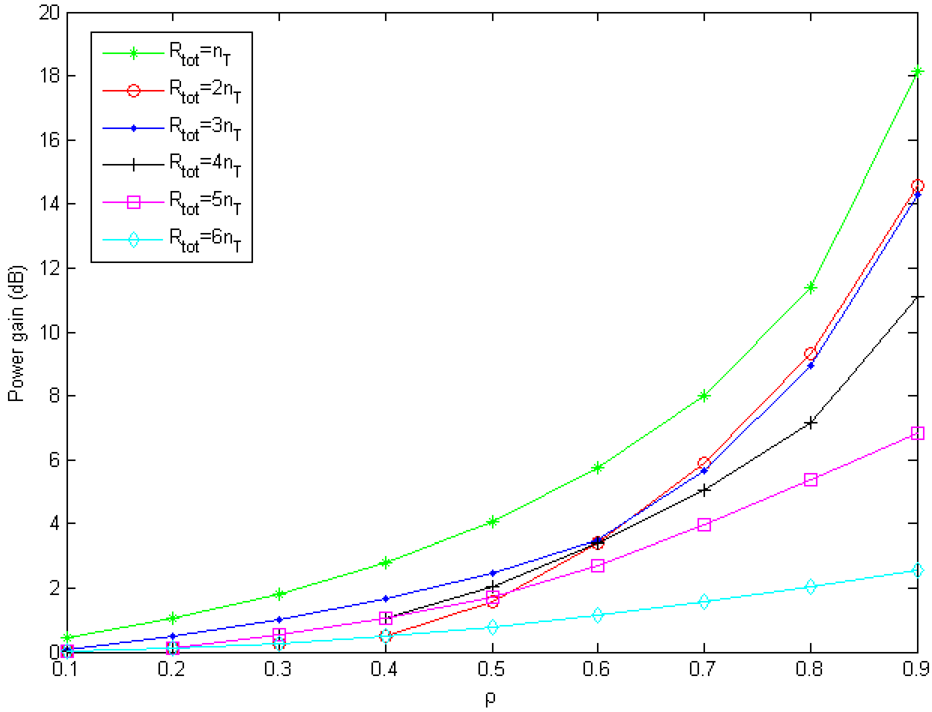

Figure 4.6: Power gain vs. ρ - 6 uncoded bit rates with $n_T = 3$, $n_R = 4$ and $\overline{\mathrm{BER}} = 10^{-2}$.

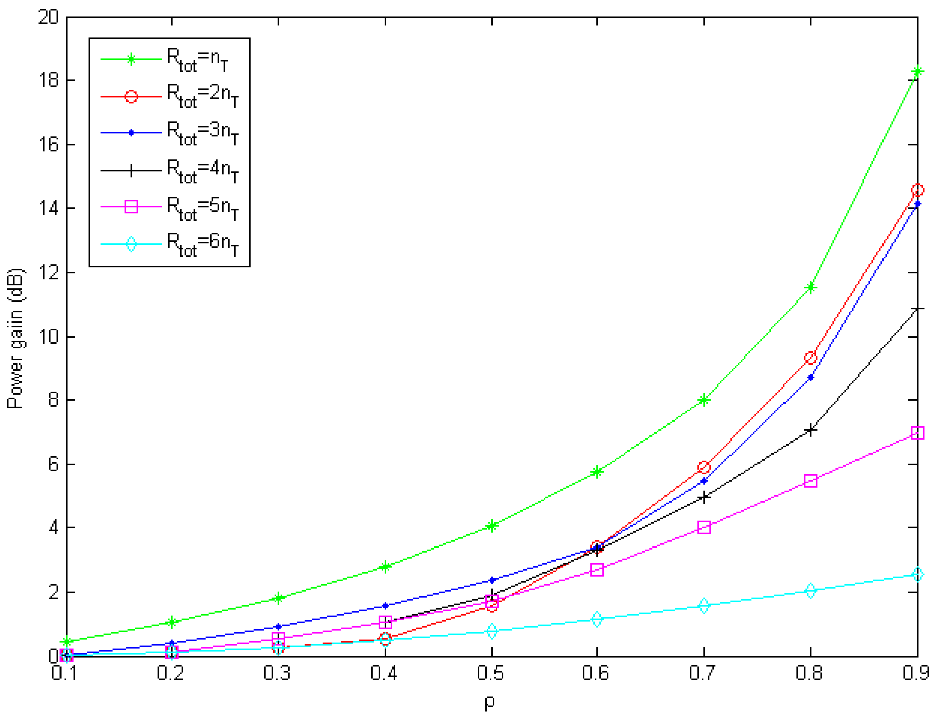

Figure 4.7: Power gain vs. $\boldsymbol{\rho}$ - 6 uncoded bit rates with $n_T = 3$, $n_R = 4$ and $\overline{\text{BER}} = 10^{-4}$.

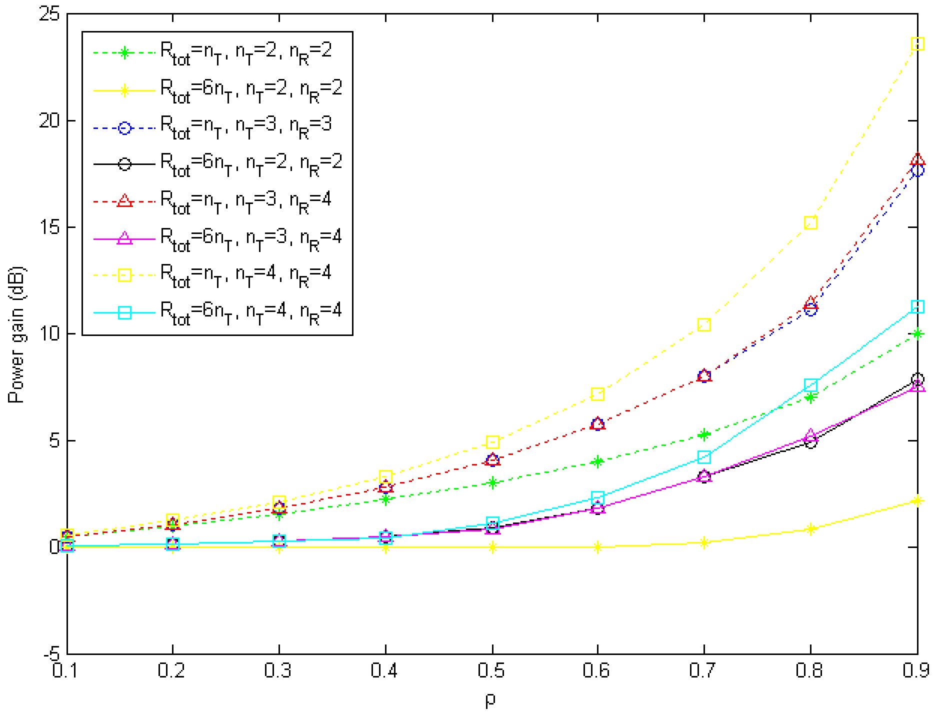

Figure 4.8: Power gain vs. ρ - 8 uncoded bit rates with $\overline{\mathrm{BER}} = 10^{-2}$.

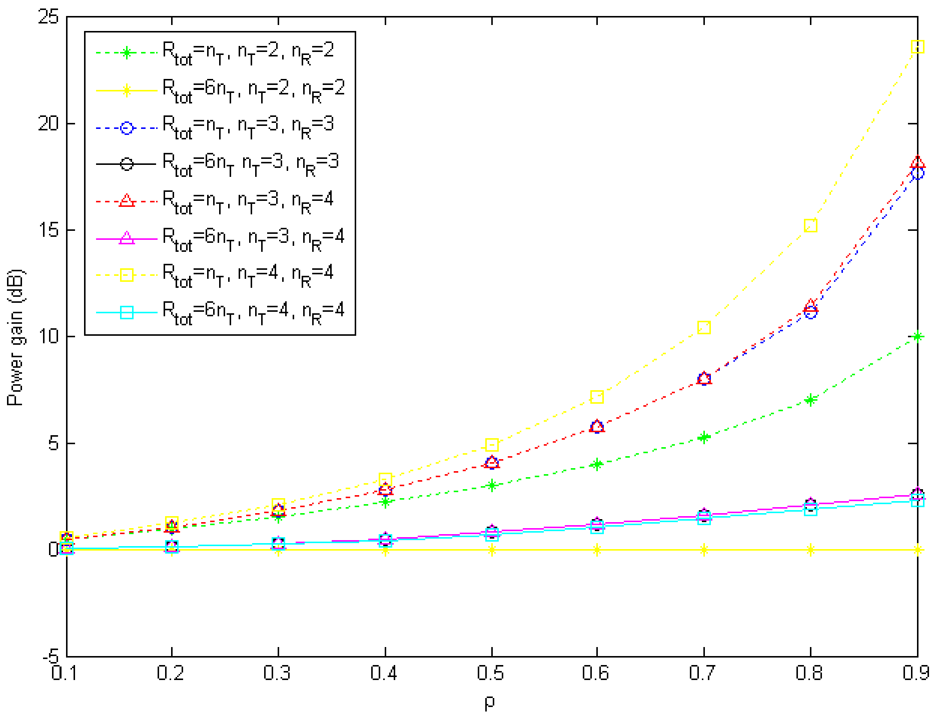

Figure 4.9: Power gain vs. ρ - 6 uncoded bit rates with $\overline{\mathrm{BER}} = 10^{-2}$.

respectively. Uncoded modulation is used, with $\overline{\mathrm{BER}} = 10^{-2}$. Contrasting these figures, it can be seen that limiting the number of bit rates without coding limits the power gain at high SNR since no higher cardinality constellations are available to profit from such high SNR. This effect does not occur at low SNR. Higher gains are achieved for $R = n_T$ (low SNR) than for $R = 6n_T$ (high SNR).

4.4 Conclusion

In the context of single-user MIMO communication, expressions have been obtained that relate the channel statistics, the precoding vectors, and the power allocation, with the average BER at the output of a ZF receiver when uncoded or coded M-QAM modulation is used. These expressions enable bit and power loading procedures that can be formalized into two dual optimization problems: bit rate maximization and power minimization. With an optimized transmission, substantially higher bit rates can be achieved and/or less power spent. The developed formulation can leverage available loading algorithms to render the optimization process highly efficient.

5

BER of a MIMO system with MMSE receiver

This chapter studies the statistical distribution of the signal-to-interference-plus-noise ratio (SINR) for the minimum mean squared error (MMSE) receiver in MIMO wireless communications. The channel model is assumed to be (transmit) correlated Rayleigh flat-fading with unequal powers for the different transmitted data streams. A Gamma distribution and a generalized Gamma distribution have been proposed in the literature as approximations to the finite sample distribution of SINR for this receiver. The BER of each stream can be approximated and simplified into closed-form with these distributions, particularized for high or low SNR. Simulations confirm that these approximate distributions can be used to accurately estimate the probability of error even for very small dimensions (e.g., 2 transmit antennas).

The performance of a general MIMO system is analyzed, with or without precoding, in transmit-correlated Rayleigh flat-fading channels with an MMSE receiver. Our analysis will be based on the signal-to-interference-plus-noise ratio (SINR) distribution. It is proved in [Gore et al. 2002] that the SINR after a ZF receiver is a Gamma random variable when a uniform power distribution is used in the transmitter. Making use of this distribution in [Armada et al. 2009] the average BER can be obtained when a ZF scheme is employed at the receiver. As regards the MMSE receiver, some expressions have been developed that are only accurate for high dimensions [Guo et al. 2002] or particularized to diversity combining receivers [Kiessling and Speidel 2003]. In [Moustakas et al. 2009] the performance is evaluated for large dimensions in terms of mutual information. None of these works contemplates the precoder.

Recently the distribution of the SINR after an MMSE receiver has been obtained for the case of transmit-correlated Rayleigh flat-fading channel [P. Li et al. 2006]. The authors show that the SINR approaches a Gamma or generalized Gamma distribution. Using both of them, the average BER can be obtained for a MIMO system employing M-ary quadrature amplitude modulation (M-QAM). As we will show it is accurate, even for a small number of antennas. We will compare our approximations with the expressions obtained in [Guo et al. 2002], that are accurate for large antenna dimensions, and [Kammoun et al. 2009]. In this last paper the authors also use a generalized Gamma distribution. However its parameters are obtained following a different procedure and assumptions [Hachem et al. 2008] and the developed expressions are accurate for both large and small dimensions but in this last case only for small signal to noise ratios, as shown in [Kammoun et al. 2009]. Also, in [Kammoun et al. 2009] the BER is averaged over all the MIMO transmitted streams while in channels that exhibit high correlation the use of a precoder may lead to substantial differences among the spatially multiplexed streams. Therefore we present several approximations that may be chosen depending on the accuracy and complexity requirements of the adaptation algorithms used to reduce the transmission power and/or enhance the data rates.

5.1 BER of MMSE receiver based on Gamma distribution

The system model for a MMSE receiver in MIMO system has been described in chapter II.

In [P. Li et al. 2006], the SINR for the MMSE is shown to be the sum of two parts, S and T, being T the SINR part when the ZF receiver is used, and T an independent part. The first two moments of this T are derived in [L. Hong 10], μ and σ^2, and they will be used to express the parameters of the Gamma distribution.

These first two moments for the ith stream can be obtained by numerically solving

$$\mu = \frac{1}{n_T - 1} \sum_{i=1}^{n_T-1} \frac{1}{\tau_i \left(1 - \upsilon + \upsilon\mu\right) + 1}, \tag{5.1}$$

$$\sigma^2 = \frac{\left(\frac{1}{n_T-1}\sum_{i=1}^{n_T-1}\frac{\tau_i\upsilon\mu+1}{(\tau_i(1-\upsilon+\upsilon\mu)+1)^2}\right)}{\left(1+\frac{1}{n_T-1}\sum_{i=1}^{n_T-1}\frac{\tau_i\upsilon}{(\tau_i(1-\upsilon+\upsilon\mu)+1)^2}\right)}. \tag{5.2}$$

where τ_i are the eigenvalues of $\mathbf{R}_{(-i,-i)}$ and $\upsilon = \frac{n_T-1}{n_R}$. $\mathbf{R}_{(-i,-i)}$ is the generalized covariance matrix (4.5) $\mathbf{R}_c = \frac{\gamma}{n_T}\mathbf{V}^H\mathbf{P}^{\frac{1}{2}}\mathbf{R}\mathbf{P}^{\frac{1}{2}}\mathbf{V}$ with the ith row and ith column removed. Although (5.1)-(5.2) are exact expressions for large antenna dimensions; they are also accurate for small antenna dimensions as shown in [P. Li et al. 2006].

For the ith stream, the parameters of the Gamma distribution for the MMSE receiver can then be written as

$$\alpha_M = \frac{(n_R - n_T + 1 + (n_T-1)\,\mu)^2}{n_R - n_T + 1 + (n_T-1)\,\sigma^2}, \tag{5.3}$$

$$\beta_{M_i} = \Sigma_i \frac{n_R - n_T + 1 + (n_T-1)\,\sigma^2}{n_R - n_T + 1 + (n_T-1)\,\mu}. \tag{5.4}$$

$\Sigma_i = \frac{1}{\left[\mathbf{R}_c^{-1}\right]_{i,\,i}}$ and $\left[\mathbf{R}_c^{-1}\right]_{i,\,i}$ indicates the ith diagonal element of the matrix $\mathbf{R}_c^{-1}$. From here, the subindex i is dropped from β_{M_i} for simplicity.

Closed-form expressions of average bit error rate for uncoded or coded M-QAM can be found in the chapter IV for a Gamma distribution of the SINR, corresponding to (4.14)-(4.16) and (4.18)-(4.20). Replacing the α_{ZF} and θ to be α_M and β_M in these equations, the BER of MMSE receiver can be computed.

5.2 BER of MMSE receiver based on generalized Gamma distribution

In [P. Li et al. 2006], it is shown how the SINR distribution (for the MIMO MMSE receiver and a Rayleigh flat-fading channel, is better approximated using a Generalized Gamma distribution, instead of a Gaussian or a Gamma distribution.

5.2.1 Parameters of the generalized gamma distribution

The generalized Gamma distribution will be defined using three parameters, *Gamma*(α_M, β_M, ξ_M). In [P. Li et al. 2006], the SINR for the MMSE is shown to be the sum of two parts, S and T, being S the SINR part when the ZF receiver is used, and T an independent part. The first two moments of this T has been shown in (5.1) and (5.2), and the third moment η is also derived in [P. Li et al. 2006], therefore they will be used to express the parameters of the generalized Gamma distribution.

The third moment of the ith stream can be approximated by numerically solving

$$\eta = \frac{\left(\frac{2}{n_T-1}\sum_{i=1}^{n_T-1}\frac{\tau_i \upsilon \sigma^2}{(\tau_i(1-\upsilon+\upsilon\mu)+1)^2} + \frac{2}{n_T-1}\sum_{i=1}^{n_T-1}\frac{\left(\tau_i\upsilon\mu-\tau_i\upsilon\sigma^2+1\right)}{(\tau_i(1-\upsilon+\upsilon\mu)+1)^3}\right)}{\left(1+\frac{1}{n_T-1}\sum_{i=1}^{n_T-1}\frac{\tau_i\upsilon}{(\tau_i(1-\upsilon+\upsilon\mu)+1)^2}\right)}, \tag{5.5}$$

For the ith stream, the third parameter of generalized gamma distribution can then be written as

$$\xi_M = \frac{2\left(1-\frac{n_T-1}{n_R}+\frac{n_T-1}{n_R}\mu\right)\left(1-\frac{n_T-1}{n_R}+\frac{n_T-1}{n_R}\eta\right)}{\left(1-\frac{n_T-1}{n_R}+\frac{n_T-1}{n_R}\sigma^2\right)^2} - 1. \tag{5.6}$$

5.2.2 Closed-form approximation of average bit error rate for uncoded M-QAM

The analysis starts with the Moment Generating Function (MGF) [Mark E. Irwin] of the SINR. The MGF of a random variable T is

$$M_T(s) = \int_{-\infty}^{\infty} e^{st} f_{gg}(t)dt. \tag{5.7}$$

where f_{gg} is the generalized Gamma probability density function. On the other side, the average BER for the ith signal stream can be obtained from the generalized Gamma parameters as

$$P_{gg} = \int_0^{\infty} P_e(t)\, f_{gg}(t)dt. \tag{5.8}$$

Where $P_e(t)$ is the instantaneous BER function for the corresponding scalar signal, which depends on the modulation and coding scheme used at the transmitter.

For M-QAM modulation, (4.7) and (4.11) in chapter IV show $Q(t)$ and an accurate approximation $\tilde{Q}(t)$. $P_e(t)$ is derived from the Q-function $Q(t)$, and its high SNR approximation $\tilde{P}_e(t)$ is obtained from the approximated Q-function $\tilde{Q}(t)$.

As SINR ≥ 0, combining (5.7) and (5.8), and considering (4.11) for the corresponding $\tilde{P}_e(t)$,

$$\begin{aligned} P_{mqam} &\simeq \int_0^\infty \tilde{P}_e(t)\, f_{gg}(t)dt \\ &\simeq A_p \int_0^\infty \left(\tfrac{1}{12} e^{\frac{s_p t}{2}} + \tfrac{1}{4} e^{\frac{2 s_p t}{3}} \right) f_{gg}(t)dt \ . \\ &= A_p \left(\tfrac{1}{12} M_T\left(\tfrac{s_p}{2}\right) + \tfrac{1}{4} M_T\left(\tfrac{2s_p}{3}\right)\right) \end{aligned} \tag{5.9}$$

For 2-QAM, $s_p = -2$, $A_p = 1$, and for 4-QAM, $s_p = -1$, $A_p = 1$, according to chapter IV, and, $s_p = \frac{-3}{(M-1)}$, $A_p = \frac{4}{\log_2 M}$ for M-QAM ($M > 4$).

Recalling the equations (69) and (70) in [P. Li et al. 2006] and combining with (6.5),

if $\xi > 1$,

$$\begin{aligned} P_{mqam} &\simeq A_p \left(\tfrac{1}{12} M_T\left(\tfrac{s_p}{2}\right) + \tfrac{1}{4} M_T\left(\tfrac{2s_p}{3}\right)\right) \\ &= \tfrac{1}{12} \exp\left(\tfrac{\alpha_M}{\xi_M - 1} \left(1 - \left(1 - \tfrac{s_p \beta_M \xi_M}{2}\right)^{\frac{\xi_M - 1}{\xi_M}} \right)\right) \ . \\ &+ \tfrac{1}{4} \exp\left(\tfrac{\alpha_M}{\xi_M - 1} \left(1 - \left(1 - \tfrac{2 s_p \beta_M \xi_M}{3}\right)^{\frac{\xi_M - 1}{\xi_M}} \right)\right) \end{aligned} \tag{5.10}$$

and if $\xi < 1$,

$$\begin{aligned} P_{mqam} &\simeq A_p \left(\tfrac{1}{12} M_T\left(\tfrac{s_p}{2}\right) + \tfrac{1}{4} M_T\left(\tfrac{2s_p}{3}\right)\right) \\ &= \tfrac{1}{12} \exp\left(\tfrac{\alpha_M}{1 - \xi_M} \left(\left(\tfrac{1}{1 - \frac{s_p \beta_M \xi_M}{2}} \right)^{\frac{1 - \xi_M}{\xi_M}} - 1 \right)\right) \ . \\ &+ \tfrac{1}{4} \exp\left(\tfrac{\alpha_M}{1 - \xi_M} \left(\left(\tfrac{1}{1 - \frac{2 s_p \beta_M \xi_M}{3}} \right)^{\frac{1 - \xi_M}{\xi_M}} - 1 \right)\right) \end{aligned} \tag{5.11}$$

5.2.3 High or low SNR approximations of average bit error rate for uncoded M-QAM

For high SNR, combining (5.7) and (5.8), and considering (4.13) corresponding to $P'_e(t)$,

$$P_{mqam} \approx \int_0^\infty P'_e(t)\, f_{gg}(t)dt \simeq A_p \int_0^\infty \frac{1}{2\sqrt{\pi}} e^{\frac{s_p t}{2}} f_{gg}(t)dt = A_p \left(\frac{1}{2\sqrt{\pi}} M_T\left(\frac{s_p}{2}\right)\right). \tag{5.12}$$

Recalling the equations (69) and (70) in [P. Li et al. 2006] and combining with (5.12), the high SNR approximations for the average BER of the ith stream are shown in Table 5.1.

Constellation	BER approximation with $\xi > 1$
2-QAM	$P_{2qam} \approx \frac{1}{2\sqrt{\pi}} \exp\left(\frac{\alpha_M}{\xi_M - 1}\left(1 - \left(1+\beta_M\xi_M\right)^{\frac{\xi_M-1}{\xi_M}}\right)\right)$
4-QAM	$P_{4qam} \approx \frac{1}{2\sqrt{\pi}} \exp\left(\frac{\alpha_M}{\xi_M - 1}\left(1 - \left(1+\frac{\beta_M\xi_M}{2}\right)^{\frac{\xi_M-1}{\xi_M}}\right)\right)$
M-QAM	$P_{Mqam} \approx \frac{2}{\log_2(M)\sqrt{\pi}} \exp\left(\frac{\alpha_M}{\xi_M - 1}\left(1 - \left(1+\frac{3}{2(M-1)}\beta_M\xi_M\right)^{\frac{\xi_M-1}{\xi_M}}\right)\right)$
Constellation	BER approximation with $\xi < 1$
2-QAM	$P_{2qam} \approx \frac{1}{2\sqrt{\pi}} \exp\left(\frac{\alpha_M}{1-\xi_M}\left(\left(\frac{1}{1+\beta_M\xi_M}\right)^{\frac{1-\xi_M}{\xi_M}} - 1\right)\right)$
4-QAM	$P_{4qam} \approx \frac{1}{2\sqrt{\pi}} \exp\left(\frac{\alpha_M}{1-\xi_M}\left(\left(\frac{1}{1+\frac{\beta_M\xi_M}{2}}\right)^{\frac{1-\xi_M}{\xi_M}} - 1\right)\right)$
M-QAM	$P_{Mqam} \approx \frac{2}{\log_2(M)\sqrt{\pi}} \exp\left(\frac{\alpha_M}{1-\xi_M}\left(\left(\frac{1}{1+\frac{3\beta_M\xi_M}{2(M-1)}}\right)^{\frac{1-\xi_M}{\xi_M}} - 1\right)\right)$

Table 5.1: Approximate average BER for uncoded modulations at high SNR.

At low SNR, the Gamma distribution and the generalized Gamma distribution are very close. Thus, $\xi_M \approx 1$. From the equation (2.6) in [Huang and Hwang 2006] it is known that the expectation of $e^{-st\xi}$ under the generalized Gamma distribution is

$$\mathrm{E}\left(e^{-st^{\xi_M}}\right) = \frac{\left(\frac{1}{\beta_M}\right)^{\alpha_M\xi_M}}{\left(\left(\frac{1}{\beta_M}\right)^{\xi_M} + s\right)^{\alpha_M}}, \tag{5.13}$$

which for $\xi_M \approx 1$ becomes

$$\mathrm{E}\left(e^{-st}\right) = \left(\left(\frac{1}{\beta_M}\right)^{\xi_M} + s\right)^{-\alpha_M} \left(\frac{1}{\beta_M}\right)^{\alpha_M\xi_M}. \tag{5.14}$$

For 2-QAM, average BER is obtained setting $s = 1$ as

$$P_{2qam} \approx \frac{1}{2\sqrt{\pi}} \int_0^\infty e^{-t} f_{gg}(t)\, dt \approx \frac{1}{2\sqrt{\pi}} E\left(e^{-t}\right) \approx \frac{1}{2\sqrt{\pi}} \left(\left(\frac{1}{\beta_M}\right)^{\xi_M} + 1\right)^{-\alpha_M} \left(\frac{1}{\beta_M}\right)^{\alpha_M\xi_M}. \tag{5.15}$$

The BER of 4-QAM and M-QAM can be also obtained following the same procedure. They are shown in Table 5.2 [Hong et al. 2010].

2-QAM	$P_{2qam} \approx \frac{1}{2\sqrt{\pi}} \left(1 + \left(\frac{1}{\beta_M}\right)^{\xi_M}\right)^{-\alpha_M} \left(\frac{1}{\beta_M}\right)^{\alpha_M \xi_M}$
4-QAM	$P_{4qam} \approx \frac{1}{2\sqrt{\pi}} \left(\frac{1}{2} + \left(\frac{1}{\beta_M}\right)^{\xi_M}\right)^{-\alpha_M} \left(\frac{1}{\beta_M}\right)^{\alpha_M \xi_M}$
M-QAM	$P_{Mqam} \approx \frac{2}{\log_2(M)\sqrt{\pi}} \left(\frac{3}{2(M-1)} + \left(\frac{1}{\beta_M}\right)^{\xi_M}\right)^{-\alpha_M} \left(\frac{1}{\beta_M}\right)^{\alpha_M \xi_M}$

Table 5.2: Approximate average BER for uncoded modulations at low SNR.

5.3 Closed-form approximation of average bit error rate for coded M-QAM

Furthermore, for M-QAM modulations in conjunction with a convolutional code of rate $r_c = k_c/n_c$ and minimum distance d_f, the BER at the output of the decoder can be approximated, for high SNR, as (4.21) shown.

Using the parameters (4.22)-(4.23) and the approximations for uncoded modulations in Table 5.1, the average BER for coded M-QAM systems can be approximated as shown in Table 5.3.

5.4 Numerical examples

The same transmit correlation matrix as in (4.29) and the power matrix $\mathbf{P} = \mathbf{I}$ of section 4.3.1 are used here.

Fig. 5.1 shows the excellent agreement between the Monte Carlo simulation (exa) and those approximations (app) in Table 5.1, for the operational range of interest ($P_e \leq 10^{-1}$).

Figure 5.2 shows the average BER of each transmitted stream with different modulation schemes when $\rho = 0$ and SNR is 5 dB or 20 dB. The four theoretical expressions here developed are represented, namely: Gamma approximation (Gamma), high SNR Gamma approximation (App Gamma), generalized Gamma approximation (g Gamma) and low SNR generalized Gamma approximation (App g Gamma). It can be seen that for high SNR the generalized Gamma approximation fits extremely well the simulation results (the curves labeled with Sim represent the 4 transmitted streams in the 4x4

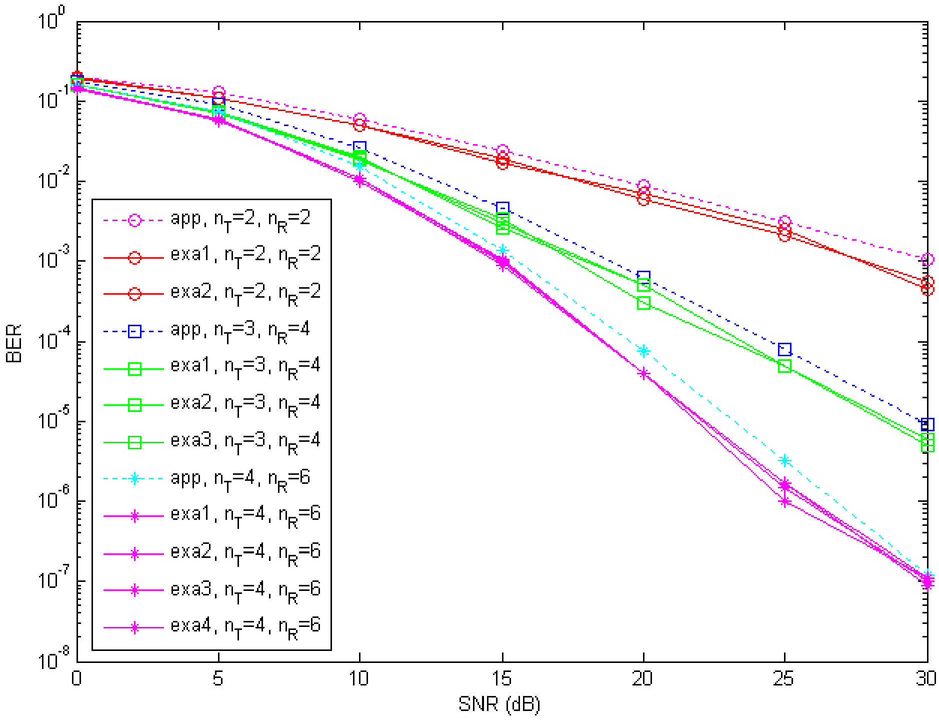

Figure 5.1: Simulated and approximate average BER for uncoded QPSK - i.i.d Rayleigh flat-fading channel.

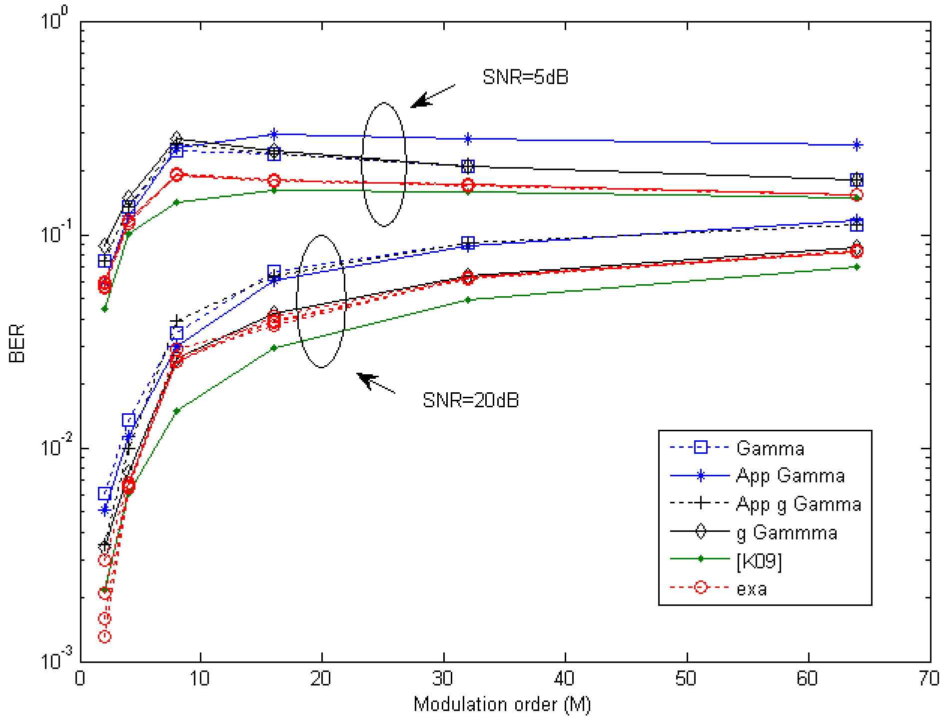

Figure 5.2: Average BER for 4×4 MIMO with precoding - several modulations (represented by modulation order M), SNR = 5 dB and 20 dB. $\rho = 0$.

Constellation	BER approximation with $\xi > 1$
2-QAM	$P_{c\_2qam} \approx D \exp\left(\frac{\alpha_M}{\xi_M - 1}\left(1 - \left(1 + \frac{d_f \beta_M \xi_M}{2}\right)^{\frac{\xi_M - 1}{\xi_M}}\right)\right)$
4-QAM	$P_{c\_4qam} \approx D \exp\left(\frac{\alpha_M}{\xi_M - 1}\left(1 - \left(1 + \frac{d_f \beta_M \xi_M}{4}\right)^{\frac{\xi_M - 1}{\xi_M}}\right)\right)$
M-QAM	$P_{c\_Mqam} \approx \frac{4D}{\log_2(M)} \exp\left(\frac{\alpha_M}{\xi_M - 1}\left(1 - \left(1 + \frac{3 d_f \beta_M \xi_M}{4(M-1)}\right)^{\frac{\xi_M - 1}{\xi_M}}\right)\right)$
Constellation	BER approximation with $\xi < 1$
2-QAM	$P_{c\_2qam} \approx D \exp\left(\frac{\alpha_M}{1 - \xi_M}\left(\left(\frac{1}{1 + \frac{d_f \beta_M \xi_M}{2}}\right)^{\frac{1 - \xi_M}{\xi_M}} - 1\right)\right)$
4-QAM	$P_{c\_4qam} \approx D \exp\left(\frac{\alpha_M}{1 - \xi_M}\left(\left(\frac{1}{1 + \frac{d_f \beta_M \xi_M}{4}}\right)^{\frac{1 - \xi_M}{\xi_M}} - 1\right)\right)$
M-QAM	$P_{c\_Mqam} \approx \frac{4D}{\log_2(M)} \exp\left(\frac{\alpha_M}{1 - \xi_M}\left(\left(\frac{1}{1 + \frac{3 d_f \beta_M \xi_M}{4(M-1)}}\right)^{\frac{1 - \xi_M}{\xi_M}} - 1\right)\right)$

Table 5.3: Approximate average BER for coded modulations.

system) while the other three approximations slightly overestimate the average BER. For low SNR the fit is not so accurate while still the generalized Gamma gives the best approximation together with its low SNR approximation (App g Gamma). Also shown in this Figure are the values obtained in [Kammoun et al. 2009] ([K09]) where it has been included the effect of the precoder. It can be seen that they are not accurate for high SNR.

Figure 5.3 shows the average BER of each transmitted stream with Quadrature Phase Shift Keying (QPSK) modulation when $\rho = 0.9$ and SNR is varied between 0 dB and 30 dB. For this value of ρ the BER of the 4 transmitted streams get very dissimilar values due to the different SINR induced by the precoder, suggesting the importance of being able to properly choose the transmitted powers. Since they are the most accurate and for the sake of clarity, here only the generalized Gamma and its low SNR approximation are represented and it can be seen that again the generalized Gamma produces very close values to the simulation results for all SNR values. On the other hand, the average BER obtained in [Guo et al. 2002] ([G02]) under the Normal approximation assumed large antenna dimensions and it can be seen that it is clearly not accurate for a small number of antennas.

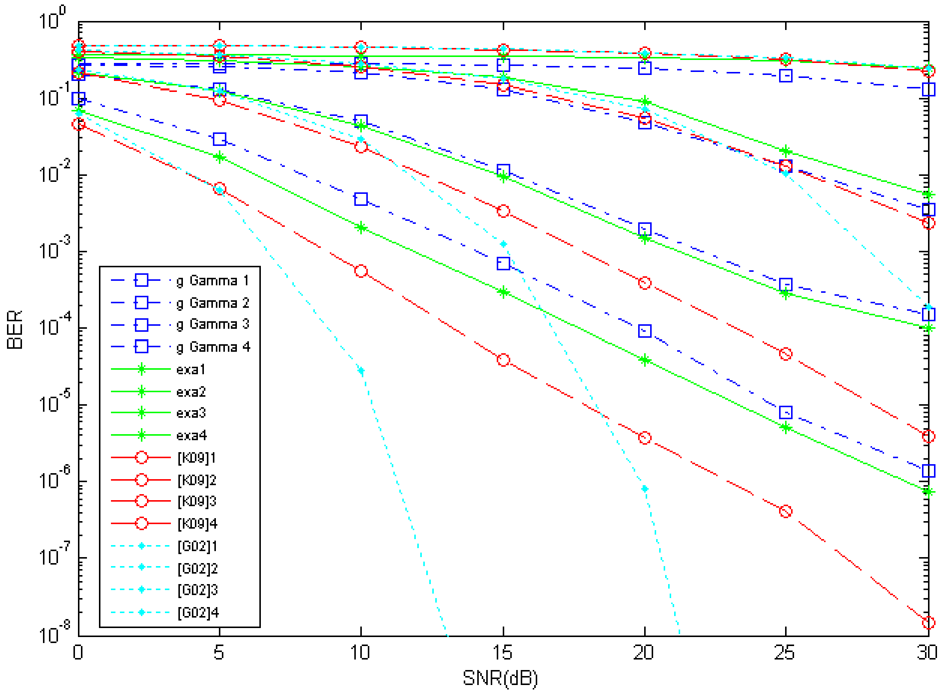

Figure 5.3: Average BER for 4×4 MIMO with precoding - QPSK modulation and several values of SNR. $\rho = 0.9$. Analytical versus simulated values.

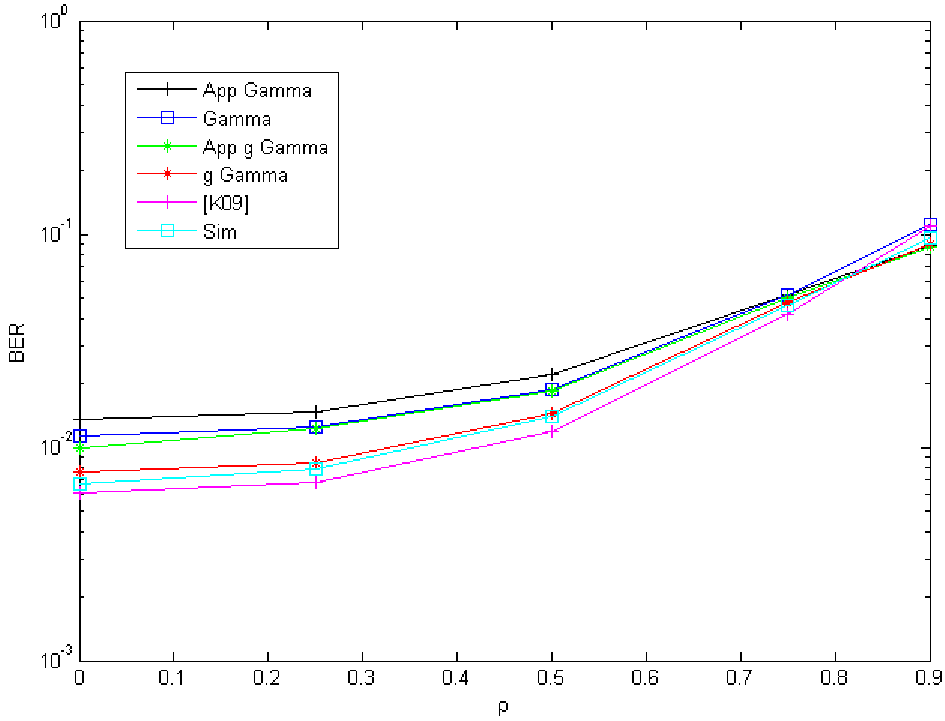

Figure 5.4: Average BER (averaged also over the 4 transmitted streams) for 4×4 **MIMO with precoding -** QPSK modulation and SNR=20dB.

Figure 5.4 shows the average BER, averaged over the 4 transmitted streams, with QPSK modulation when SNR=20 dB and different values of ρ. It can be seen that the generalized Gamma gives a very good fit for all values of ρ. Reference [Kammoun et al. 2009] ([K09]) assumes correlation only at the receiver side so it can be expected to be accurate only for the smallest values of ρ. However, even for these values it can be seen that our expressions give a better fit to the simulation results because [Kammoun et al. 2009] ([K09]) is not accurate for high SNR values.

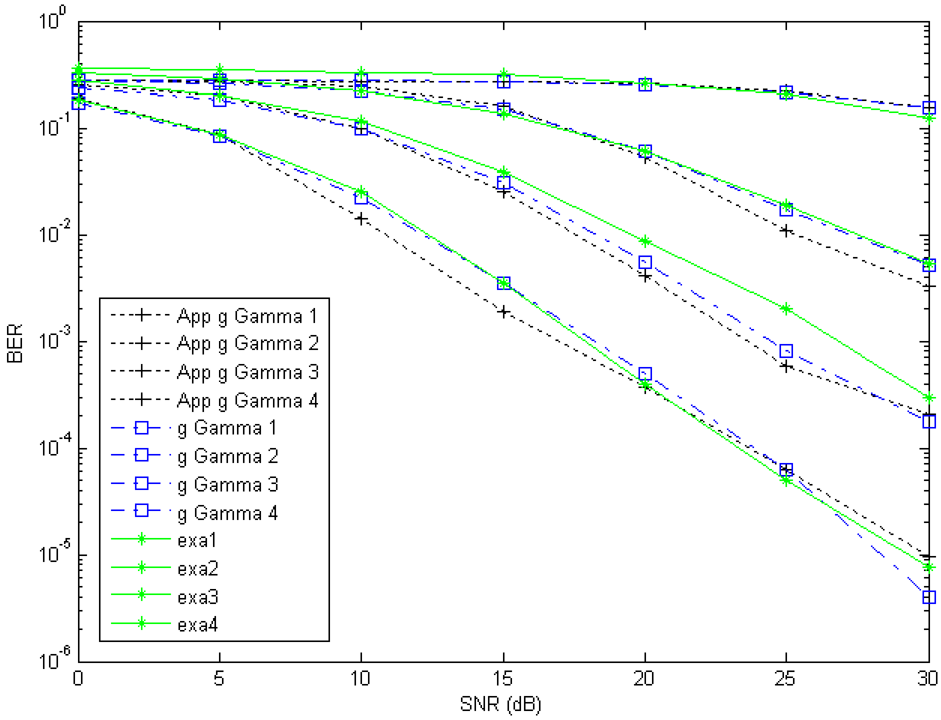

Figure 5.5: Analytical versus simulated values - Average BER for 4×4 MIMO with precoding and nonuniform power [1.8,1.2,0.6,0.4]. QPSK modulation and several values of SNR. $\rho = 0.9$.

The results shown until now considered a uniform power allocation. In Figure 5.5 the average BER is shown for a non-uniform power allocation example where the values of the $[p_1, p_2, p_3, p_4]$ are set to 1.8, 1.2, 0.6 and 0.4, so the stream that is transmitted through the worst channel is enhanced with a higher power (i.e. the effect of the channel is somehow compensated by the power allocation). It can be again seen a good fit of the analytical and Monte Carlo simulations.

5.5 Conclusion

Analytical expressions for the average BER of MIMO systems in transmit-correlated Rayleigh flat-fading channels with or without precoding and with MMSE receivers have been obtained in this chapter. These expressions, whose accuracy even for small dimensions has been shown by analysis of numerical results, can be used to optimize the transmitter for a given target BER or, in general, as a useful tool for the system design.

6

Optimization of a MIMO system with MMSE receiver

Bit and power loading schemes for a single user MIMO system using a Minimum Mean-Squaree Error (MMSE) receiver are proposed. The schemes define the precoding at the transmitter, based on the knowledge of statistical channel information. The relationship between the average bit error probability at the receiver and the powers allocated at the transmitter is used, when the signal goes through a correlated Rayleigh flat-fading channel, in order to improve the system performance by either maximizing the bit rate or minimizing the power. Finally, the performance of the proposed schemes is analyzed and benchmarked with respect to a non-optimized transmission and a bitloaded scheme with Zero Forcing (ZF) receiver.

6.1 Optimization problem

As we mention in previous chapters, it is feasible to assume that the receiver has perfect instantaneous channel state information (CSIR). However, since this information is usually estimated at the receiver side and fed back to the transmitter, it can be assumed that only the channel distribution information is known at the transmitter (CDIT). Optimal design of linear MMSE precoders and decoders with perfect channel knowledge at both transmitter and receiver ends is analyzed in [Scaglione et al. 2002]. In [Tulino et al. 2006] the input covariance of the Gaussian input that achieves capacity when the channel is known at the receiver (CSIR) but only the channel distribution is known at the transmitter (CDIT) is obtained.

In [Chien-Chang Li et al. 2009], the optimization of the transceiver jointly with bitloading is proposed for MIMO assuming perfect channel state information at the transmitter (CSIT) and a ZF receiver. Chengshan Xiao and Yahong Rosa Zheng propose an iterative algorithm for MIMO precoding systems with partial but instantaneous channel state information at the transmitter and discrete-constellation inputs in [Xiao et al. 2009].

Here, making use of the SINR distribution, the bit and power loading problem for precoded MIMO systems is solved, based on the average bit error probability achieved at the MMSE receiver when the signal goes over a correlated Rayleigh flat-fading channel. For M-QAM MIMO MMSE receivers over a correlated Rayleigh flat-fading channel, some closed-form BER approximations are presented in the previous chapter and [Hong et al. 2010]. These approximations are used to realize the bit loading and power allocation.

The problems of bit maximization and power minimization have been described by (4.27) and (4.28). Now the optimization is done searching for the best combinations of bit (i.e., constellation cardinalities) and power loads. For each possible bit allocation, and using the approximations in Table 5.1 that relate the BER with the power matrix $\mathbf{P} = \mathrm{diag}\,[p_1,\ \cdots,\ p_i,\ \cdots,\ p_{n_T}]$, the appropriate constraints can be enforced. Clearly, for a given set of constraints, the total number of bits with an MMSE receiver cannot be less than with a ZF receiver. Therefore, the starting point for the search is always the solution derived in chapter IV for ZF receivers, and the search progresses from that point towards higher loads until the constraints set in. The process is usually quick and, even if truncated before termination, it always returns a performance point that is superior to that achieved with a ZF receiver.

Nevertheless, the complexity of exhaustive search is exponential, so the main target of the following steps is to add more feasible constraints to the exhaustive search to speed up the solution of these two optimization problems.

6.2 Optimal bit distribution ordering

Because of the effect of the precoder matrix $\mathbf{V}$ and the channel correlation parameter $\rho \geq 0$, $\mathbf{R}_a = \mathbf{H}_c^H \mathbf{H}_c$ is a positive definite matrix and its eigenvalues are all positive real values, which can be sorted as

$$\lambda_1 \leq \lambda_2 \leq \cdots \leq \lambda_i \leq \lambda_j \leq \cdots \leq \lambda_{n_T},\ \lambda_i \geq 0. \tag{6.1}$$

We conjuncture that according to the relationship (6.1), the optimal bit distribution ordering should be

$$b_1 \leq b_2 \leq \cdots \leq b_i \leq \cdots \leq b_{n_T}. \tag{6.2}$$

with b_i meaning the number of bits allocated to the ith stream. The derivation of the proof of this conjecture is described in four parts. Firstly, an accurate BER approximation is derived by using the Moment Generating Function (MGF) of SINR. The second part shows the expression of the three moments of SINR. BER expressions based on these moments of SINR are addressed in the third part. Finally, through considering any two randomly selected antennas i and j, the relationship (6.2) is proved mathematically.

6.2.1 BER based on the SINR moments

It is known that the equations (3) and (71) of [P. Li et al. 2006] based on the normal distribution are accurate for large dimensions. But for small dimensions, they are not accurate, because the higher moments introduce non-negligible errors. So not only the first moment but also higher moments are taken into consideration in the following analysis.

The equation (45) of [P. Li et al. 2006] shows the first moment of SINR, which can be approximated as

$$\mathrm{E}\left(\mathrm{SINR}\right) = \mathrm{E}\left(\mathrm{SINR_{ZF}}\right) + \mathrm{E}\left(\mathrm{T}\right) \approx \frac{n_R - n_T + 1}{n_R}\Sigma + \frac{n_T - 1}{n_R}\Sigma\mu. \tag{6.3}$$

μ can be calculated directly by the expression (5.1). However, in order to facilitate the following derivation, another expression for μ, σ^2 and η in the equations (22)-(24) in [P. Li et al. 2006] can also be used for small antenna dimensions, which are

$$\mu = \frac{1}{n_T - 1}\sum_{i=1}^{n_T - 1}\frac{1}{\left(1 + \frac{1}{n_R}\left(\lambda_i \gamma p\left(i\right)\frac{n_R}{n_T}\right)^2\right)}, \tag{6.4}$$

$$\sigma^2 = \frac{1}{n_T - 1} \sum_{i=1}^{n_t - 1} \frac{1}{\left(1 + \frac{1}{n_R}\left(\lambda_i \gamma p\left(i\right) \frac{n_R}{n_T}\right)^2\right)^2}, \tag{6.5}$$

$$\eta = \frac{1}{n_T - 1} \sum_{i=1}^{n_t - 1} \frac{1}{\left(1 + \frac{1}{n_R}\left(\lambda_i \gamma p\left(i\right) \frac{n_R}{n_T}\right)^2\right)^3}. \tag{6.6}$$

For antenna i, coupled with antenna j and (any other antenna besides i and j) z, from (6.4)-(6.6), α_M in (5.3) can be seen as a function of the following variables

$$\alpha_M\left(\lambda_i p_i, \lambda_j p_j, \lambda_z p_z\right). \tag{6.7}$$

Similarly, β_M in (5.4) and ξ_M in (5.6) can also be seen as a functions of the following variables

$$\beta_M\left(\lambda_i p_i, \lambda_j p_j, \lambda_z p_z\right), \tag{6.8}$$

and

$$\xi_M\left(\lambda_i p_i, \lambda_j p_j, \lambda_z p_z\right). \tag{6.9}$$

respectively.

Plugging (6.7)-(6.9) into (5.10) or (5.11), $P_{mqam}\left(\alpha_M, \beta_M, \xi_M\right)$ can be expressed as

$$P_{mqam}\left(A_{p_i}, s_{p_i}, \alpha_M\left(\lambda_i p_i, \lambda_j p_j, \lambda_z p_z\right), \beta_M\left(\lambda_i p_i, \lambda_j p_j, \lambda_z p_z\right), \xi_M\left(\lambda_i p_i, \lambda_j p_j, \lambda_z p_z\right)\right), \tag{6.10}$$

so that can be further simplified as

$$P_{mqam}\left(A_{p_j}, s_{p_j}, \lambda_i p_i, \lambda_j p_j, \lambda_z p_z\right). \tag{6.11}$$

6.2.2 Comparison of any two randomly selected antennas with the target $\overline{\mathrm{BER}}$

If the maximum number of bits is B for each antenna, for any two randomly selected antennas i and j, the possible combinations of the bits allocated to them are $\{b_i,\ b_j\}$.

All the combinations of $\{b_i,\ b_j\}$ can build a matrix $\mathrm{C}_{n,m}$, $n, m = 0, \cdots, B$, where n is the number of allocated bits for antenna i and m is the number of allocated bits for antenna j. That is, each $(n,\ m)$th entry of $\mathrm{C}_{n,m}$ equals to $\{n,\ m\}$.

At first, only the $\mathrm{C}_{n,n}$ combinations are concerned, in order to derive some equations for the next step. And then, combining the previous results, the comparisons of $\mathrm{C}_{m,n}$ and $\mathrm{C}_{n,m}$ are introduced to conclude the proof.

6.2.2.1 Analysis of $\mathrm{C}_{n,n}$

When the bit distribution is $\mathrm{C}_{n,n}$, considering (6.11), the average BER of antenna i and j can be obtained.

For the same target $\overline{\mathrm{BER}}$, for antenna i, its average BER satisfies

$$P_{mqam}\left(A_{p_i}^{\mathrm{C}_{n,n}}, s_{p_i}^{\mathrm{C}_{n,n}}, \lambda_i p_i^{\mathrm{C}_{n,n}}, \lambda_j p_j^{\mathrm{C}_{n,n}}, \lambda_z p_z^{\mathrm{C}_{n,n}}\right) = \overline{\mathrm{BER}}. \tag{6.12}$$

For antenna j,

$$P_{mqam}\left(A_{p_j}^{\mathrm{C}_{n,n}}, s_{p_j}^{\mathrm{C}_{n,n}}, \lambda_j p_j^{\mathrm{C}_{n,n}}, \lambda_i p_i^{\mathrm{C}_{n,n}}, \lambda_z p_z^{\mathrm{C}_{n,n}}\right) = \overline{\mathrm{BER}}. \tag{6.13}$$

As the modulation type of antenna i and j are the same,

$$A_{p_i}^{\mathrm{C}_{n,n}} = A_{p_j}^{\mathrm{C}_{n,n}}, \tag{6.14}$$

$$s_{p_i}^{\mathrm{C}_{n,n}} = s_{p_j}^{\mathrm{C}_{n,n}}. \tag{6.15}$$

Equations (6.12) and (6.13) have the same structure, and the part $\left(\lambda_i p_i^{\mathrm{C}_{n,n}}, \lambda_j p_j^{\mathrm{C}_{n,n}}\right)$ is symmetrical with $\left(\lambda_j p_j^{\mathrm{C}_{n,n}}, \lambda_i p_i^{\mathrm{C}_{n,n}}\right)$. After plugging (6.14) and (6.15) into (6.12) and (6.13), and combining them, the relation of the assigned powers $p_i^{\mathrm{C}_{n,n}}$ and $p_j^{\mathrm{C}_{n,n}}$ is found

$$\lambda_i p_i^{\mathrm{C}_{n,n}} = \lambda_j p_j^{\mathrm{C}_{n,n}}. \tag{6.16}$$

6.2.2.2 Comparisons of $\mathrm{C}_{m,n}$ and $\mathrm{C}_{n,m}$

For any two randomly selected antennas i and j, starting with the same modulation $\mathrm{C}_{n,n}$, additional Δb bits will be added to one of them. Obviously, there are two possible ways to do it. One is adding Δb to antenna i, and another is adding Δb to antenna j.

$\mathrm{C}_{m,n}$ and $\mathrm{C}_{n,m}$ can be expressed as

1.

$$\mathrm{C}_{m,n}, \quad m = n + \Delta b, \tag{6.17}$$

where Δb can be any one of the set $\{0,\ 1,\ \cdots,\ B-n\}$, and only added on antenna i. Alternatively

2.

$$\mathrm{C}_{n,m}, \quad m = n + \Delta b. \tag{6.18}$$

In case 1, if Δb is only added to the antenna i, and the bits of any other antenna are not changed, the bit distribution of these two antennas is now $\mathrm{C}_{m,n}$. To load more Δb bits, the incremental energy of antenna i, j and z can be respectively denoted as

$$\Delta p_i^{\mathrm{C}_{m,n}},\ \Delta p_j^{\mathrm{C}_{m,\ n}},\ \Delta p_z^{\mathrm{C}_{m,\ n}}. \tag{6.19}$$

Their assigned powers are

$$\begin{array}{l} p_i^{\mathrm{C}_{m,n}} = p_i^{\mathrm{C}_{n,n}} + \Delta p_i^{\mathrm{C}_{m,n}} \\ p_j^{\mathrm{C}_{m,n}} = p_j^{\mathrm{C}_{n,n}} + \Delta p_j^{\mathrm{C}_{m,n}} \\ p_z^{\mathrm{C}_{m,n}} = p_z^{\mathrm{C}_{n,n}} + \Delta p_z^{\mathrm{C}_{m,n}} \end{array} . \tag{6.20}$$

In case 2, if additional Δb bits are only added to the antenna j, and the bits of any other antenna are not changed, the bit distribution of these two antennas is now $\mathrm{C}_{n,m}$. Similarly to case 1, the incremental energy of each antenna can also be respectively denoted as

$$\Delta p_i^{\mathrm{C}_{n,m}},\ \Delta p_j^{\mathrm{C}_{n,\ m}},\ \Delta p_z^{\mathrm{C}_{n,\ m}}. \tag{6.21}$$

and their assigned powers can be expressed as

$$p_i^{\mathrm{C}_{n,m}},\ p_j^{\mathrm{C}_{n,\ m}},\ p_z^{\mathrm{C}_{n,\ m}}. \tag{6.22}$$

For these two cases, their new average bit error rates satisfy

$$\begin{aligned}&P_{mqam}\left(A_{p_i}^{\mathrm{C}_{m,n}}, s_{p_i}^{\mathrm{C}_{m,n}}, \lambda_i p_i^{\mathrm{C}_{m,n}}, \lambda_j p_j^{\mathrm{C}_{m,n}}, \lambda_z p_z^{\mathrm{C}_{m,n}}\right)\\&= \overline{\mathrm{BER}} \qquad ,\\&= P_{mqam}\left(A_{p_i}^{\mathrm{C}_{n,m}}, s_{p_i}^{\mathrm{C}_{n,m}}, \lambda_i p_i^{\mathrm{C}_{n,m}}, \lambda_j p_j^{\mathrm{C}_{n,m}}, \lambda_z p_z^{\mathrm{C}_{n,m}}\right)\end{aligned} \tag{6.23}$$

$$\begin{aligned}&P_{mqam}\left(A_{p_j}^{\mathrm{C}_{m,n}}, s_{p_j}^{\mathrm{C}_{m,n}}, \lambda_j p_j^{\mathrm{C}_{m,n}}, \lambda_i p_i^{\mathrm{C}_{m,n}}, \lambda_z p_z^{\mathrm{C}_{m,n}}\right)\\&= \overline{\mathrm{BER}} \qquad ,\\&= P_{mqam}\left(A_{p_j}^{\mathrm{C}_{n,m}}, s_{p_j}^{\mathrm{C}_{n,m}}, \lambda_j p_j^{\mathrm{C}_{n,m}}, \lambda_i p_i^{\mathrm{C}_{n,m}}, \lambda_z p_z^{\mathrm{C}_{n,m}}\right)\end{aligned} \tag{6.24}$$

$$\begin{aligned}&P_{mqam}\left(A_{p_z}^{\mathrm{C}_{m,n}}, s_{p_z}^{\mathrm{C}_{m,n}}, \lambda_z p_z^{\mathrm{C}_{m,n}}, \lambda_i p_i^{\mathrm{C}_{m,n}}, \lambda_j p_j^{\mathrm{C}_{m,n}}\right)\\&= \overline{\mathrm{BER}} \qquad .\\&= P_{mqam}\left(A_{p_z}^{\mathrm{C}_{n,m}}, s_{p_z}^{\mathrm{C}_{n,m}}, \lambda_z p_z^{\mathrm{C}_{n,m}}, \lambda_j p_j^{\mathrm{C}_{n,m}}, \lambda_i p_i^{\mathrm{C}_{n,m}}\right)\end{aligned} \tag{6.25}$$

From the definition of $\mathrm{C}_{m,n}$ and $\mathrm{C}_{n,m}$,

$$A_{p_i}^{\mathrm{C}_{n,m}} = A_{p_j}^{\mathrm{C}_{m,n}}, \tag{6.26}$$

$$s_{p_i}^{\mathrm{C}_{n,m}} = s_{p_j}^{\mathrm{C}_{m,n}}, \tag{6.27}$$

$$A_{p_i}^{\mathrm{C}_{m,n}} = A_{p_j}^{\mathrm{C}_{n,m}}, \tag{6.28}$$

$$s_{p_i}^{\mathrm{C}_{m,n}} = s_{p_j}^{\mathrm{C}_{n,m}}, \tag{6.29}$$

$$A_{p_z}^{\mathrm{C}_{m,n}} = A_{p_z}^{\mathrm{C}_{n,m}}, \tag{6.30}$$

$$s_{p_z}^{\mathrm{C}_{m,n}} = s_{p_z}^{\mathrm{C}_{n,m}}. \tag{6.31}$$

Plugging (6.26)-(6.31) into (6.23)-(6.25), according to the principle of least action [Maupertuis 1744] [Maupertuis 1744], and considering the symmetrical structure of (6.23)-(6.25), the relations of the antenna powers at these two cases are

$$\lambda_i p_i^{\mathrm{C}_{m,n}} = \lambda_j p_j^{\mathrm{C}_{n,m}} = f_1 > 0, \tag{6.32}$$

$$\lambda_i p_i^{\mathrm{C}_{n,\,m}} = \lambda_j p_j^{\mathrm{C}_{m,\,n}} = f_2 > 0, \tag{6.33}$$

$$\lambda_z p_z^{\mathrm{C}_{m,\,n}} = \lambda_z p_z^{\mathrm{C}_{n,\,m}} = f_3. \tag{6.34}$$

When the relation (6.34) $\lambda_z p_z^{\mathrm{C}_{m,\,n}} = \lambda_z p_z^{\mathrm{C}_{n,\,m}}$ is fixed, if

$$\lambda_i p_i^{\mathrm{C}_{m,\,n}} = \lambda_i p_i^{\mathrm{C}_{n,\,m}} = f_4, \tag{6.35}$$

$$\lambda_j p_j^{\mathrm{C}_{m,\,n}} = \lambda_j p_j^{\mathrm{C}_{n,\,m}} = f_5. \tag{6.36}$$

Then, from (5.8) and (6.34)-(6.36), we can see that $f_{gg}\left(t\right)$ is equal for $\mathrm{C}_{m,\,n}$ and $\mathrm{C}_{n,\,m}$ for antenna i, and only the part of $P_e\left(t\right)$ is different. For antenna j, $f_{gg}\left(t\right)$ is also equal for $\mathrm{C}_{m,\,n}$ and $\mathrm{C}_{n,\,m}$, and only the part of $P_e\left(t\right)$ is different. Observing (5.8) and (6.23), the BERs for these two cases $\mathrm{C}_{m,\,n}$ and $\mathrm{C}_{n,\,m}$ are

$$P_{mqam}\left(A_{p_i}^{\mathrm{C}_{m,\,n}}, s_{p_i}^{\mathrm{C}_{m,\,n}}, \lambda_i p_i^{\mathrm{C}_{m,\,n}}, \lambda_j p_j^{\mathrm{C}_{m,\,n}}, \lambda_z p_z^{\mathrm{C}_{m,\,n}}\right) = \int_0^\infty P_e\left(t, A_{p_i}^{\mathrm{C}_{m,\,n}}, s_{p_i}^{\mathrm{C}_{m,\,n}}\right) f_{gg}\left(t\right) dt, \tag{6.37}$$

$$P_{mqam}\left(A_{p_i}^{\mathrm{C}_{n,\,m}}, s_{p_i}^{\mathrm{C}_{n,\,m}}, \lambda_i p_i^{\mathrm{C}_{n,\,m}}, \lambda_j p_j^{\mathrm{C}_{n,\,m}}, \lambda_z p_z^{\mathrm{C}_{n,\,m}}\right) = \int_0^\infty P_e\left(t, A_{p_i}^{\mathrm{C}_{n,\,m}}, s_{p_i}^{\mathrm{C}_{n,\,m}}\right) f_{gg}\left(t\right) dt. \tag{6.38}$$

In (6.37) and (6.38), the modulation cardinality of $\left(A_{p_i}^{\mathrm{C}_{m,\,n}}, s_{p_i}^{\mathrm{C}_{m,\,n}}\right)$ is more than $\left(A_{p_i}^{\mathrm{C}_{n,\,m}}, s_{p_i}^{\mathrm{C}_{n,\,m}}\right)$. In [Proakis 2000], when the mean energy of the constellation is to remain the same (see (6.34)-(6.36)), the points must be closer together and are thus more susceptible to noise. This results in a higher bit error rate (See chapter V and Fig5.2-5 in [Proakis 2000])

$$P_e\left(t, A_{p_i}^{\mathrm{C}_{m,\,n}}, s_{p_i}^{\mathrm{C}_{m,\,n}}\right) > P_e\left(t, A_{p_i}^{\mathrm{C}_{n,\,m}}, s_{p_i}^{\mathrm{C}_{n,\,m}}\right). \tag{6.39}$$

Combining (6.39) and (6.37)-(6.38),

$$\begin{aligned} & P_{mqam}\left(A_{p_i}^{\mathrm{C}_{m,\,n}}, s_{p_i}^{\mathrm{C}_{m,\,n}}, \lambda_i p_i^{\mathrm{C}_{m,\,n}}, \lambda_j p_j^{\mathrm{C}_{m,\,n}}, \lambda_z p_z^{\mathrm{C}_{m,\,n}}\right) \\ & > P_{mqam}\left(A_{p_i}^{\mathrm{C}_{n,\,m}}, s_{p_i}^{\mathrm{C}_{n,\,m}}, \lambda_i p_i^{\mathrm{C}_{n,\,m}}, \lambda_j p_j^{\mathrm{C}_{n,\,m}}, \lambda_z p_z^{\mathrm{C}_{n,\,m}}\right) \end{aligned}. \tag{6.40}$$

Also, observing (6.35) and (6.36), for antenna j,

$$\begin{aligned} &P_{mqam}\left(A_{p_j}^{\mathrm{C}_{n,m}}, s_{p_j}^{\mathrm{C}_{n,m}}, \lambda_j p_j^{\mathrm{C}_{n,m}}, \lambda_i p_i^{\mathrm{C}_{n,m}}, \lambda_z p_z^{\mathrm{C}_{n,m}}\right) \\ &> P_{mqam}\left(A_{p_j}^{\mathrm{C}_{m,n}}, s_{p_j}^{\mathrm{C}_{m,n}}, \lambda_j p_j^{\mathrm{C}_{m,n}}, \lambda_i p_i^{\mathrm{C}_{m,n}}, \lambda_z p_z^{\mathrm{C}_{m,n}}\right) \end{aligned}. \tag{6.41}$$

From (6.40) and (6.41), to achieve the target $\overline{\mathrm{BER}}$ in (6.32) and (6.33), the antenna powers of two cases should satisfy

$$f_1 > f_2. \tag{6.42}$$

Combining (6.32) and (6.33), and recalling (6.1),

$$p_i^{\mathrm{C}_{m,n}} - p_j^{\mathrm{C}_{n,m}} = f_1\left(\frac{1}{\lambda_i} - \frac{1}{\lambda_j}\right) \geq 0, \tag{6.43}$$

$$p_i^{\mathrm{C}_{n,m}} - p_j^{\mathrm{C}_{m,n}} = f_2\left(\frac{1}{\lambda_i} - \frac{1}{\lambda_j}\right) \geq 0. \tag{6.44}$$

Observing (6.42)-(6.44),

$$p_i^{\mathrm{C}_{m,n}} + p_j^{\mathrm{C}_{m,n}} \geq p_i^{\mathrm{C}_{n,m}} + p_j^{\mathrm{C}_{n,m}}. \tag{6.45}$$

From (6.34),

$$p_z^{\mathrm{C}_{m,n}} = p_z^{\mathrm{C}_{n,m}}. \tag{6.46}$$

From (6.45) and (6.46), it requires more sum power on antennas i and j, if Δb are added to the antenna i (6.45) and it requires the same power for antenna z in either case (6.46). So it is better to place Δb in antenna j, which corresponds to bigger λ_j.

Considering this, the bit distribution relationship of these two randomly selected antennas should follow

$$b_i \leq b_j. \tag{6.47}$$

Because these two antennas i and j are randomly selected, (6.47) can be extended to be

$$b_1 \leq b_2 \leq \cdots \leq b_{n_T}. \tag{6.48}$$

which concludes the proof.

6.3 Search procedure and its complexity

In the above part, it is shown that the best of two channels should be used to transmit a number of bits greater or equal than the worst one. And the optimal bit distribution follows (6.48).

Consider that the total required power of MMSE is always slightly lower than the one of ZF for a given $\overline{\mathrm{BER}}$, so the maximum total number of bits of MMSE is not less than that of ZF for each SNR value.

For problem (4.27), the maximum total number of loaded bits of ZF, R_{zf}, is calculated in chapter IV, and this value will be chosen as the starting value for the exhaustive search.

The maximum possible number of bits allocated for each antenna is denoted as $B = \max\{\log_2 M_i\}$, the whole point is to restrict the search to the solutions that lie between the ZF one R_{zf} and the fully-loaded one (B bits on every antenna) with the restriction that eigenvectors having larger eigenvalues receive more bits.

For problem (4.28), given (6.48) and R_{tot}, the minimum power can be obtained by comparing the exhaustive search results calculated when the constrains (6.48) and R_{tot} are all satisfied.

It is interesting to analyze the complexity of the proposed approach.

Denote that the maximal cardinality of each stream is q, then the complexity of complete exhaustive search is $(q+1)^{n_t}$.

Utilizing the proposed method, the complexity of exhaustive search can be decreased noticeably. By adding the constraint (6.48) the calculations of exhaustive search can be reduced to be $\frac{(q+1)^{n_t}}{2^{(n_T-1)}}$.

In problem (4.28), for the target total number of bits R_{tot}, the number of different possible bit combinations is extremely limited. That is the reason why the complexity of problem (4.27) is the main concern.

In the Table 6.1, there is a comparison of the maximum number of trials required to solve problem (4.27), at a typical value $\rho = 0.5$ and $\overline{\mathrm{BER}} = 10^{-2}$, and M_i takes values in the set $\{0, 2, 4, 8, 16, 32, 64\}$ ($q = 6$). The maximum number of trials is required in a medium SNR regime, for both in low and high SNR scenarios, we have seen that the convergence of the process is much faster. When SNR is varying from 0 dB to 30 dB, we have seen that the maximum number of trials is required at an SNR of around 15 dB.

$n_T \times n_R$	Exhaustive search	Exhaustive search with (6.48)	Exhuastive search with (6.48) and the initial value R_{zf}
3×4	343	86	15
8×10	5764801	45038	197

Table 6.1: Maximum number of trials.

6.4 Numerical examples

The transmit covariance matrix $\mathbf{R}$ and the three evaluation scenarios are the same as in chapter IV.

6.4.1 Bit Rate Maximization

Fig. 6.1 shows the achievable bit rate R with optimized power allocation. Two typical values of the correlation parameter ρ are chosen, n_t is 3, n_R is 4 and $\overline{\mathrm{BER}} = 10^{-2}$. Here, the scenario is the second one (6 uncoded bit rates). The effect of correlation on the channel capacity is already known from works like [Joham et al. 2005]. In Fig. 6.1, it can be checked this effect: with high channel correlation, the bit loading algorithm works better for low SNR regimes, while for low correlation, the performance is much better for high SNR values. Apart from that, the performance at high SNR of receivers MMSE and ZF is more similar, so the curves tend to converge in that regime, while MMSE has a clear advantage at low SNR.

The results for the scenario with convolutional codes are shown in Fig. 6.2.

In Fig. 6.3, again the second scenario, in this case with a configuration of $n_T \times n_R = 8 \times 10$, is simulated, showing the applicability of the proposed optimization even under such extreme dimensions.

6.4.2 Power Minimization

The following figures represent the power gain, in dB, of the proposed optimized $\mathbf{P}$ with respect to the uniform power distribution $\mathbf{P} = \mathbf{I}$.

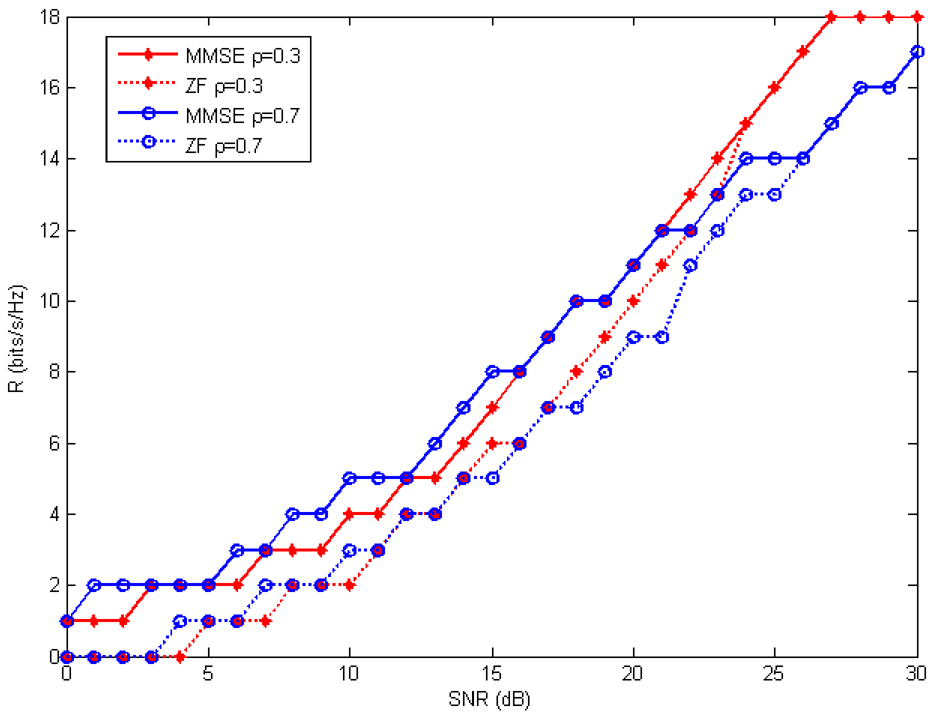

Figure 6.1: Bit rate vs. SNR - 6 uncoded bit rates with $n_T = 3$, $n_R = 4$, and $\overline{\mathrm{BER}} = 10^{-2}$.

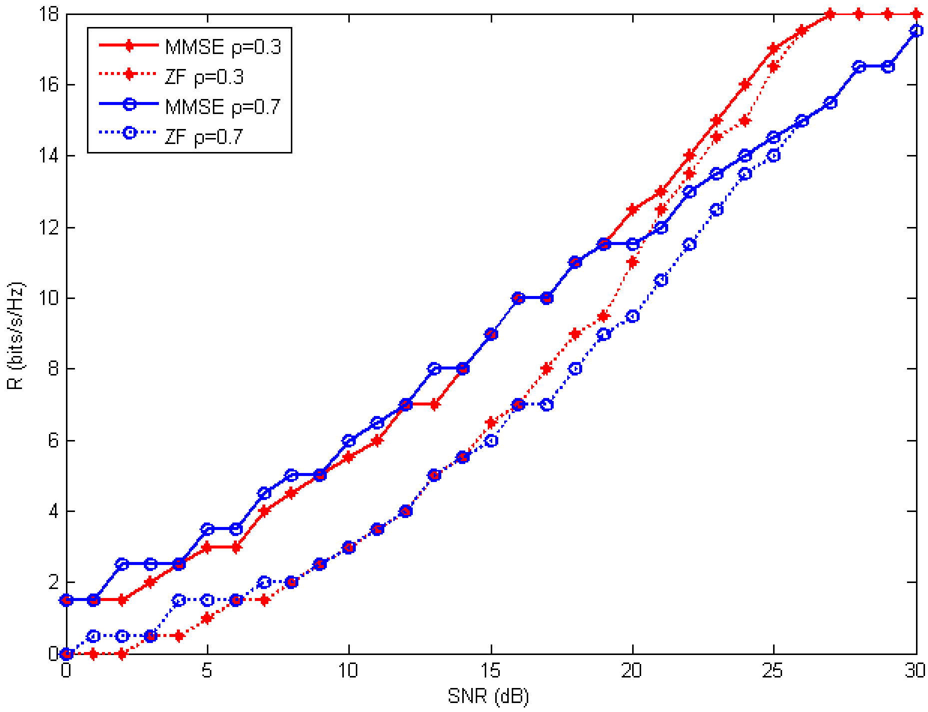

Figure 6.2: Bit rate vs. SNR - 12 uncoded bit rates with $n_T = 3$, $n_R = 4$, and $\overline{\mathrm{BER}} = 10^{-2}$.

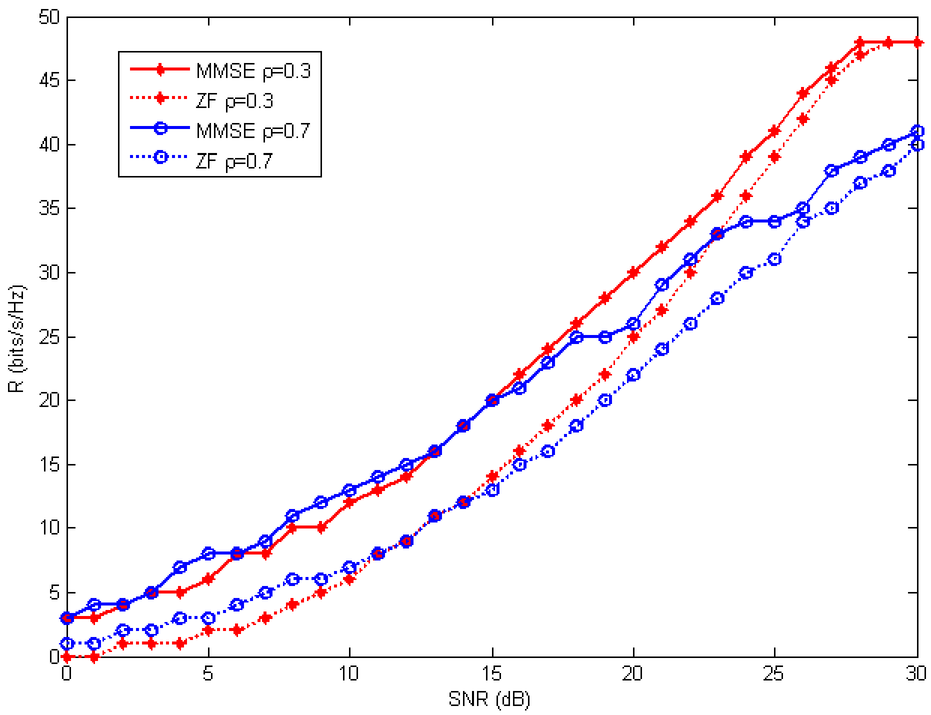

Figure 6.3: Bit rate vs. SNR - 6 uncoded bit rates with $n_T = 8$, $n_R = 10$, and $\overline{\mathrm{BER}} = 10^{-2}$.

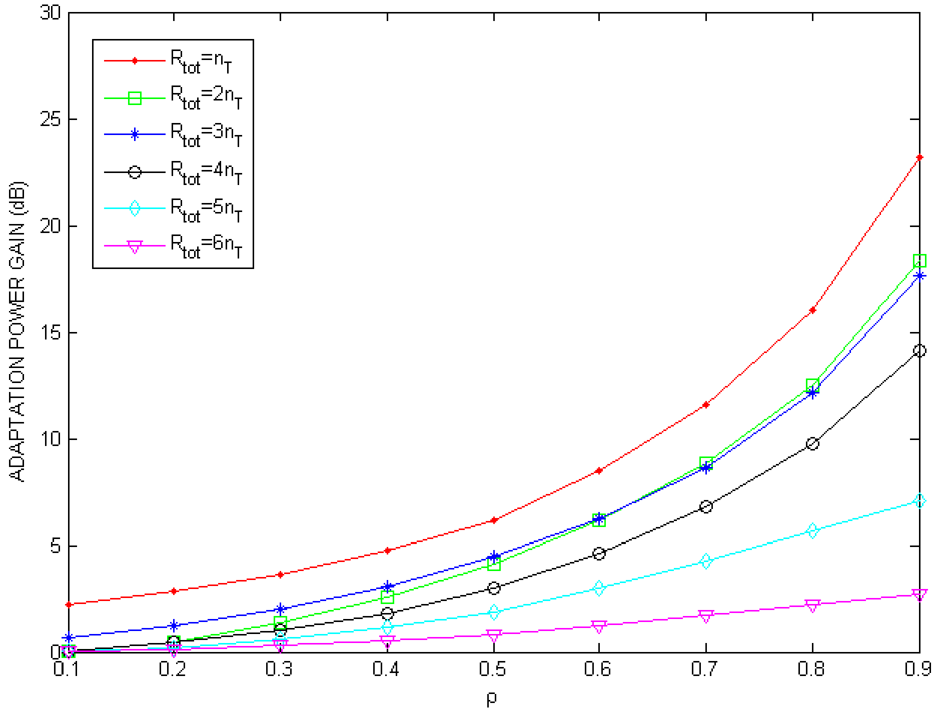

Figure 6.4: Power gain vs. ρ - 6 uncoded bit rates with $n_T = 3$, $n_R = 4$, and $\overline{\mathrm{BER}} = 10^{-2}$.

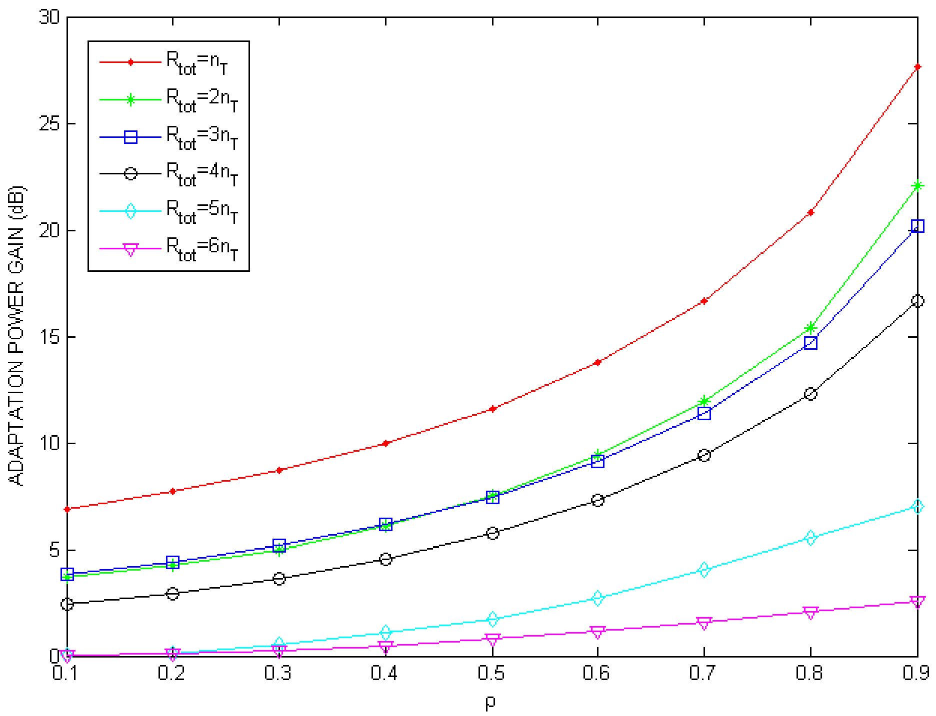

Figure 6.5: Power gain vs. ρ - 6 uncoded bit rates with $n_T = 3$, $n_R = 4$, and $\overline{\mathrm{BER}} = 10^{-4}$.

Fig. 6.4 shows the power gain when $\overline{\text{BER}} = 10^{-2}$ and $n_T \times n_R = 3 \times 4$.

In Fig. 6.5, the only parameter changed with respect to Fig. 4 is the target $\overline{\text{BER}}$, that now is 10^{-4}. We can see that it has little effect on the performance comparison.

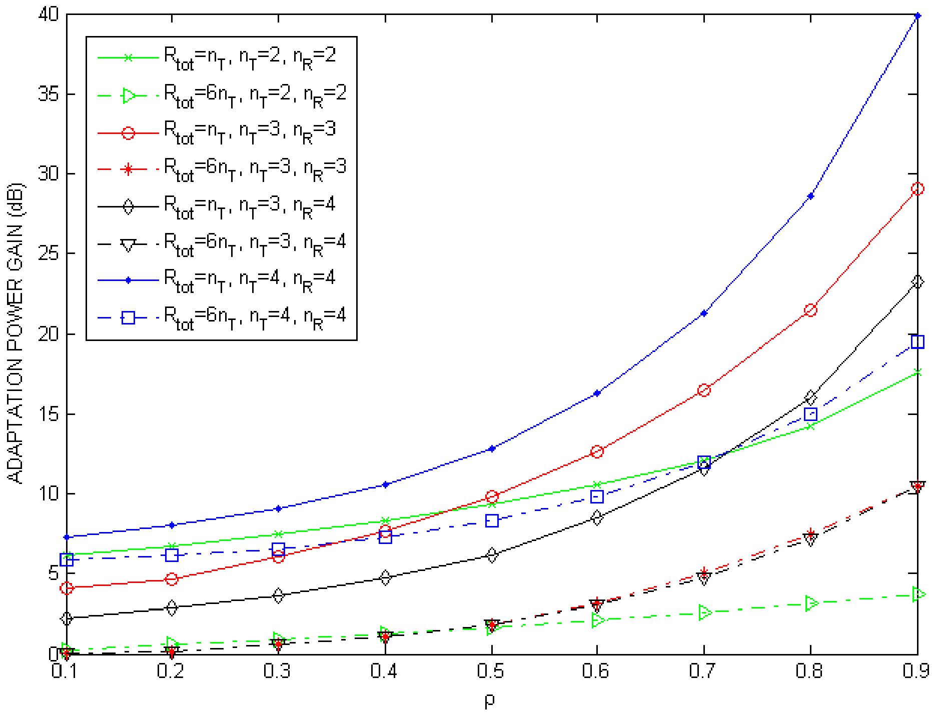

Figure 6.6: Power gain vs. $\boldsymbol{\rho}$ - 8 uncoded bit rates with $\overline{\text{BER}} = 10^{-2}$.

Finally, Fig. 6.6 and Fig. 6.7 show two extreme cases with the constraint $\overline{\text{BER}} = 10^{-2}$, when the required bit rate is either $R_{tot} = n_T$ or $R_{tot} = 6n_T$. When $R_{tot} = n_T$, the low SNR behaviour is illustrated, and the high SNR performance is explored when $R_{tot} = 6n_T$. From these Figs. 6.6 and 6.7, it can be seen that attainable gain in the low SNR regime is higher than that in the high SNR regime. This is so, as in high SNR regime the constellations used are always the higher cardinality constellations, leaving no gap for improvement.

The power gain in Fig. 6.8 and Fig. 6.9 is defined for the optimized MMSE approach as compared to the ZF power allocated by using the Levin-Campello algorithm in chapter IV. From this comparison, the difference of power gain between MMSE and ZF is varying from 0.2 dB to 5.5 dB in Fig. 6.8 and the gain is within the range 0-9.5

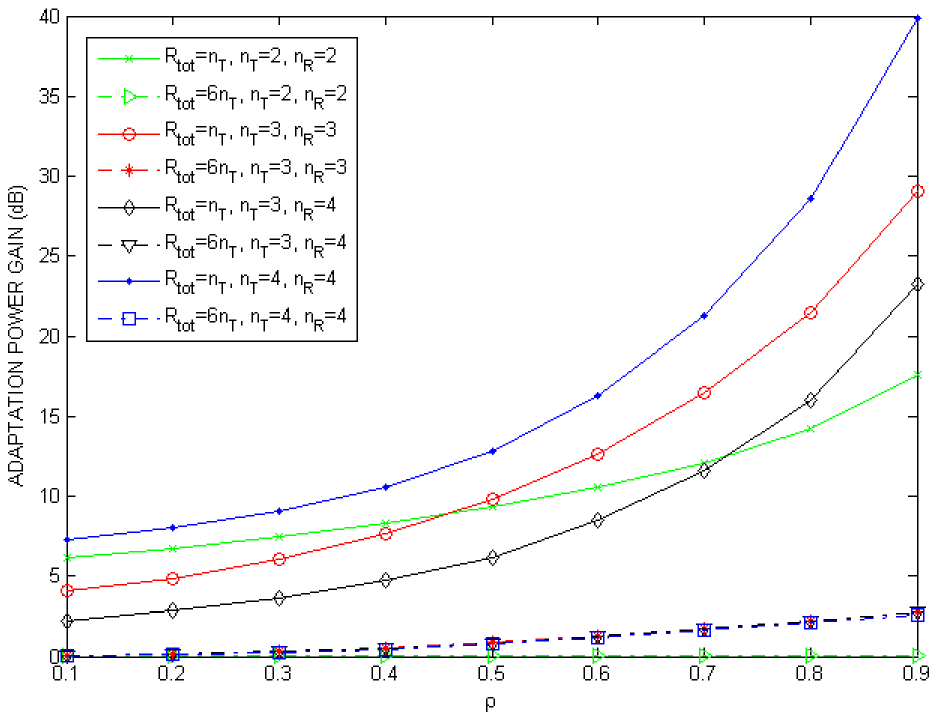

Figure 6.7: Power gain vs. ρ - 6 uncoded bit rates with $\overline{\mathrm{BER}} = 10^{-2}$.

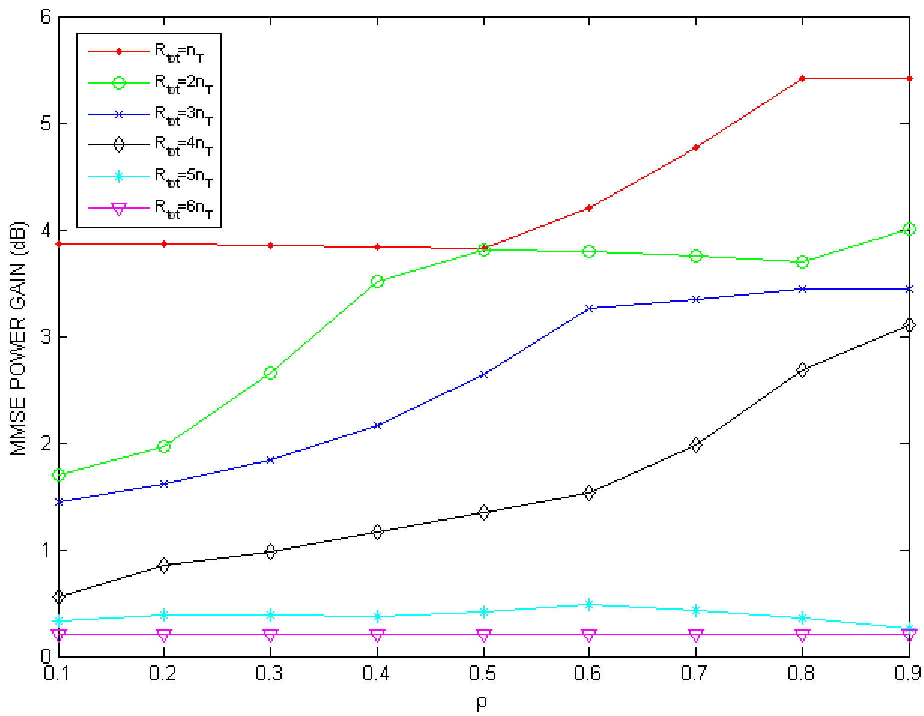

Figure 6.8: Power gain vs. ρ - 6 uncoded bit rates with $n_T = 3$, $n_R = 4$, and $\overline{\mathrm{BER}} = 10^{-2}$.

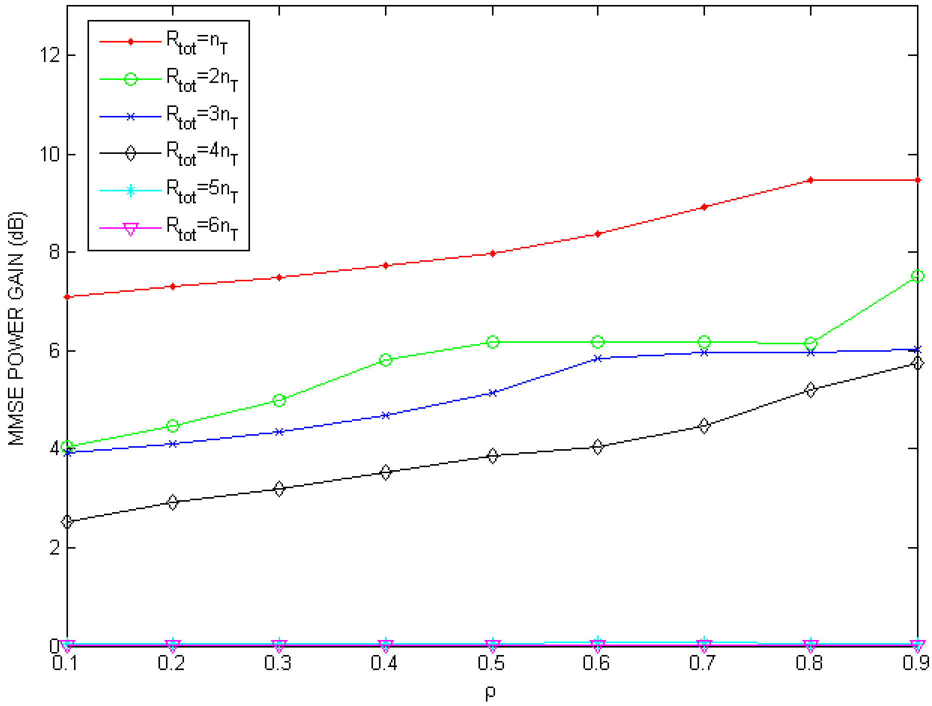

Figure 6.9: Power gain vs. ρ - 6 uncoded bit rates with $n_T = 3$, $n_R = 4$, and $\overline{\text{BER}} = 10^{-4}$.

dB in Fig. 6.9.

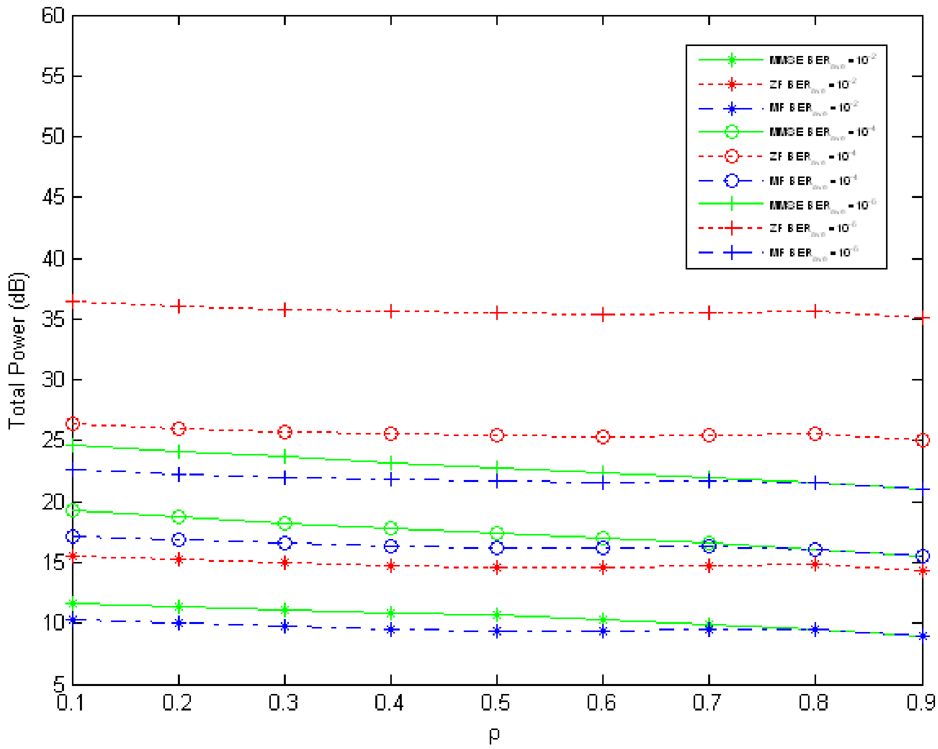

Figure 6.10: Total power vs. ρ - 6 uncoded bit rates with $n_T = 3$, $n_R = 4$, and $R_{tot} = n_T$.

In order to benchmark the performance of the previous schemes with the corresponding to a MF (matched filter) receiver, the bit and power allocation for the later can be obtained following the scheme in chapter IV, similarly to that of the ZF receiver, assuming there is no interference. The MF is an optmimum receiver that assumes there is no interference among the spatial streams. Even though it is not practical, we use it here as an upper bound of the performance that may be achieved. It is known that MMSE approaches MF performance for low SNR.

In figures Fig. 6.10 and Fig. 6.11 we plot the total required transmit power when the SNR is fixed to 0 dB, and the target total number of bits R_{tot} equals n_T for Fig. 6.10, and $6n_T$ for Fig. 6.11.

In Fig. 6.10 it can be seen how the total power remains approximately constant for

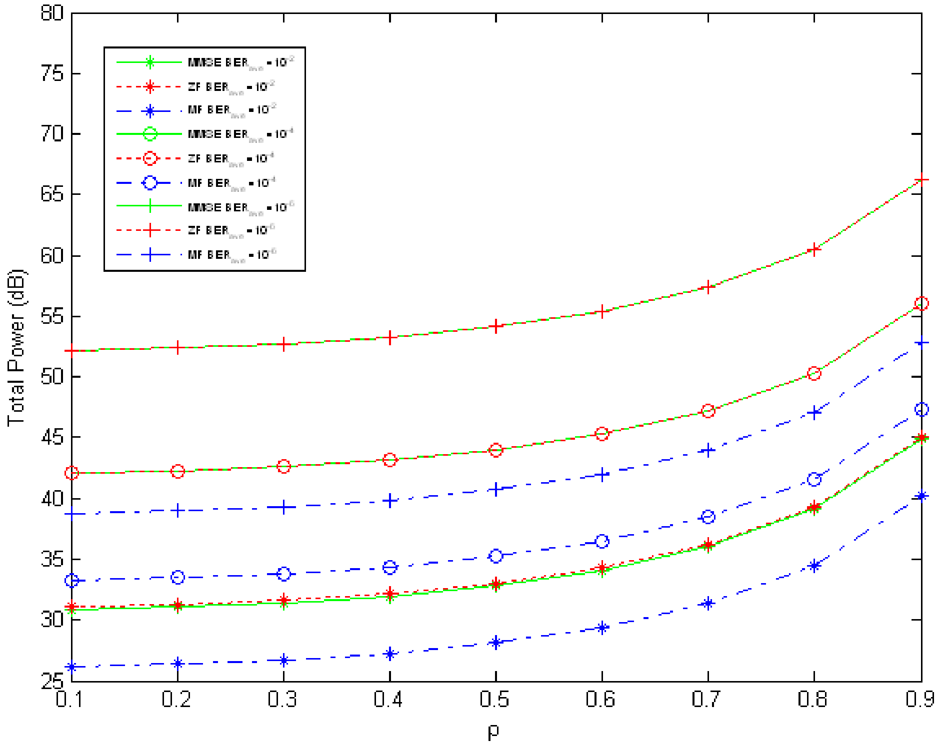

Figure 6.11: Total power vs. $\boldsymbol{\rho}$ - 6 uncoded bit rates with $n_T = 3$, $n_R = 4$, and $R_{tot} = 6n_T$.

all values of the correlation parameter ρ, as for lower values of this parameter the bits and power are allocated evenly through out all the channels, while for higher values of ρ the optimization process assigns higher number of bits and power to those channels with better characteristics. The performance of MMSE is very close to MF for this low SNR situation, as it should be expected.

In Fig. 6.11, as $R_{tot} = 6n_T$, it is hard to assign more bits to better channels when ρ is high, the result is an increasing total required power. Another characteristic that is observed is that the difference between MMSE and ZF tends to vanish, with respect to the result shown in Fig. 6.10, as it corresponds to high SNR.

6.5 Conclusion

For uncoded or coded modulation in a single-user MIMO communication system with a MMSE receiver, using the developed BER approximations, an efficient method is proposed for solving the two dual optimization problems, bit rate maximization and power minimization. As shown by the simulations, lower power cost and higher bit rates are achieved with this optimization scheme. The asymptotical performance (low and high SNR) of MMSE is also analyzed and compared with ZF and MF.

7

Optimization of a MIMO system with ZF-SIC receiver

This chapter analyzes the bit error rate (BER) after a zero-forcing successive interference cancellation (ZF-SIC) receiver over uncorrelated or (transmit) correlated Rayleigh flat-fading channels in MIMO wireless communication. Since the decoding ordering is important for this kind of receivers, we will take it into account for the development of the BER expressions. Using a Gamma approximation for the SINR of the ZF receiver, a closed-form formulation can be derived and simplified for the average BER. Furthermore, bit and power loading schemes for a single user MIMO system using a ZF-SIC receiver are proposed. The schemes define precoding at the transmitter, based on the knowledge of statistical channel information. The developed approximations for the BER and decoding ordering are used in order to improve the system performance by either maximizing the bit rate or minimizing the power. We obtain some bounds for the bit rate of ZF-SIC and a tree search algorithm facilitates the search process to be more efficient. Finally, to show the accuracy of the proposed expressions, the theoretical results are compared with those of Monte Carlo simulations and the performance of the proposed schemes is analyzed and benchmarked with respect to bitloaded schemes with more simple linear receivers.

7.1 BER of ZF-SIC receiver based on the Gamma distribution

Despite the simplicity of the ZF receiver it is suboptimum and it can be outperformed by other receiver choices, or by more advanced receivers such as successive interference cancelation (SIC) [Paulraj 2003]. With the aim of improving the performance of the ZF scheme of Chapter IV, in this chapter a bit loading procedure will be proposed for a MIMO system with ZF-SIC receiver.

For the development of such a bit loading scheme a relationship between the average bit error rate (BER) after the ZF-SIC receiver and the powers allocated at the transmitter under the premise of CDIT is required. A number of papers estimate the BER of MIMO ZF-SIC receivers based on their SINR distribution. In [Gore et al. 2002], the authors proposed a chi-square distribution to approximate the SINR of a ZF receiver while it is proved in [Xin Li and Nie 2004] that the SINR of ZF-SIC may be approximated by a chi-square distribution in correlated channels at both transmitter side and receiver side. The error performance bounds of ZF and perfect ZF-SIC in M-QAM MIMO systems are analyzed in [XU et al. 2008] without considering channel correlation and receiver error propagation. In [Wang and Blostein 2007] the SINR of ZF-SIC is approximated by a noncentral chi-square density function.

While [Gore et al. 2002] used a chi-square approximation of the SINR, it is shown in [P. Li et al. 2006] that the SINR obtained after a MIMO ZF follows a Gamma distribution. The BER of MIMO ZF after a correlated Rayleigh flat-fading channel is derived in [P. Li et al. 2006] using a Gamma distribution and the approximation is shown to be much better than the previous works.

Also, [Xin Li and Nie 2004], [XU et al. 2008] and [Wang and Blostein 2007] omitted the error propagation in their derivations. Considering the error propagation, the authors of [Shen et al. 2004] provide a method to calculate the BER of ZF-SIC with BPSK modulation. Moreover, the BER of space-time block codes for ZF-SIC with MPSK modulation is analyzed in [Kim 2004]. However, the approximations in [Shen et al. 2004] and [Kim 2004] do not include channel correlation.

Since the ordering of the decoding process can dramatically impact the system performance when using ZF-SIC [Wolniansky et al. 1998; Xiaofeng et al. 2002; Zhiheng et al. 2007; HAN et al. 2009], often the BER formulations are obtained for a particular ordering. The authors of [HAN et al. 2009] propose an analytical SER expression for the decoding ordering that maximizes the achievable rate [Wolniansky et al. 1998] assuming Gaussian inputs. As we will show, this particular ordering does not necessarily maximize the achievable rate when discrete constellations are used.

Here we will obtain accurate approximations for the average BER of each M-QAM transmitted data stream in a MIMO system with precoding and ZF-SIC receiver. Channel correlation at the transmitter side and error propagation are considered.

7.1.1 Average Bit Error Probability

There are again two cases that should be analyzed respectively to obtain the average bit error rate : with and without coding.

7.1.1.1 Average bit error rate without coding

For the first stage $i = 1$, since $\hat{s}_1$ may be detected with errors, we define E_1 that represents the occurrence of error events (bit errors) at the first stage. The SINR corresponding to the reception of the signal of the first transmit stream can be expressed as

$$\mathrm{SINR}\left(E_1\right) = \frac{1}{\left[\left(\mathbf{H}^H\mathbf{H}\right)^{\dagger}\right]_{1,1}}, \tag{7.1}$$

where $[\cdot]_{1,1}$ means the first diagonal element.

The bit error probability of $\hat{s}_1$ can be calculated based on the Gamma distribution (4.2) with two parameters $Gamma\left(\alpha_1,\ \beta_1\right)$ of $\mathrm{SINR}_{\mathrm{ZF}}$, which has been proposed in Chapter IV,

$$P\left(E_1\right) \approx A_m\left(1 - s\beta_1\right)^{-\alpha_1}, \tag{7.2}$$

where $A_m = \frac{1}{2\sqrt{\pi}}$ for 2-QAM and 4-QAM and $A_m = \frac{2}{\log_2(M)\sqrt{\pi}}$ for M-QAM($M > 4$). And $s = -1$ for 2-QAM, $s = -\frac{1}{2}$ for 4-QAM and $s = -\frac{3}{2(M-1)}$ for M-QAM($M > 4$).

Although (7.2) is a high SNR approximation, it is also accurate for low SNR calculation as we discussed in Chapter IV.

When the precoder $\mathbf{V}$ diagonalizes $\mathbf{R}$ in (2.4), the parameters in (7.2) can be expressed as

$$\begin{array}{l} \alpha_1 = n_R - n_T + 1 \\ \beta_1 = \lambda_1 \gamma p_1 \frac{1}{n_T} \end{array} , \tag{7.3}$$

where $\lambda_i,\ i = 1, \cdots, n_T$ are the eigenvalues of the covariance matrix $\mathbf{R}$ in (2.2).

The feedback symbol to the ith stage only can belong to one of these two possible status: with or without bit errors. Considering that in the ith stage there are $i-1$ feedbacks from the previous stages, so there is ${}_{i-1}C_0 = 1$ possible combination when all feedbacks do not contain error events, where ${}_{i-1}C_0$ is the binomial coefficient ${}_{i-1}C_n = \frac{(i-1)!}{((i-1)-n)!n!}$, $0 \le n \le i-1$. There are also ${}_{i-1}C_1 = i-1$ possible combinations when any one feedback contains some error events. There are ${}_{i-1}C_2 = \frac{(i-1)(i-2)}{2}$ possible combinations when any two given feedbacks contain error events. And so on, there are ${}_{i-1}C_{i-1} = 1$ possible combinations when any $i-1$ feedbacks contain error events. Thus the number of total combinations is denoted as $N_{i-1} = {}_{i-1}C_0 + {}_{i-1}C_2 + {}_{i-1}C_2 + \cdots + {}_{i-1}C_{i-1} = \sum\limits_{j=0}^{i-1} {}_{i-1}C_j = 2^{i-1}$.

The error probability at stage i will be obtained, looking at all the possible combinations of feedback errors in previous stages. Define E_i as the occurrence of error events (bit errors) at the ith stage. Then $\bar{E}_i$ represents the complementary event of E_i and the probability $P\left(\bar{E}_i\right) = 1 - P\left(E_i\right)$.

The total probability of bit error for signal $\hat{\mathrm{s}}_i$ of stage i is

$$\begin{array}{l} P\left(E_i\right) = P\left(E_i \left| E_{i-1} \cap E_{i-2} \cdots E_2 \cap E_1 \right.\right) P\left(E_{i-1} \cap E_{i-2} \cdots E_2 \cap E_1\right) \\ \qquad + P\left(E_i \left| E_{i-1} \cap E_{i-2} \cdots E_2 \cap \bar{E}_1 \right.\right) P\left(E_{i-1} \cap E_{i-2} \cdots E_2 \cap \bar{E}_1\right) \\ \qquad + P\left(E_i \left| E_{i-1} \cap E_{i-2} \cdots \bar{E}_2 \cap E_1 \right.\right) P\left(E_{i-1} \cap E_{i-2} \cdots \bar{E}_2 \cap E_1\right) \\ \qquad + P\left(E_i \left| E_{i-1} \cap E_{i-2} \cdots \bar{E}_2 \cap \bar{E}_1 \right.\right) P\left(E_{i-1} \cap E_{i-2} \cdots \bar{E}_2 \cap \bar{E}_1\right) \\ \qquad + \cdots \\ \qquad + P\left(\bar{E}_i \left| \bar{E}_{i-1} \cap \bar{E}_{i-2} \cdots \bar{E}_2 \cap \bar{E}_1 \right.\right) P\left(\bar{E}_{i-1} \cap \bar{E}_{i-2} \cdots \bar{E}_2 \cap \bar{E}_1\right) \end{array} . \tag{7.4}$$

Using the conditional probability formula $P\left(A \cap B\right) = P\left(B \left| A\right.\right) P\left(A\right)$, (7.4) can be expanded as

$$
\begin{aligned}
P\left(E_i\right) = {} & P\left(E_i \left| E_{i-1} \cap E_{i-2} \cdots E_2 \cap E_1\right.\right) P\left(E_{i-1} \left| E_{i-2} \cap E_{i-3} \cdots E_2 \cap E_1\right.\right) \\
& P\left(E_{i-2} \left| E_{i-3} \cap E_{i-4} \cdots E_2 \cap E_1\right.\right) \cdots P\left(E_1\right) + \\
& P\left(E_i \left| E_{i-1} \cap E_{i-2} \cdots E_2 \cap \bar{E}_1\right.\right) P\left(E_{i-1} \left| E_{i-2} \cap E_{i-3} \cdots E_2 \cap \bar{E}_1\right.\right) \\
& P\left(E_{i-2} \left| E_{i-3} \cap E_{i-4} \cdots E_2 \cap \bar{E}_1\right.\right) \cdots P\left(\bar{E}_1\right) + \\
& P\left(E_i \left| E_{i-1} \cap E_{i-2} \cdots \bar{E}_2 \cap E_1\right.\right) P\left(E_{i-1} \left| E_{i-2} \cap E_{i-3} \cdots \bar{E}_2 \cap E_1\right.\right) \\
& P\left(E_{i-2} \left| E_{i-3} \cap E_{i-4} \cdots \bar{E}_2 \cap E_1\right.\right) \cdots P\left(E_1\right) + \\
& P\left(E_i \left| E_{i-1} \cap E_{i-2} \cdots \bar{E}_2 \cap \bar{E}_1\right.\right) P\left(E_{i-1} \left| E_{i-2} \cap E_{i-3} \cdots \bar{E}_2 \cap \bar{E}_1\right.\right) \\
& P\left(E_{i-2} \left| E_{i-3} \cap E_{i-4} \cdots \bar{E}_2 \cap \bar{E}_1\right.\right) \cdots P\left(\bar{E}_1\right) + \cdots + \\
& P\left(E_i \left| \bar{E}_{i-1} \cap \bar{E}_{i-2} \cdots \bar{E}_2 \cap \bar{E}_1\right.\right) P\left(\bar{E}_{i-1} \left| \bar{E}_{i-2} \cap \bar{E}_{i-3} \cdots \bar{E}_2 \cap \bar{E}_1\right.\right) \\
& P\left(\bar{E}_{i-2} \left| \bar{E}_{i-3} \cap \bar{E}_{i-4} \cdots \bar{E}_2 \cap \bar{E}_1\right.\right) \cdots P\left(\bar{E}_1\right)
\end{aligned} . \quad (7.5)
$$

Define $E_i^{(1)} = E_i \left| E_{i-1} \cap E_{i-2} \cdots E_2 \cap E_1\right.$, $E_i^{(2)} = E_i \left| E_{i-1} \cap E_{i-2} \cdots E_2 \cap \bar{E}_1\right.$, and the others follow this order one by one.

And similarly define $E_{i-1}^{(1)} = E_{i-1} \left| E_{i-2} \cap E_{i-3} \cdots E_2 \cap E_1\right.$, and then the others are defined similarly.

$$
\begin{aligned}
P\left(E_i\right) = {} & P\left(E_i^{(1)}\right) P\left(E_{i-1}^{(1)}\right) P\left(E_{i-2}^{(1)}\right) \cdots P\left(E_1\right) \\
& + P\left(E_i^{(2)}\right) P\left(E_{i-1}^{(2)}\right) P\left(E_{i-2}^{(2)}\right) \cdots P\left(\bar{E}_1\right) \\
& + P\left(E_i^{(3)}\right) P\left(E_{i-1}^{(3)}\right) P\left(E_{i-1}^{(3)}\right) \cdots P\left(E_1\right) \\
& + P\left(E_i^{(4)}\right) P\left(E_{i-1}^{(4)}\right) P\left(E_{i-2}^{(4)}\right) \cdots P\left(\bar{E}_1\right) \\
& + \cdots \\
& + P\left(E_i^{(N_{i-1})}\right) P\left(\bar{E}_{i-1}^{(N_{i-1})}\right) P\left(\bar{E}_{i-2}^{(N_{i-1})}\right) \cdots P\left(\bar{E}_1\right)
\end{aligned} . \quad (7.6)
$$

If $\hat{\mathrm{s}}_1, \cdots, \hat{\mathrm{s}}_{i-1}$ are all detected incorrectly, to get $P\left(E_i^{(1)}\right)$ in (7.6), the SINR of the second transmit antenna can be expressed as

$$
\mathrm{SINR}\left(E_i^{(1)}\right) = \frac{1}{\left[\left(\mathbf{H}_{-(i-1)}^H \mathbf{H}_{-(i-1)}\right)^{-1} \left(\left|\left(\mathrm{s}_1 - \hat{\mathrm{s}}_1\right) \mathbf{h_1}\right|^2 + \cdots + \left|\left(\mathrm{s}_{i-1} - \hat{\mathrm{s}}_{i-1}\right) \mathbf{h}_{i-1}\right|^2 + \sigma^2\right)\right]_{1,1}} . \quad (7.7)
$$

According to [Hong et al. 2011a], $\frac{1}{\left[\left(\mathbf{H}_{-(i-1)}^{H}\mathbf{H}_{-(i-1)}\right)^{\dagger}\right]_{1,1}}$ is a Gamma random variable and its distribution follows

$$Gamma\left(n_r - n_t + i,\ \lambda_i \gamma p_i \frac{1}{n_t}\right). \tag{7.8}$$

The expectation of the part $|(\mathrm{s}_1 - \hat{\mathrm{s}}_1)\,\mathbf{h}_1|^2 + \cdots + |(\mathrm{s}_{i-1} - \hat{\mathrm{s}}_{i-1})\,\mathbf{h}_{i-1}|^2$ in (7.7) is denoted as $\bar{\mu}_i^{(1)}$. As the following subsection of examples will show, the BER is calculated accurately by using $\bar{\mu}_i^{(1)}$. Thus, omitting its higher moments, the part $|(\mathrm{s}_1 - \hat{\mathrm{s}}_1)\,\mathbf{h}_1|^2 + \cdots + |(\mathrm{s}_{i-1} - \hat{\mathrm{s}}_{i-1})\,\mathbf{h}_{i-1}|^2$ in (7.7) can be approximated by its expectation value $\bar{\mu}_i^{(1)}$. As $\kappa_i^{(1)} = \bar{\mu}_i^{(1)} + \sigma^2$ is a positive constant, according to the scaling property of Gamma distribution, $\mathrm{SINR}_i\left(E_i^{(1)}\right)$ can also approximated by a Gamma distribution

$$Gamma\left(n_r - n_t + i,\ \lambda_i \gamma p_i \frac{1}{n_t \kappa_i^{(1)}}\right). \tag{7.9}$$

Therefore the BER of ith transmit antenna with the error events $E_i^{(1)}$ also can be approximated by (7.2) with new parameters, so we have

$$P\left(E_i^{(1)}\right) \approx A_m \left(1 - s\beta_i\left(E_i^{(1)}\right)\right)^{-\alpha_i\left(E_i^{(1)}\right)}. \tag{7.10}$$

Following (7.7), the parameters of the Gamma distribution of the ith transmit antenna are

$$\alpha_i\left(E_i^{(1)}\right) = n_R - n_T + i, \tag{7.11}$$

$$\begin{aligned}\beta_i\left(E_i^{(1)}\right) &= \frac{\lambda_i \gamma p_i \frac{1}{n_T}}{\mathrm{E}\left(|(\mathrm{s}_1-\hat{\mathrm{s}}_1)\mathbf{h}_1|^2\right)+\cdots+\mathrm{E}\left(|(\mathrm{s}_{i-1}-\hat{\mathrm{s}}_{i-1})\mathbf{h}_{i-1}|^2\right)+1} \\ &= \frac{\lambda_i \gamma p_i \frac{1}{n_T}}{d_1\lambda_1\gamma p_1\frac{1}{n_T}+\cdots+d_{i-1}\lambda_{i-1}\gamma p_{i-1}\frac{1}{n_T}+1}\end{aligned}, \tag{7.12}$$

where $d_{i-1} = \mathrm{E}\left(|(\mathrm{s}_{i-1} - \hat{\mathrm{s}}_{i-1})|^2\right)$ can be approximated by the minimum square Euclidean distance in the constellation and its value depends on the modulation type.

For the event $E_{i-1}^{(1)}$, the parameters of the Gamma distribution $Gamma\left(\alpha_{i-1},\ \beta_{i-1}\right)$ can be expressed similarly following the above analysis.

$$\alpha_{i-1}\left(E_{i-1}^{(1)}\right) = n_r - n_t + i - 1, \tag{7.13}$$

$$\begin{aligned}\beta_{i-1}\left(E_{i-1}^{(1)}\right) &= \frac{\lambda_{i-1}\gamma p_i \frac{1}{n_t}}{\mathrm{E}\left(\left|(\mathrm{s}_1-\hat{\mathrm{s}}_1)\mathbf{h}_1\right|^2\right)+\cdots+\mathrm{E}\left(\left|(\mathrm{s}_{i-2}-\hat{\mathrm{s}}_{i-2})\mathbf{h}_{i-2}\right|^2\right)+1} \\ &= \frac{\lambda_{i-1}\gamma p_i \frac{1}{n_t}}{d_1\lambda_1\gamma p_1 \frac{1}{n_t}+\cdots+d_{i-2}\lambda_{i-2}\gamma p_{i-2}\frac{1}{n_t}+1}\end{aligned}, \tag{7.14}$$

The parameters α_i and β_i of the other cases $P\left(E_i^{(1)}\right)$, $2 \leq i \leq i-2$ can be obtained by calculating similarly to the above (7.13) and (7.14). The probabilities of bit errors for these cases are similar to the equation (7.10), only changing the parameters α_i and β_i.

Because α_i comes from $\frac{1}{\left(\mathbf{H}_{-(i-1)}^H \mathbf{H}_{-(i-1)}\right)^{\dagger}}$, its value is a constant for all error events. As it does not depend on $E_i^{(1)}$, we have

$$\alpha_i = n_R - n_T + i. \tag{7.15}$$

While calculating $P\left(E_i^{(2)}\right)$, since the first stage is totally detected correctly, we have $\mathrm{s}_1 - \hat{\mathrm{s}}_1 = 0$ in (7.7) and (7.12). So we have

$$\beta_i\left(E_i^{(2)}\right) = \frac{\lambda_i\gamma p_i \frac{1}{n_T}}{d_2\lambda_2\gamma p_2\frac{1}{n_T} + \cdots + d_{i-1}\lambda_{i-1}\gamma p_{i-1}\frac{1}{n_T} + 1}. \tag{7.16}$$

The parameter β_i of the other cases $P\left(E_i^{(j)}\right)$, $3 \leq j \leq N_{i-1}$ can be obtained by calculating similarly to the above (7.16). The probabilities of bit errors for these cases are similar to the equation (7.10), only changing the parameter β_i.

7.1.1.2 Average bit error rate with coding

Furthermore, for M-QAM modulations in conjunction with a convolutional code of rate $r_c = k_c/n_c$ and minimum distance d_f, the BER at the output of the decoder can be approximated, for high SNR, as shown in (4.21).

Similarly to the uncoded case, the total bit error rate for the ith stream in coded

M-QAM systems is,

$$\begin{aligned} P_c\left(E_i\right) = & P_c\left(E_i^{(1)}\right) P_c\left(E_{i-1}^{(1)}\right) P_c\left(E_{i-2}^{(1)}\right) \cdots P_c\left(E_1\right) \\ & + P_c\left(E_i^{(2)}\right) P_c\left(E_{i-1}^{(2)}\right) P_c\left(E_{i-2}^{(2)}\right) \cdots P_c\left(\bar{E}_1\right) \\ & + P_c\left(E_i^{(3)}\right) P_c\left(E_i^{(3)}\right) P_c\left(\bar{E}_{i-2}^{(2)}\right) \cdots P_c\left(E_1\right) \\ & + P_c\left(E_i^{(4)}\right) P_c\left(E_{i-1}^{(4)}\right) P_c\left(\bar{E}_{i-2}^{(4)}\right) \cdots P_c\left(\bar{E}_1\right) \\ & + \cdots \\ & + P_c\left(E_i^{(N_{i-1})}\right) P_c\left(\bar{E}_{i-1}^{(N_{i-1})}\right) P_c\left(\bar{E}_{i-2}^{(N_{i-1})}\right) \cdots P_c\left(\bar{E}_1\right) \end{aligned}, \tag{7.17}$$

where in (7.17)

$$P_c\left(E_i^{(1)}\right) \approx D_f\left(1 - c_f \beta_i\left(E_i^{(1)}\right)\right)^{-\alpha_i\left(E_i^{(1)}\right)}. \tag{7.18}$$

and $c_f = \frac{-d_f}{2}$ for 2-QAM, $c_f = \frac{-d_f}{4}$ for 4-QAM and $c_f = \frac{-3d_f}{4(M-1)}$ for M-QAM($M > 4$). And for 2-QAM and 4-QAM $D_f = D$, $D_f = \frac{4D}{\log_2(M)}$ for M-QAM.

In particular, for the first stage we have

$$P_c\left(E_1\right) \approx D_f\left(1 - c_f \beta_1\right)^{-\alpha_1}, \tag{7.19}$$

which is shown in [Armada et al. 2009].

7.2 Decoder ordering

Let us define the precoder

$$\mathbf{V} = \left[\mathbf{v}_1, \cdots, \mathbf{v}_j, \cdots, \mathbf{v}_{n_T}\right]. \tag{7.20}$$

Changing the order of $\mathbf{v}_j$, the total power will be different. We would like to find an ordering $\mathbf{V}^n$ from the permutation of the columns $\mathbf{v}_j$, which can realize the maximization of bit rate with a power limitation or minimization of power with a rate limitation.

Once the bit distribution $\{b_1, b_2, \cdots, b_i, \cdots, b_{n_T}\}$ is fixed, A_m and s in (7.10) can be determined for each stage. Moreover, we define $c_1 = \lambda_1 p_1$ and it can be calculated by solving (7.6), when $i = 1$. Furthermore, we define $c_i = \lambda_i P$ and it can also be computed one by one, by using the results of the previous steps from c_1 to c_{i-1}, Until c_{n_T} has been solved. This set is

$$\{c_1, \cdots, c_i, \cdots c_{n_T}\}, \tag{7.21}$$

and it can be sorted in ascending order as

$$\left\{c^1 \leq \cdots \leq c^k \leq \cdots \leq c^{n_T}\right\}, \ 1 \leq k \leq n_T. \tag{7.22}$$

The mapping relationship between the unordered index i and the ordered one k is

$$A\left(i,\ k\right). \tag{7.23}$$

Because $\mathbf{R}$ is a positive definite matrix [Chu et al. 1997], its eigenvalues are all positive real values, which can be sorted as

$$\{\lambda_1 \leq \cdots \leq \lambda_k \leq \cdots \leq \lambda_{n_T}\}, \ 1 \leq k \leq n_T. \tag{7.24}$$

To minimize the total power or maximize the rate, we propose that (7.24) is the right order since the biggest λ_k should be coupled with the biggest c^k.

Then, we have to go back to the original ordering of (7.21) by using (7.23), so λ_i can be obtained by reordering (7.24)

$$\left\{\lambda^1, \cdots, \lambda^i, \cdots \lambda^{n_T}\right\}, \tag{7.25}$$

corresponding to

$$\mathbf{V}^n = \left[\mathbf{v}^1, \cdots,\ \mathbf{v}^i, \cdots,\ \mathbf{v}^{n_T}\right]. \tag{7.26}$$

The above proposition should be proven to be an optimal solution for power minimization. This means that a payoff $\sum\limits_{i=1}^{n_T} p_i = \sum\limits_{i=1}^{n_T} \frac{c_i}{\lambda^i}$ can be minimized after processing according to the above steps.

We conjecture that the above steps can minimize the payoff, then it can be seen that the sets $\{c_1, \cdots, c_i, \cdots c_{n_T}\}$ and $\{\lambda_1, \cdots, \lambda_j, \cdots \lambda_{n_T}\}$ are sorted monotonically increasing to be (7.22) and (7.24). Consider any indices k and l such that $k < l$, and consider the terms $\frac{c_k}{\lambda^k}$ and $\frac{c_l}{\lambda^l}$. Since the sets $\{c_1, \cdots, c_i, \cdots c_{n_T}\}$ and $\{\lambda_1, \cdots, \lambda_j, \cdots \lambda_{n_T}\}$

are sorted into monotonically increasing order and $k < l$, we have $0 \leq c_k \leq c_l$ and $0 \leq \lambda_k \leq \lambda_l$. Since c_k and c_l are positive and $\lambda_l - \lambda_k$ is nonnegative, we have

$$\frac{c_k}{\lambda^k} + \frac{c_l}{\lambda^l} \leq \frac{c_k}{\lambda^l} + \frac{c_l}{\lambda^k}. \tag{7.27}$$

So far, the proof that this method yields an optimal solution is completed. Since the order of multiplication doesn't matter, sorting the sets $\{c_1, \cdots, c_i, \cdots c_{n_T}\}$ and $\{\lambda_1, \cdots, \lambda_j, \cdots \lambda_{n_T}\}$ into monotonically decreasing order works as well.

7.3 Bit loading and power allocation

Consider that M_i is the cardinality of the modulation applied to the ith eigenvector of $\mathbf{V}$, P_{e_i} its average BER, and $\overline{\text{BER}}$ is the target average bit error rate.

With the relations between these parameters and the power matrix $\mathbf{P}$ for different modulation schemes, and considering $\mathbf{V}^n$ (Section 7.2), the optimization problems (4.27) and (4.28) can be solved.

The method of Section 7.2 can not only be applied to power minimization (4.28), but also to bit rate maximization (4.27), because the total power is limited.

The optimization is conducted by searching for the best combinations of bit (i.e., constellation cardinalities) and power loads. For each possible bit allocation, and using the approximations in (7.6) and (7.17) that relate the BER with the power matrix $\mathbf{P}$= diag $[p_1 p_2 \cdots p_{n_T}]$, the appropriate constraints can be enforced.

For (4.28), given (6.48) and R_{tot}, the minimum power can be obtained by comparing the exhaustive search results calculated when the constrains (6.48) and R_{tot} are all satisfied.

For problem A, the complexity of exhaustive search is exponential, so some constraint should be added to simplify the exhaustive search.

Checking (20) in [XU et al. 2008], a BER relationship among the perfect ZF-SIC (ZF-PSIC), ZF-SIC and ZF is given, in which the perfect ZF-SIC refers to the ZF-SIC without considering error propagation and channel correlation, while utilizing the same detection order for ZF-PSIC and ZF-SIC. From figure 2 of [XU et al. 2008], it can be seen that the upper bound and lower bound of the average BER over all antennas are tight.

Following [XU et al. 2008], the Gamma distribution is available to calculate the BER for ZF-PSIC, which can be approximated for any ith stage by

$$P_{\mathrm{ZF-PSIC}} \approx A_m \left(1 - s\beta_{\mathrm{ZF-PSIC}}\right)^{-\alpha_{\mathrm{ZF-PSIC}}}, \tag{7.28}$$

with the parameters

$$\begin{array}{l} \alpha_{\mathrm{ZF-PSIC}} = n_R - n_T + i \\ \beta_{\mathrm{ZF-PSIC}} = \lambda_i \gamma p_i \frac{1}{n_T} \end{array}. \tag{7.29}$$

Since each stage of ZF-PSIC does not contain the coupling effect of the transmitted power, which is caused by the error propagation, the Levin-Campello algorithm is still valid for the bit loading and power allocation with this receiver. Thus, by utilizing the Levin-Campello algorithm for bit and power optimization with ZF and ZF-SIC, their total number of bits can be individually calculated.

Therefore, for ZF-SIC, we conjecture that its total number of bits $R_{\mathrm{ZF-SIC}}$ is bounded by

$$R_{\mathrm{ZF}} \leq R_{\mathrm{ZF-SIC}} \leq R_{\mathrm{ZF-PSIC}}. \tag{7.30}$$

If utilizing (7.30) as a constraint, the exhaustive search can be more simplified and efficient. So (7.30) should be proved.

For the ith stage, observing (7.4) and (7.28),

$$P_{\mathrm{ZF-PSIC}} = P\left(\bar{E}_i \left| \bar{E}_{i-1} \cap \bar{E}_{i-2} \cdots \bar{E}_2 \cap \bar{E}_1 \right.\right). \tag{7.31}$$

Obviously, we have

$$\begin{array}{l} P\left(\bar{E}_i \left| \bar{E}_{i-1} \cap \bar{E}_{i-2} \cdots \bar{E}_2 \cap \bar{E}_1 \right.\right) \leq P\left(E_i \left| E_{i-1} \cap E_{i-2} \cdots E_2 \cap E_1 \right.\right) \\ P\left(\bar{E}_i \left| \bar{E}_{i-1} \cap \bar{E}_{i-2} \cdots \bar{E}_2 \cap \bar{E}_1 \right.\right) \leq P\left(E_i \left| E_{i-1} \cap E_{i-2} \cdots E_2 \cap \bar{E}_1 \right.\right) \\ \cdots \\ P\left(\bar{E}_i \left| \bar{E}_{i-1} \cap \bar{E}_{i-2} \cdots \bar{E}_2 \cap \bar{E}_1 \right.\right) \leq P\left(E_i \left| E_{i-1} \cap \bar{E}_{i-2} \cdots \bar{E}_2 \cap \bar{E}_1 \right.\right) \end{array}. \tag{7.32}$$

Combining (7.4) and (7.32),

$$\begin{aligned} P_{\mathrm{ZF-SIC}} &= P\left(E_i\right) \\ &= P\left(E_i \left| E_{i-1} \cap E_{i-2} \cdots E_2 \cap E_1 \right.\right) P\left(E_{i-1} \cap E_{i-2} \cdots E_2 \cap E_1\right) \\ &\quad + \cdots + P\left(\bar{E}_i \left| \bar{E}_{i-1} \cap \bar{E}_{i-2} \cdots \bar{E}_2 \cap \bar{E}_1 \right.\right) P\left(\bar{E}_{i-1} \cap \bar{E}_{i-2} \cdots \bar{E}_2 \cap \bar{E}_1\right) \\ &\geq P\left(\bar{E}_i \left| \bar{E}_{i-1} \cap \bar{E}_{i-2} \cdots \bar{E}_2 \cap \bar{E}_1 \right.\right) P\left(E_{i-1} \cap E_{i-2} \cdots E_2 \cap E_1\right) \\ &\quad + \cdots + P\left(\bar{E}_i \left| \bar{E}_{i-1} \cap \bar{E}_{i-2} \cdots \bar{E}_2 \cap \bar{E}_1 \right.\right) P\left(\bar{E}_{i-1} \cap \bar{E}_{i-2} \cdots \bar{E}_2 \cap \bar{E}_1\right) \\ &= P\left(\bar{E}_i \left| \bar{E}_{i-1} \cap \bar{E}_{i-2} \cdots \bar{E}_2 \cap \bar{E}_1 \right.\right) \end{aligned} . \tag{7.33}$$

Plugging (7.31) into (7.33),

$$P_{\mathrm{ZF-SIC}} \geq P_{\mathrm{ZF-PSIC}}. \tag{7.34}$$

For the ith stream, the relationship between $P_{\mathrm{ZF-SIC}}$ and $P_{\mathrm{ZF-SIC}}$ can be known from [Wang and Blostein 2007],

$$P_{\mathrm{ZF}} \geq P_{\mathrm{ZF-SIC}}. \tag{7.35}$$

So far, it can be seen that the relationship (7.30) holds true.

7.4 Search procedure and its complexity

It is interesting to analyze the complexity of the proposed approach.

From Chapter VI, it is known that the complexity of complete exhaustive search is $(q+1)^{n_T}$.

In (4.28), for the target number of total allocated bits R_{tot}, the number of different bit combinations is extremely limited. That is the reason why the complexity of (4.27) is the main concern.

Utilizing the proposed method, the complexity of exhaustive search can be decreased noticeably. By adding the constraint (7.30), the calculations of exhaustive search can be reduced efficiently.

In Table 7.1, there is a comparison of the search limitation of bit rate for (4.27), at a typical value $\rho = 0.5$ and $\overline{\mathrm{BER}} = 10^{-2}$, and M_i takes values in the set {0, 2, 4, 8, 16, 32, 64}. When SNR is varying from 0 dB to 30 dB, from the simulation results, we found that the maximum number of trials is required at an SNR of around 15 dB. From Table 7.1, it can be observed that the convergence of the process is much faster with (7.30).

$n_T \times n_R$	$R_{\mathrm{ZF-SIC}}$	Limitation of bit rate for exhaustive search	Limitation of bit rate for exhaustive search with (7.30)
3×4	7	$0 \leq R_{\mathrm{ZF-SIC}} \leq 7^3$	$5 \leq R_{\mathrm{ZF-SIC}} \leq 8$
8×10	20	$0 \leq R_{\mathrm{ZF-SIC}} \leq 7^8$	$13 \leq R_{\mathrm{ZF-SIC}} \leq 22$

Table 7.1: $R_{\mathbf{ZF-SIC}}$ and limitation of bit rate for search.

Since $c_i = \lambda_i P$, $\mathrm{Tr}\,[\mathbf{R}] = n_T$ and $\mathrm{Tr}\,[\mathbf{P}] \leq n_T$, there is

$$c_i \leq n_T^2. \tag{7.36}$$

From Table 7.1, it can be seen that the exhaustive search with (7.30) is still not efficient enough. Because the BER of any stage depends on the BER of its prior stages, a tree search with (7.30) can facilitate the computation.

For the first stage, if the maximum number of bits of each channel is limited to $B = \max\{\log_2 M_i\}$, there are $B + 1$ possible bits loaded, which are selected from 0 to B. Checking among all these B possibilities of c_1, which ones satisfies (7.30), then the second stage can start with these ones, which are also $B + 1$ possible numbers for each one.

This search loop can proceed until the last stage. Finally the ultimate assigned powers are calculated, as it was mentioned in the Section 7.2.

7.5 Numerical examples

The transmit covariance matrix $\mathbf{R}$ and the three evaluation scenarios are the same as in Chapter IV.

7.5.1 BER of ZF-SIC

The numerical results of our developed expressions and the equations of reference [Paulraj 2003] are compared to Monte Carlo simulation results in a MIMO system with ZF-SIC receiver.

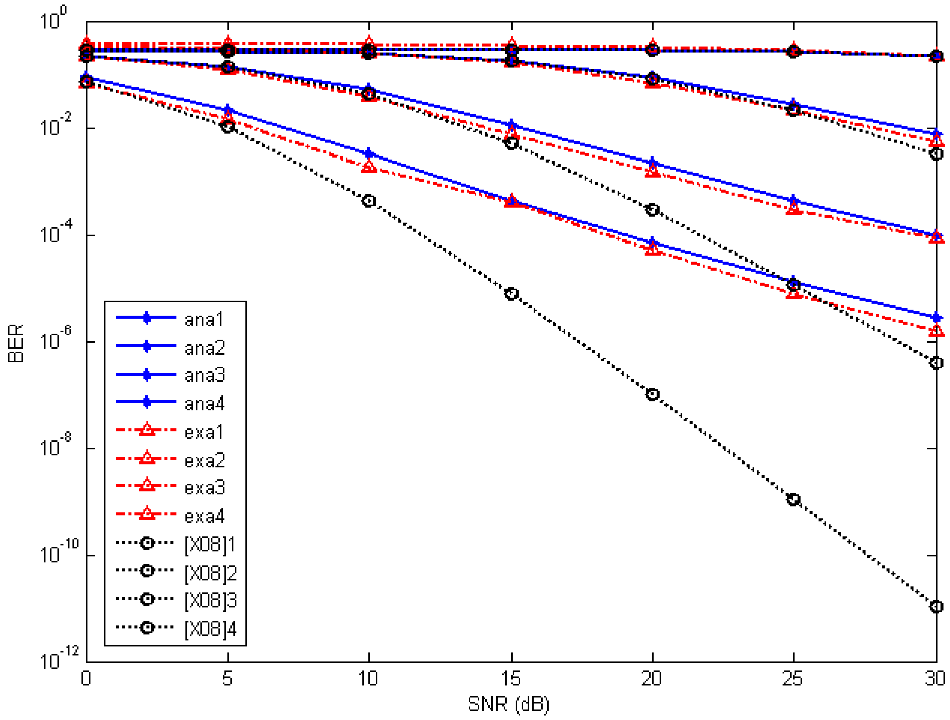

Figure 7.1: Average BER vs. SNR - QPSK modulation with $n_T = 4$, $n_R = 4$ and $\rho = 0.9$; Order 1.

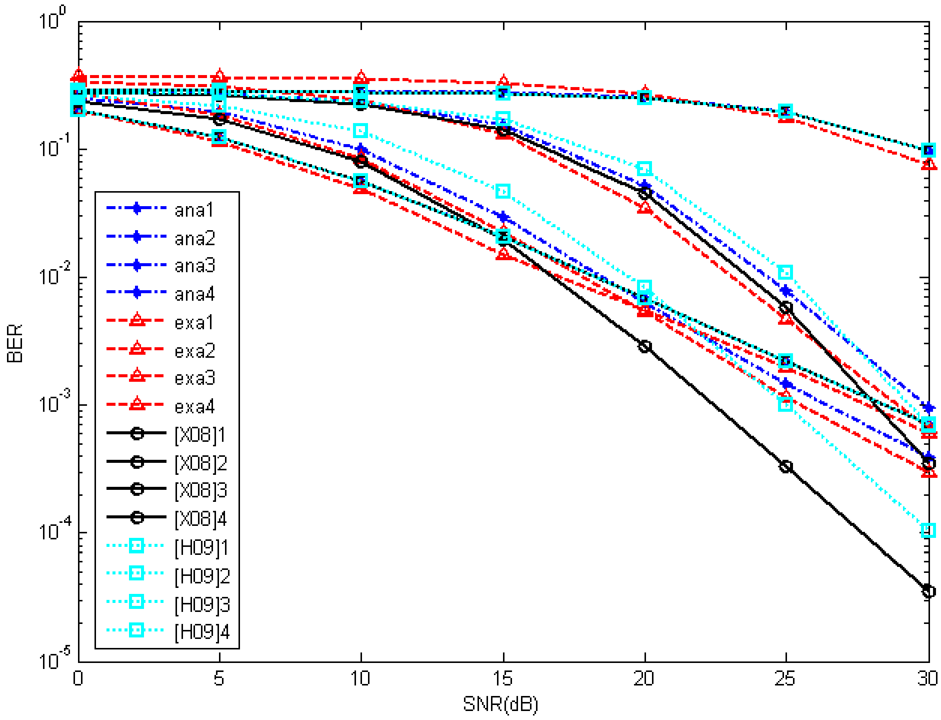

Figure 7.2: Average BER vs. SNR - QPSK modulation with $n_T = 4$, $n_R = 4$ and $\rho = 0.9$; Order 2.

Figure 7.1 shows the average BER of each transmitted stream with QPSK modulation when the detection order follows the sort order of the eigenvalues $\lambda_1 \leq \lambda_2 \leq \cdots \leq \lambda_{n_T}$, which is denoted as Order 1. Here $\rho = 0.9$ and SNR is varied between 0 dB and 30 dB, when $n_T = 4$, $n_R = 4$. It can be seen that our analytical expressions give a very good fit for all values of SNR. The results of [XU et al. 2008] ([X08]) exhibit more estimation errors for higher stage streams in the high SNR regime.

In order to verify the accuracy of the developed expressions, a detection order different from Order 1 is used. Figure 7.2 shows the average BER of each transmitted stream with QPSK modulation when the detection order is completely reversed, which is denoted as Order 2, where $\rho =$ 0.9 and SNR is varied between 0 dB and 30 dB in 4×4 MIMO system. It also demonstrates a good fit of the results between the developed expressions and Monte Carlo simulations for all values of SNR. Although the results of [XU et al. 2008] ([X08]) have less estimation errors for this new detection order, they are still worse than our analytical results. These comparisons also verify that the developed expressions are accurate for different detection orders. Since the optimal ordering in [XU et al. 2008] ([X08]) corresponds to Order 2, the results of [HAN et al. 2009] ([H09]) are more accurate than those of [XU et al. 2008] ([X08]). However, the results of our proposed expression are more accurate if we consider all antennas and SNRs, even though it may outperform ours in some special SNR regimes, and this is only for that particular given decoding order.

7.5.2 Bit Rate Maximization

The following three scenarios, in terms of modulation and coding schemes available at the transmitter, are considered.

- 6 uncoded bit rates: M_i takes values in the set {0, 2, 4, 8, 16, 32, 64}. This is a realistic uncoded scenario.
- 12 bit rates with convolutional coding: M_i takes values in the set {0, 2, 4, 8, 16, 32, 64}. Each of the signals will either be uncoded or coded with a rate - 1/2 convolutional code of generator polynomials (133, 171) and $d_f = 10$.
- 16 bit rates with convolutional coding: M_i takes values in the set {0, 2, 4, 8, 16, 32, 64, 128, 256}, to compare with capacity. Each of the signals will either be

uncoded or coded with a rate - 1/2 convolutional code of generator polynomials (133, 171) and $d_f = 10$.

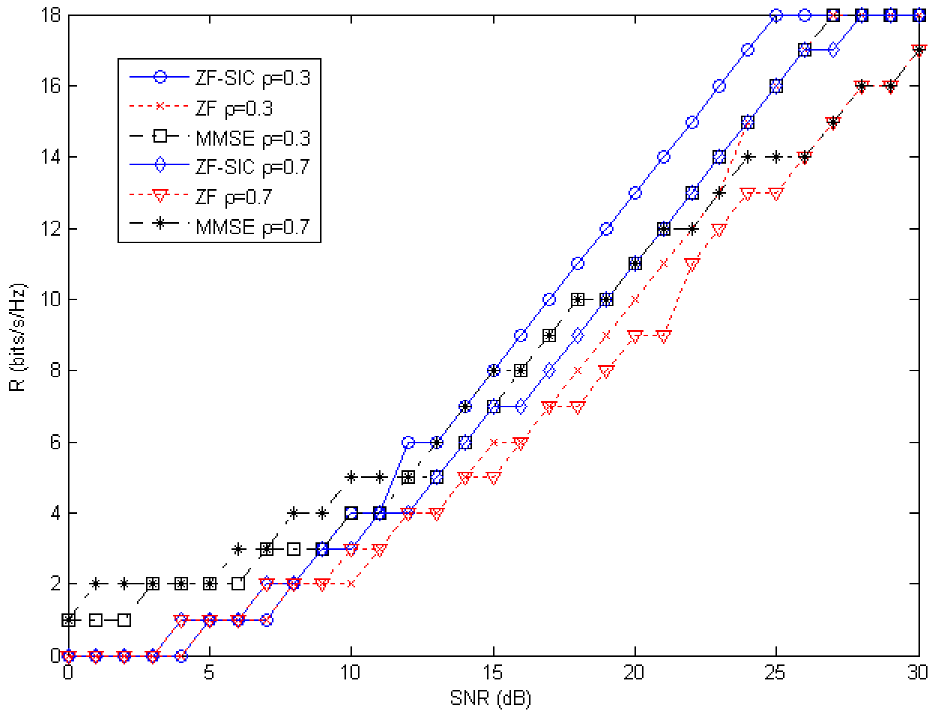

Figure 7.3: Bit rate vs. SNR - 6 uncoded bit rates with $n_T = 3$, $n_R = 4$ and $\overline{\text{BER}} = 10^{-2}$.

Fig. 7.3 shows the achievable bit rate R with optimized power allocation. Two typical values of the correlation parameter ρ are chosen, n_T is 3, n_R is 4 and $\overline{\text{BER}} = 10^{-2}$. Here, the scenario is the first one (6 uncoded bit rates). Bit rates of ZF and MMSE are obtained in previous chapters. In Fig. 7.4, it can be checked the same dependence with correlation as in the previous chapters: with high channel correlation, the bit loading algorithm works better for low SNR regimes, while for low correlation, the performance is much better for high SNR values. Apart from that, the performance at low SNR of receivers ZF-SIC and ZF is more similar, due to the propagation of a high number of errors, so the curves tend to converge in that regime. At high SNR, a considerably higher bit rate can be achieved by the optimized systems with the ZF-SIC receiver.

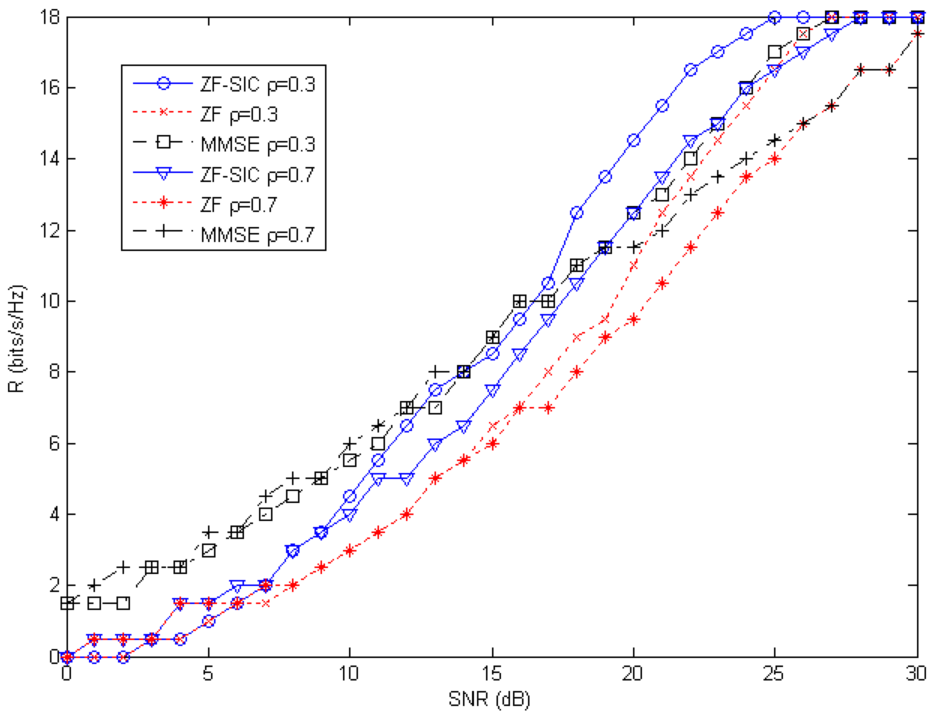

Figure 7.4: Bit rate vs. SNR - 12 coded bit rates with $n_T = 3$, $n_R = 4$ and $\overline{\mathrm{BER}} = 10^{-2}$.

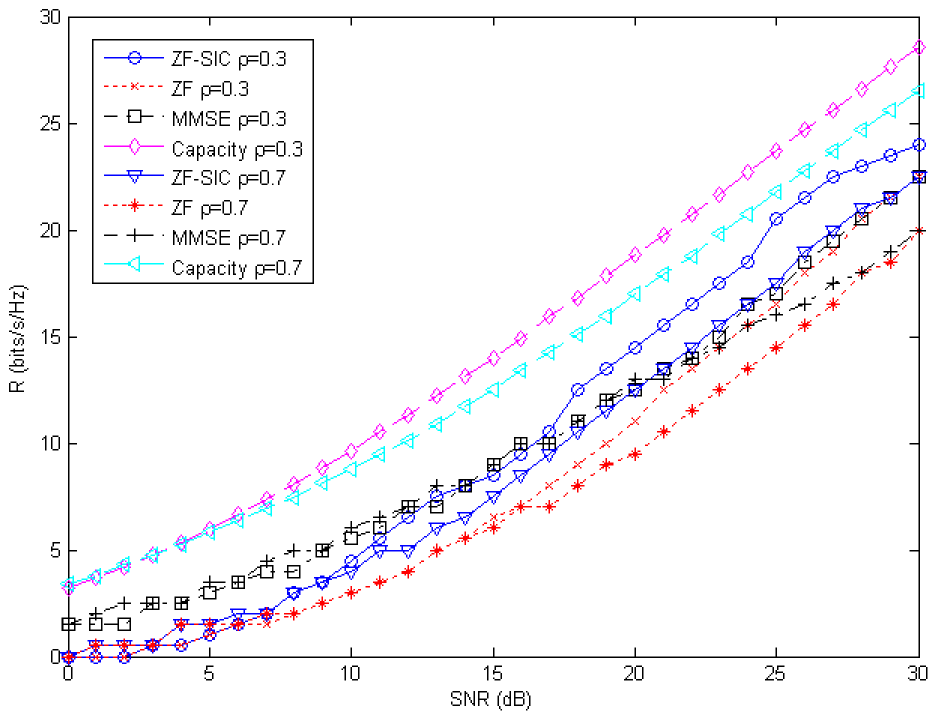

Figure 7.5: Bit rate vs. SNR - 16 coded bit rates with $n_T = 3$, $n_R = 4$ and $\overline{\text{BER}} = 10^{-2}$.

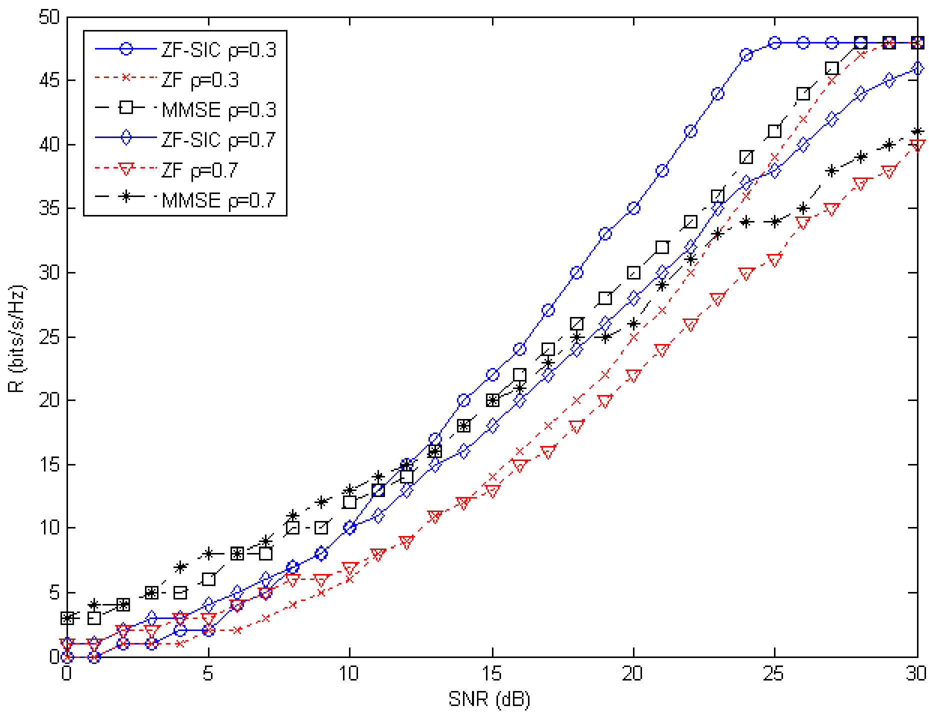

Figure 7.6: Bit rate vs. SNR - 6 uncoded bit rates with $n_T = 8$, $n_R = 10$ and $\overline{\text{BER}} = 10^{-2}$.

The results for the scenario with 12 convolutional codes are shown in Fig. 7.4. the results for the third scenario with 16 convolutional codes are compared with the CDIT capacity in Fig. 7.5. We can see that the difference between capacity and ZF-SIC is about 3-4 bits, at 25 dB of SNR, which shows that the percentage of rate of ZF-SIC compared to capacity is at the region 80%-86.5%.

In Fig. 7.6, the first scenario, in this case with a configuration of $n_T = 8$, $n_R = 10$, is simulated, showing the applicability of the proposed optimization even under such extreme dimensions.

7.5.3 Power Minimization

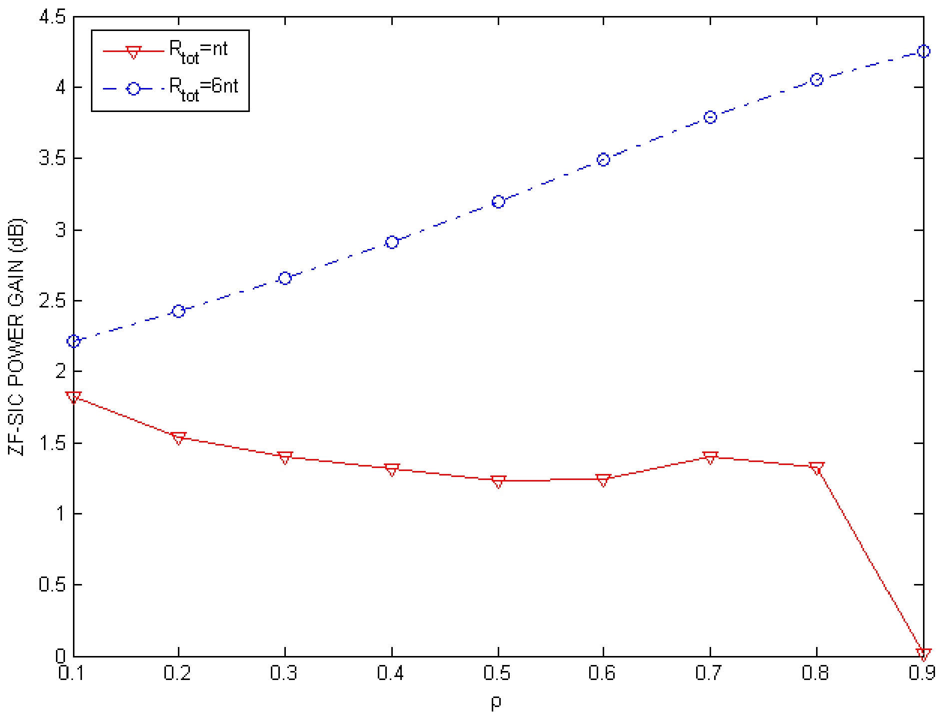

Figure 7.7: ZF-SIC power gain vs. ρ - 6 uncoded bit rates with $n_T = 3$, $n_R = 4$ and $\overline{\mathrm{BER}} = 10^{-2}$.

The power gain in Fig. 7.7 and Fig. 7.8 compares the optimized $\mathbf{P}$ of the proposed approach (using the optimum $\mathbf{V}^n$) with respect to the ZF power allocated by using the Levin-Campello algorithm (Chapter IV). We can see that the difference of power gain

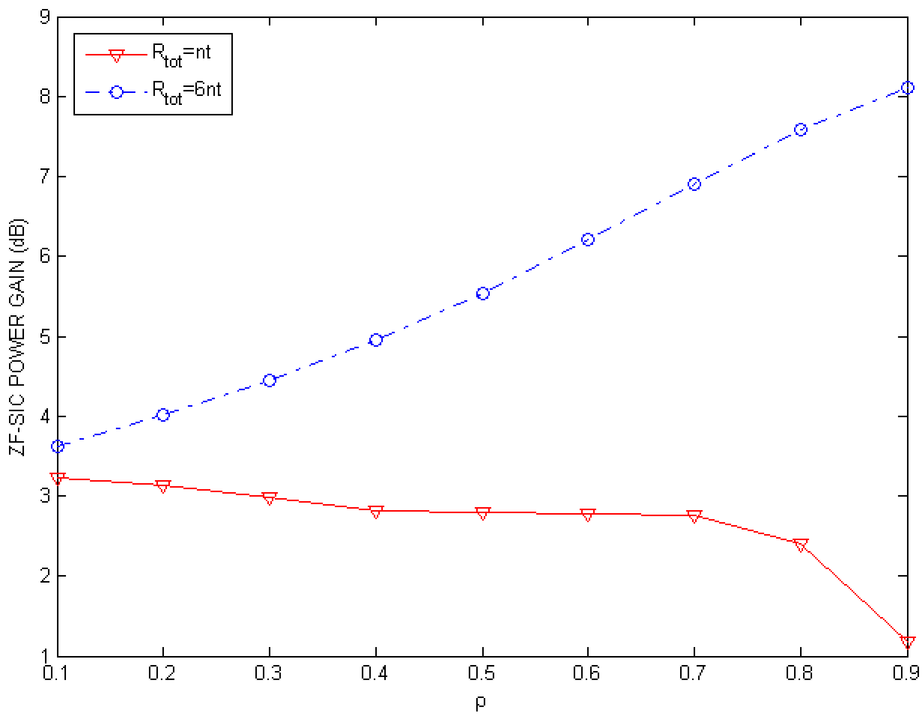

Figure 7.8: ZF-SIC power gain vs. ρ - 6 uncoded bit rates with $n_T = 3$, $n_R = 4$ and $\overline{\mathrm{BER}} = 10^{-4}$.

between ZF-SIC and ZF is varying from 0 dB to 4.3 dB in Fig. 7.7 and the gain is within the range 1-8.5 dB in Fig. 7.8. In these two figures, for high SNR, the power gain is increasing with ρ, but for low SNR, the power gain between ZF-SIC and ZF is small, as the error propagation is large. For low SNR, with high correlation ($\rho = 0.9$), the performance of ZF-SIC is sharply deteriorated to be close to ZF.

7.6 Conclusion

Analytical approximations for the BER of MIMO systems in transmit-correlated Rayleigh flat-fading channels with ZF-SIC receiver are obtained, taking into account the decoding order. These approximations can be used to optimize the transmitter for a given target BER, following a decoding order, or in general, for the system design. Their accuracy has been shown by comparison with numerical results.

From these BER approximations, a method is proposed for solving the two dual optimization problems, bit rate maximization and power minimization. As shown by the simulations, lower power cost and higher bit rates are achieved with this optimization scheme compared to ZF or MMSE approaches.

8

Conclusions

For a single user MIMO system, the BER of three typical receivers, ZF, MMSE and ZF-SIC, has been estimated and simplified, when possible, to convenient closed-form approximations, by using the statistical information of the channel matrix with correlation at the transmitter side. Numerical results show the accuracy of the developed expressions.

By utilizing these BER approximations, two dual optimization problems, bit rate maximization and power minimization, are solved for the practical case of statistical channel knowledge at the transmitter side and discrete constellations.

The comparison of the power gain of the three mentioned types of receivers relative to a non-optimized transmission explicitly shows the performance gains of the proposed methods in this Thesis. As it happens without optimization, ZF performs close to MMSE at high SNR while ZF-SIC approaches ZF at low SNR. Otherwise, the performance of ZF-SIC is the best of the three considered schemes while MMSE gives intermediate rates or power requirements with a lower complexity.

8.1 Future work

This Thesis focuses on the flat fading Rayleigh channel model with correlation only at the transmitter side. Following the proposed method in this Thesis, the way of solving the two optimization problems could be considered for other kinds of channel models, or even considering correlation at both sides, that is, not only at the transmitter side, but also at the receiver side. The extension to frequency selective fading seems quite straightforward with the use of multicarrier modulation to create a set of parallel flat fading channels. However, with the new frequency dimension the complexity of the system may grow in such a way that possibly more efficient algorithms will be needed.

In particular, for MMSE and ZF-SIC receivers, although the proposed algorithms in this Thesis are accurate and efficient, more efficient algorithms could be considered and developed in future work. Moreover, other different types of receivers, modulation, and coding schemes may also be considered and analyzed.

The focus of this Thesis is on single-user systems. This work paves the way to developing optimization algorithms for multi-user systems, where the same obtained BER formulations can be leveraged and the problem formulation must include the interaction of several users and contemplate a particular access scheme.

Finally, in this Thesis we have optimized the power allocation matrix, considering a known precoding matrix that actually achieves capacity for Gaussian inputs. It remains to find if this precoder is also optimum for discrete constellations or, otherwise, find some guidelines to construct the optimum precoder for these conditions.

References

[Arimoto 1972] S. Arimoto, "An algorithm for computing the capacity of arbitrary discrete memoryless channels," IEEE Trans. Inf. Theory, Vol. 18, No. 1, pp. 12-20, Jan. 1972.

[Armada et al. 2009] Ana García Armada, L. Hong and A. Lozano, "Bit loading for MIMO with statistical channel information at the transmitter and ZF receiver," Proc. Int'l Conf. on Communications (ICC'09), June 2009.

[Armada 2006] Ana García Armada, "SNR gap approximation for MPSK- Based bit loading," IEEE Transactions on Wireless Communications, Vol. 5, No. 1, pp. 57-60, 2006.

[Biglieri 2004] E. Biglieri, "Transmission and reception with multiple antennas: Theoretical foundations," Foundations and Trends in Communications and Information Theory, Vol. 1, 2004.

[Blahut 1972] R. E. Blahut, "Computation of channel capacity and rate distortion functions," IEEE Trans. Inf. Theory, Vol. 18, pp. 460-473, July 1972.

[Campello et al. 1999] J. Campello, "Practical bit loading for DMT," IEEE International Conference on Communications, Proc. Int'l Conf. Communications, Vancouver, Canada, Vol. 2, pp. 801-805, June 1999.

[Chiani et al. 2003] Marco Chiani, Davide Dardari and Marvin K. Simon, "New exponential bounds and approximations for the computation of error probability in fading channels," IEEE Trans. on Wireless Comm., Vol. 2, No. 4, pp. 840-845, Jul. 2003.

[Chien-Chang Li et al. 2009] Chien-Chang Li, Yuan-Pei Lin, Shang-Ho Tsai, and P. P. Vaidyanathan, "Optimization of transceivers with bit allocation to maximize bit rate for MIMO transmission," IEEE Trans. on Communications, Vol. 57, No. 12, pp. 3556- 3560, Dec. 2009.

[Chow et al. 1995] J. S. Chow, J. M. Cioffi, and J. Bingham, "A practical discrete multitone ransceiver loading algorithm for data transmission over spectrally shaped channels," IEEE Trans. Commun., Vol. 43, No. 234, pp.773-775, Feb./Mar./Apr. 1995.

[Chu et al. 1997] T.-S. Chu and L. J. Greenstein, "A semiempirical representation of antenna diversity gain at cellular and PCS base stations," IEEE Trans. Commun., Vol. 45-46, pp. 644-646, June 1997.

[Chuah et al. 1998] C. Chuah, J. Kahn and D. Tse. "Capacity of multi-antenna arry systems in indoor environment," Porc. IEEE GLOBECOM, 4, 1894-1899, Sydney, Australia, Nov. 1998.

[Chuah et al. 2002] C. Chuah, D. Tse, J. Kahn and R. Valenzuela. "Capacity scaling in MIMO wireless under correlated faidng," IEEE Trans. Inf. Theory, 48(3), 637-650, Mar. 2002.

[Cioffi] J. M. Cioffi, EE379A course notes, Stanford University, http://www.stan ford.edu/class/ee379c/readerfiles/chap4.pdf.

[Cioffi et al. 1995] J. M. Cioffi, G.P. Dudevoir, M.V. Eyuboglu and G.D. Forney, Jr., "MMSE decision-feedback equalizers and coding-Part II: Coding results," IEEE Transactions on Communications, Vol. 43, No. 10, pp. 2595-2604, Oct. 1995.

[Cover and Thomas 1991] Cover, T. M. and Thomas, J. A. (1991). Elements of Information Theory. 1991.

[Forney and Ungerboeck 1998] Forney, G.D., Jr. Ungerboeck, G., "Modulation and coding for linear Gaussian channels," Information Theory, IEEE Transactions, Vol. 44, Issue 6, pp. 2384 - 2415, Oct. 1998.

[Froschini 1996] G. Froschini. “Layered space-time architecture for wireless communication in a fading environment when using multi-element antennas,” Bell Labs Tech. J., 41-59, 1996.

[Fung and Lim 2007] C.-H. F. Fung, W. Yu, T. J. Lim, “Precoding for the multi-antenna downlink: Multiuser SNR gap and optimal user ordering,” IEEE Trans. Communications, Vol. 55, No. 1, pp. 188-197, 2007.

[Gesbert 2003] D. Gesbert, “Robust linear MIMO receivers: A minimum error-rate approach,” IEEE Trans. Signal Processing, Vol. 51, No. 11, pp. 2863- 2871, Nov. 2003.

[Goldsmith and Varaiya 1997] A. J. Goldsmith and P. Varaiya, “Capacity of fading channels with channel side information,” IEEE Trans. on Inform. Theory, Vol. 43, No. 6, pp. 1986-1992, Nov. 1997.

[Gore et al. 2002] D. Gore, R. W. Heath Jr. and A. Paulraj, “On performance of the zero forcing receiver in presence of transmit correlation,” ISIT Lausanne, Switzerland, p. 159, July 2002.

[Guo et al. 2005] D. Guo, S. Shamai, and S. Verdú, “Mutual information and minimum mean-square error in Gaussian channels,” IEEE Trans. Inf. Theory, Vol. 51, No. 4, pp. 1261-1283, Apr. 2005.

[Guo et al. 2002] D. Guo, S. Verdú, and L. K. Rasmussen, “Asymptotic normality of linear multiuser receiver outputs,” IEEE Trans. Inform. Theory, Vol. 48, pp. 3080-3095, Dec. 2002.

[Hachem et al. 2008] W. Hachem, O. Khorunzhiy, Ph. Loubaton, J. Najim, and L. Pastur, “A new approach for capacity analysis of large dimensional multiple-antenna channels,” IEEE Trans. Inf. Theory, Vol. 54, No. 9, pp. 3987-4004, Sept. 2008.

[HAN et al. 2009] Juan HAN, Xiaofeng TAO, Qimei CUI, “Lower bound of BER in M-QAM MIMO system with ordered ZF-SIC receiver,” IEEE, VTC Spring 69th, pp. 1-5, 2009.

[Hong et al. 2009] L. Hong, Juan José García Fernádez, Ana García Armada, "On the optimality of Levin-Campello bit and power Loading," International OFDM-Workshop, Hamburg, 2009.

[Hong et al. 2010] L. Hong, A. García-Armada, "Bit error rate performance of MIMO MMSE receivers in correlated Rayleigh flat-fading channels," IEEE Trans. on Vehicular Technology, Vol. 60, No. 1, pp. 313-317, Jan. 2010.

[Huang and Hwang 2006] Ping Huang Huang and Tea Yuan Hwang, "On new moment estimation of parameters of the generalized Gamma distribution using its characterization," Taiwanese journal of mathematics, Vol. 10, No. 4, pp. 1083-1093, Jun. 2006.

[Irwin] Mark E. Irwin, Moment Generating Function, http://markirwin.net/stat110/Lecture/Section45.pdf.

[Joham et al. 2005] Michael Joham, Wolfgang Utschick and Josef A. Nossek, "Linear Transmit Processing in MIMO Communications Systems," IEEE Trans. on Signal Processing, Vol. 53, No. 8, Aug. 2005.

[Kammoun et al. 2009] A. Kammoun, M. Kharouf, W. Hachem, and J. Najim, "BER and outage probablity approximations for LMMSE detectors on correlated MIMO channels," IEEE Trans. Information Theory, Vol. 55, No.10, pp. 4386- 4397, Oct. 2009.

[Kiessling and Speidel 2003] M. Kiessling and J. Speidel, "Analytical performance of MIMO MMSE receivers in correlated Rayleigh fading environments," Proc. IEEE Vehicular Technology Conference, Vol. 3, pp. 1738-1742, Oct. 2003.

[Kim 2004] Il-Min Kim, "Space-time power optimization of variable-Rate space-Time block codes based on successive interference cancellation," IEEE Trans. on communications, Vol. 52, No. 7, pp. 1204-1213, Jul. 2004.

[L. Li et al. 2001] L. Li, A. M. Tulino, and S. Verdú, "Asymptotic eigenvalue moments for linear multiuser detection," Communications in Information and Systems, Vol. 1, No. 3, pp. 273-304, 2001.

[Lozano and Papadias 2002] A. Lozano and C. Papadias. "layered space-time receivers for frequency selective wireless channels." IEEE Trans. Comm, 50(1), 65-73, Jan, 2002.

[Lozano et al. 2006a] Angel Lozano, A. M. Tulino, and S. Verdú, "Opitmum power allocation for parallel Gaussian channels with arbitrary input distributions," IEEE Trans. Inf. Theory, Vol. 52, No. 7, pp. 3033-3051, Jul. 2006.

[Lozano et al. 2006b] Angel Lozano, A. M. Tulino, and S. Verdú, "Opitmum power allocation for parallel Gaussian channels with arbitrary input distributions," IEEE Trans. Inf. Theory, Vol. 52, No. 7, pp. 3033-3051, Jul. 2006.

[Lozano et al. 2008] Angel Lozano, A. M. Tulino, and S. Verdú, "Optimum power allocation for multiuser OFDM with arbitrary signal constellations," IEEE Trans. Communications, Vol. 56, pp. 828-837, May. 2008.

[Matas and Lamarca 2007] David Matas, Meritxell Lamarca, "Optimum power allocation and bit loading for systems with suboptimum receivers," Global Telecommunications Conference, 2007. GLOBECOM '07. IEEE, pp. 3085-3090, Nov. 2007.

[Maupertuis 1744] P.L.M. de Maupertuis, Accord de différentes lois de la nature qui avaient jusquíci paru incompatibles. Mém. As. Sc. Paris p. 417, 1744.

[Maupertuis 1746] P.L.M. de Maupertuis, Le lois de mouvement et du repos, déduites dún principe de métaphysique. Mém. Ac. Berlin, p. 267, 1746.

[Mosier and Clabaugh 1958] R. R. Mosier and R. G. Clabaugh, "Kineplex, a bandwidth efficient binary transmission system," AIEE Trans. AIEE, Vol. 76, pp. 723-728, Jan. 1958.

[Moustakas et al. 2009] A. L. Moustakas, K. R. Kumar, and G. Caire, "Performance of MMSE MIMO receivers: A large N analysis for correlated channels," Proc. Vehicular Technology Conference, Vol. 1, pp. 1-5, Dec. 2009.

[Neeser and Massey 1993] F. Neeser and J. Massey. "Proper complex random processes with applications to information theory," IEEE Trans. Inf. Theory, 39(4), 1293-1302, July, 1993.

[P. Li et al. 2006] P. Li, D. Paul, R. Narasimhan, and J. Cioffi, "On the distribution of SINR for the MMSE MIMO receiver and performance analysis," IEEE Trans. Inform. Theory, Vol. 52, No. 1, pp. 271-286, Jan. 2006.

[Paulraj 2003] A. Paulraj, Introduction to Space-Time Wireless Communications. Cambridge University Press, 2003.

[Poor and Sergio V. 1997] H. V. Poor and S. Verdú, "Probability of error in MMSE multiuser detection," IEEE Trans. Inform. Theory, Vol. 43, pp. 858-871, May 1997.

[Proakis 2000] J. Proakis, Digital Communications, 4th ed. McGraw Hill, 2000.

[Ralf R. M. 2002] Ralf R. Müler, "On the asymptotic eigenvalue distribution of concatenated vector-valued fading channels," IEEE Trans. Inform. Theory, Vol. 48, No. 7, pp. 2086-2091, 2002.

[Rungnes and Gesbert 2004] A. H. rungnes and D. Gesbert, "Exact ser-precoding of orthogonal spacetime block coded correlated MIMO channels: An iterative approach," in Proceedings of the 6th Nordic Signal Processing Symposium, NORSIG 2004, Espoo, Finland, pp. 336-339, June 2004.

[Scaglione et al. 1999] A. Scaglione, G. Giannakis, and S. Barbarossa, "Redundant filterbank precoders and equalizers. I. Unification and optimal designs," IEEE Trans. On Signal Processing, Vol. 47, No. 7, pp. 1988-2006, Jul. 1999.

[Sergio V. 1998] S. Verdú, Multiuser Detection. Cambridge, U.K.: Cambridge Univ. Press, 1998.

[Shannon 1948] C. Shannon. A mathematical theory of communication. Bell Labs Tech. J., 27, 379-423, 623-656, July and Oct., 1948.

[Sergio V. and Shamai 1999] S. Verdú and S. Shamai, "Spectral efficiency of CDMA with random spreading," IEEE Trans. Inform. Theory, Vol. 45, No. 2, pp. 622-640, Mar. 1999.

[Scaglione et al. 2002] Anna Scaglione, Petre Stoica, Sergio Barbarossa, and etc, "Optimal designs for space-Time linear precoders and decoders," IEEE Trans. On Signal Processing, Vol. 50, No. 5, pp. 1051-1064, May 2002.

[Shen et al. 2004] Cong Shen, Yan Zhu, Shidong Zhou, Jinjing Jiang, “On the performance of V-BLAST with zero-forcing successive interference cancellation receiver,” IEEE Globecom, pp. 2818-2822, 2004.

[Taouk and Peacock 2006] Michael M.Taouk, Matthew J. M. Peacock, “Statistical power allocation and coded bit allocation optimization in Mercury/Waterfilling,” Communications Theory Workshop, 2006. Proceedings. 7th Australian, pp. 159-164, Feb. 2006.

[Telatar 1999] I. Telatar. “Capacity of multi-antenna Gaussian channels,” European Trans. Tel., 10(6), 585-595, Nov./Dec., 1999.

[Tse and Hanly 1999] D. N. C. Tse and S. V. Hanly, “Linear multiuser receivers: Effective interference, effective bandwidth and user capacity,” IEEE Trans. Inform. Theory, Vol. 45, No. 2, pp. 641-657, Mar. 1999.

[Tse and Zeitouni 2000] D. N. C. Tse and O. Zeitouni, “Linear multiuser receivers in random environments,” IEEE Trans. Inform. Theory, Vol. 46, No. 1, pp. 171-188, Jan. 2000.

[Tulino and Sergio V. 2004] A. M. Tulino and S. Verdú, “Random matrix theory and wireless communications,” Foundations and Trends in Communications and Information Theory, Vol. 1, June 2004.

[Tulino et al. 2005] A. M. Tulino, A. Lozano, and S. Verdú, “Impact of Antenna Correlation on the Capacity of Multiantenna Channels,” IEEE Trans. on Information Theory, vol. 51, no. 7, pp. 2491-2509, July 2005.

[Tulino et al. 2006] A. M. Tulino, A. Lozano, and S. Verdú, “Capacity-achieving input covariance for single-user multi-antenna channels,” IEEE Trans. on Wireless Communications, Vol. 5, No. 3, pp. 662-671, March 2006.

[Varnica et al. 2002] N. Varnica, Ma Xiao, and A. Kavcic, “Capacity of power constrained memoryless AWGN channels with fixed input constellations,” Proc. IEEE, GLOBECOM 2002, Vol. 2, pp. 1339-1343, Nov. 2002.

[Wang and Blostein 2007] Neng Wang and Steven D. Blostein, "Approximate minimum BER power allocation for MIMO spatial multiplexing systems," IEEE Trans. On Communications, Vol. 55, No. 1, pp. 180-187, Jan. 2007.

[Winters et al. 1994] J. Winters, J. Salz and R. Gitlin, "The impact of antenna diversity on the capapcity of sireless communications systems," IEEE Trans. Comm., 42(2), 1740-1751, Feb. 1994.

[Wolniansky et al. 1998] P. W. Wolniansky, G. J. Foschini, G. D. Golden, R. A. Valenzuela, "V-BLAST: An architecture for realizing very high data rates over the rich-scattering wireless channel," International Symposium on Signals, Systems, and Electronics, pp. 295 - 300, 29 Sept.- 2 Oct. 1998.

[Xiaofeng et al. 2002] Tao Xiaofeng, Yu Zhuizhuan, Qin Haiyan, Zhang Ping, Haas H. and Costa E., "New sub-optimal detection algorithm of layered pace-time code," VTC Spring 2002. Vol. 4, pp. 1791 - 1794, May 2002.

[Xiao et al. 2009] Chengshan Xiao, Yahong Rosa Zheng, "Transmit precoding for MIMO systems with partial CSI and discrete-constellation inputs," ICC 2009.

[Xin Li and Nie 2004] Xin Li, Zaiping Nie, "Performance losses in V-BLAST due to correlation," IEEE Antennas and Wireless Propagation Letters, Vol. 3, pp. 291-294, 2004.

[XU et al. 2008] Jin XU, Xiaofeng TAO, Ping ZHANG, "Analytical SER performance bound of M-QAM MIMO system with ZF-SIC receiver," ICC 2008 Proceedings, pp. 5103-5107,2008.

[Zhang et al. 2001] J. Zhang, E. K. P. Chong, and D. N. Tse, "Output MAI distribution of linear MMSE multiuser receivers in DS-CDMA systems," IEEE Trans. Inform. Theory, Vol. 47, pp. 1128-1144, Mar. 2001.

[Zhi-heng et al. 2007] GUO Zhi-heng, LI Li-hua and TAO Xiao-feng, "Fast ordering detection algorithm for V-BLAST system," Journal of Beijing University of Posts and Telecommunications, Vol. 30, No. 04, pp. 83-87, 2007.

Publications

[1] L. Hong, Juan José García Fernádez, Ana García Armada, "On the Optimality of Levin-Campello Bit and Power Loading," International OFDM-Workshop, Hamburg, 2009.

[2] A. García Armada, L. Hong and A. Lozano, "Bit Loading for MIMO with Statistical Channel Information at the Transmitter and ZF Receiver," Proc. Int'l Conf. on Communications (ICC'09), June 2009.

[3] L. Hong, A. García-Armada, "Bit Error Rate Performance of MIMO MMSE Receivers in correlated Rayleigh Flat-fading Channels," IEEE Trans. on Vehicular Technology, Vol. 60, No. 1, pp. 313-317, Jan. 2010.

[4] L. Hong, A. García.Armada and A. Lozano, "Bit Loading for MIMO with Statistical Channel Information at the Transmitter and MMSE Receivers," 2011. (in revision)

[5] L. Hong, A. García.Armada and A. Lozano, "Bit Loading for MIMO with Statistical Channel Information at the Transmitter and ZF-SIC Receiver," 2011. (in preparation)